THREE DIMENSIONAL FINITE ELEMENT KNEE JOINT MODEL FOR THE INVESTIGATION OF MENISCECTOMY AND THE IMPACT OF LANDING FROM A JUMP ON THE KNEE COMPONENTS

MODÉLE TRIDIMENSIONNEL PAR ÉlÉMENTS FINIS DE L'ARTICULATION DU GENOU POUR L'ÉTUDE DE LA MÉNISCECTOMIE ET DE L'IMPACT DE L'ATTERRISSAGE D'UN SAUT SUR LES COMPOSANTES DU GENOU.

A Thesis Submitted to the Division of Graduate studies
of the Royal Military College of Canada
by

Sohaila ElSagheir, Ph.D. Candidate, M.Sc.

In Partial Fulfillment of the Requirements for the Degree of
Doctor of Philosophy

July 2016

To my daughter Layla and my beloved husband Mohammed for their continuous support.

ACKNOWLEDGMENTS

I would like to express my gratitude to my advisor, Dr. Kodjo Moglo for his guidance and support in the completion of this thesis.

Additional thanks to Dr. Diane Wowk and Dr. Wissal Mesfar for their helpful input through the course of this project.

I would also like to thank Pierre Seguin for his helpful feedback in SolidWorks.

Finally, special thanks to my husband who supported me during this long journey and helped me with technical advice whenever needed.

ABSTRACT

Three Dimensional Finite Element Knee Joint Model for the Investigation of Meniscectomy and the Impact of Landing from a Jump on the Knee Components.

The aim of this research is to investigate the effect of total and unilateral meniscectomy on various knee components and to investigate the internal contact and ligaments forces acting at the knee as a result of landing from a jump. The injury zone was determined for each knee component and a new landing technique was proposed to minimize the injury.

Previous studies have provided very little information on internal components' stresses and forces which is crucial for improving knee function. A full 3D knee joint model was constructed based on MRI images of a male subject to investigate these scenarios. The model includes both tibio-femoral and patello-femoral joints and considers the complex 3D geometry of the joint with large relative displacements, articular surfaces, menisci, articular cartilages, ligaments, as well as the quadriceps muscles of the knee.

Two studies were undertaken in this research. In the first study, the investigation provides a full comparison between the intact menisci and fully or unilateral meniscectomized knee joint. It was found that total meniscectomy is the worst case scenario as it resulted in much higher cruciate ligament forces, contact pressure, femoral and tibial cartilages' stress, and contact force in all cases processed. This worst condition was follow by the unilateral medial meniscectomy. This highlights that the medial compartment contributes more to load bearing as reported in previous studies. These results showed that clinically, unilateral medial meniscectomy has a higher impact on knee joint function than lateral meniscectomy and that medial meniscus should have a higher priority for preservation either by grafting or transplantation.

In the second study, landing from a jump impact was investigated at five different points on the landing (pre toe-landing (P1), toe-landing (P2), between toe-landing and heel strike (P3), heel strike (P4) and after heel strike (P5)). From the results, the worst condition with respect to injury was recorded at P5, followed by P4 in severity. The ratio between the patellar tendon forces FPT and the quadriceps forces FQ versus the knee flexion of the presented model showed that the patella tendon joint did not act as a perfect pulley. By increasing the flexion angle increments of 5 degrees at toe landing and rerunning the analysis under same previous loading conditions, predicted results of the model showed substantial decrease in the stress levels and the contact forces acting at the knee. These results suggest that landing technique can be improved by changing knee flexion angle at toe landing. Overall, the results obtained in these studies were found to be in general agreement with the available reported experimental measurements.

RÉSUMÉ

Modèle Tridimensionnel par Éléments Finis de l'Articulation du Genou pour l'Étude de la Méniscectomie et de l'Impact de l'atterrissage d'un Saut sur les Composantes du Genou.

Le but de cette recherche est d'étudier l'effet de la méniscectomie totale et unilatérale sur diverses composantes du genou et d'évaluer les forces internes de contact et ligamentaires agissant sur l'articulation du genou à la suite de l'atterrissage d'un saut. La zone de lésion est déterminée pour chaque composant de genou et une nouvelle technique d'atterrissage est proposée afin de réduire au minimum la blessure.

Les études antérieures ont fourni très peu d'information sur les forces et contraintes des composants internes, information qui est cruciale pour l'amélioration de la fonction du genou. Un modèle 3D complet de l'articulation du genou a été construit à partir d'images IRM d'un sujet masculin pour évaluer ces scénarios. Le modèle comprend à la fois les articulations tibio-fémorale et fémoro-patellaire et considère la géométrie complexe 3D de l'articulation avec de grands déplacements relatifs, les surfaces articulaires, les ménisques, les cartilages articulaires, les ligaments, ainsi que les muscles quadriceps du genou.

Deux études ont été menées dans cette recherche. Dans la première étude, l'investigation fournit une comparaison complète entre l'articulation du genou avec ménisques intacts et la méniscectomie unilatérale ou totale. Il a été constaté que la méniscectomie totale est le pire des cas, car il a donné lieu à plus de forces des ligaments croisés, de pression de contact, de contraintes sur les cartilages fémoral et tibial, et de force de contact sur les cartilages dans toutes les analyses considérées. Cette pire situation était suivie par la méniscectomie médiale unilatérale. Cela a mis en évidence que le compartiment médial contribuait plus à supporter des charges comme rapporté dans les études précédentes. Ces résultats ont montré que, cliniquement, la méniscectomie médiale unilatérale a un impact plus important sur la fonction articulaire du genou que la méniscectomie unilatérale latérale et que le ménisque médial devrait avoir une priorité plus élevée pour la conservation soit par le greffage ou la transplantation.

Dans la deuxième étude, l'impact de l'atterrissage d'un saut a été étudié en cinq points différents sur la courbe d'atterrissage (pré-atterrissage d'orteil (P1), atterrissage d'orteil (P2), entre l'atterrissage d'orteil et l'impact de talon (P3), l'impact du talon (P4) et après l'impact du talon (P5)). D'après les résultats, la pire situation concernant le dommage aux composants du genou a été enregistrée à P5, suivie par P4 dans la sévérité. Le rapport entre les forces du tendon rotulien et les forces quadriceps par rapport à la flexion du genou du modèle a montré que l'articulation rotulienne du tendon n'a pas agi comme une poulie parfaite. En augmentant les incréments d'angle de flexion de 5 degrés à l'atterrissage de l'orteil et en recommençant les analyses dans les mêmes conditions de chargement

précédentes, les résultats obtenus du modèle ont montré la diminution substantielle de niveaux de contraintes et de forces de contact qui agissent au niveau du genou. Ces résultats suggèrent que la technique d'atterrissage peut être améliorée en modifiant l'angle de flexion du genou à l'atterrissage de l'orteil. Dans l’ensemble, les résultats obtenus dans ces études sont en accord général avec les mesures expérimentales disponibles rapportées.

STATEMENT OF CONTRIBUTIONS

A full 3D knee joint model including tibio-femoral, patello-femoral and tibio-fibular joints was constructed based on MRI images of a male subject, which considered the complex geometry of the joint articular surfaces, menisci , ligaments, tendons and quadriceps muscles. This model was used as a tool to investigate the following scenarios:

1) The impact of total and unilateral meniscectomy on articular cartilages and ligaments in the knee joint, and comparing results with the menisci intact case. In addition to determining the worst condition in all studied cases. This study proved the harmful impact of meniscectomy surgeries, where the case of unilateral meniscectomy had more of an impact on the knee function.

2) The impact of landing from a jump on various knee parts under various large quadriceps forces at five different stages of the landing curve (pre toe-landing, toe-landing, after toe-landing, heel strike and after heel strike). A detailed insight of the internal contact and ligament forces is presented, which was not fully discussed in previous studies as there are ethical concerns to measure experimentally due to the invasive nature of the procedure needed can cause real injury.

3) The injury zone for each knee part during each landing stage, and to specify the worst case scenario among the five stages studied. This new finding will help identify the zone in which injury may occur so a modified landing technique can be proposed to avoid this injury.

4) A new landing technique is proposed based on results of the jump impact study that minimizes the injury occurrence.

TABLE OF CONTENTS

LIST OF TABLES

Table **Page**

LIST OF FIGURES

Figure **Page**

LIST OF ACRONYMS

2D: Two Dimensional

3D: Three Dimensional

ACL: Anterior Cruciate Ligaments

CT: Computed Tomography

FQ: Quadriceps Force

FPT: Patella Tendon Force

F.E.: Finite Element

GRF: Ground Reaction Force

LCL: Lateral Collateral Ligaments

MCL: Medial Collateral Ligaments

MIMICS: Materialise's Interactive Medical Image Control System

MRI: Magnetic Resonance Imaging

PCL: Posterior Cruciate Ligaments

PT: Patellar Tendon

RF: Rectus Femoris.

VL: Vastus Lateralis

VMO: Vastus Medialis Obliqus

CHAPTER 1

INTRODUCTION

1.1 Motivation

Knee joint injuries are considered to be the most common and crucial lower extremity injuries. These injuries are due to many reasons, among which are:

1) Knee joint osteoarthritis (OA) due to cartilage degeneration as a result of meniscectomy.
2) Excessive impact forces due to improper landing from a jump.

OA is defined as a degenerative condition of the joint articular cartilage and is the most common form of arthritis affecting 27 million people in the USA (as of 2005) [1]. OA treatment is costly; a study conducted in 2009 showed that knee and hip replacements due to OA costs nearly $42.3 billion [1]. Previous studies reported that menisci surgical removal or meniscectomy is a procedure associated with a high risk of knee osteoarthritis [2]. OA is estimated to be the fourth leading cause of disability [3]. Although OA can affect any joint (hip, knee, ankle and hand), the greatest disability burden is attributed to OA at the hip and the knee [3]. Total and unilateral meniscectomy removes the shock absorbing factor of the knee joint by removing the menisci. This causes the articular cartilages to have hard contact and degeneration occurs. In this study, a full investigation of total and unilateral meniscectomy is presented to determine the effect on articular contact forces and compare it with menisci preserved conditions.

Landing from jump knee injuries affects both military and civilian personnel. For military, paratroopers and parachutists are at high risk of serious knee injuries due to jumping from flying helicopters into an operation field subjecting the knee joint to a hard landing impact. For civilians, athletes and gymnastic players are also subjected to severe knee injuries due to their excessive training protocol and high jump impacts. Previous experimental studies lacked a detailed analysis of the contact forces acting on various knee parts and determining the injury zone for each part. The present study will investigate in detail the impact of landing from a jump on various knee parts and determine the zone of injury for each part in addition to recommending a landing technique to lower the possibility of injury.

It is difficult to test directly the previous two applications on a subject as it involves invasive procedures and internal measurements that are difficult to determine. Difficulties associated with the measurement and calculation of contact and ligament forces have slowed progress in evaluating the internal state of the joint during high impact. Alternatively, computer simulation techniques and finite element knee models allow estimations of such parameters to be obtained noninvasively.

1.2 Contributions

A full 3D knee joint model including tibio-femoral, patello-femoral and tibio-fibular joints was constructed based on MRI images of a male subject, which considered the complex geometry of the joint articular surfaces, meniscii, ligaments, tendons and quadriceps muscles. This model was used as a tool to investigate the following scenarios:

1) Investigating the impact of total and unilateral meniscectomy on articular cartilages and ligaments in the knee joint, and comparing results with menisci intact case. This study proved the harmful impact of meniscectomy surgeries and which case of unilateral meniscectomy had more impact on the knee function.

2) Investigating the impact of landing from a jump on various knee parts under various large quadriceps forces at five different stages of the landing curve (pre toe-landing, toe-landing, after toe-landing, heel strike and after heel strike). A detailed insight of the internal contact and ligament forces is presented, which was not fully discussed in previous studies as there are ethical concerns to measure experimentally due to the invasive nature of the procedure needed that can cause real injury.

3) Determining the injury zone for each knee part during each landing stage. Also specifying the worst case scenario among the five stages studied. This new finding will help identify the zone in which injury occur so a modified landing technique to avoid this injury can be proposed.

4) Proposing a new landing technique-based on results of the jump impact study that minimizes the injury occurrence.

CHAPTER 2

LITERATURE REVIEW

The knee is one of the most important joints of the human body. It plays an essential role in movement related to carrying the body weight in horizontal (running and walking) and vertical (jumps) directions. The knee is a hinge type synovial joint, which is composed of three joints, the patellofemoral joint, the tibiofemoral joint and the tibiofibular joint.

The knee joint is surrounded by a joint capsule with ligaments strapping the inside and outside of the joint (collateral ligaments) as well as crossing within the joint (cruciate ligaments) as shown in Figure 2.1. These ligaments provide stability and strength to the knee joint. The knee joint is bathed in synovial fluid which is contained inside the synovial membrane (joint capsule). The functions of the synovial fluid include reduction of friction and lubricating the articulating joints. The meniscus is a thickened cartilage pad between the two joints formed by the femur and tibia. The meniscus acts as a smooth surface for the joint to move on. There is a large tendon (patellar tendon) which envelopes the knee cap and attaches to the front of the tibia bone. The large muscles of the thigh (quadriceps muscles) move the knee. They extend, or straighten, the knee joint by pulling on the patellar tendon. This complex joint with many components is very vulnerable to injury. Injury can affect any of the ligaments or tendons surrounding the knee joint. Injury can also affect the cartilage, menisci (plural for meniscus), and bones forming the joint. The complexity of the design of the knee joint and the fact that it is an active weight-bearing joint are factors in making the knee one of the most commonly injured joints.

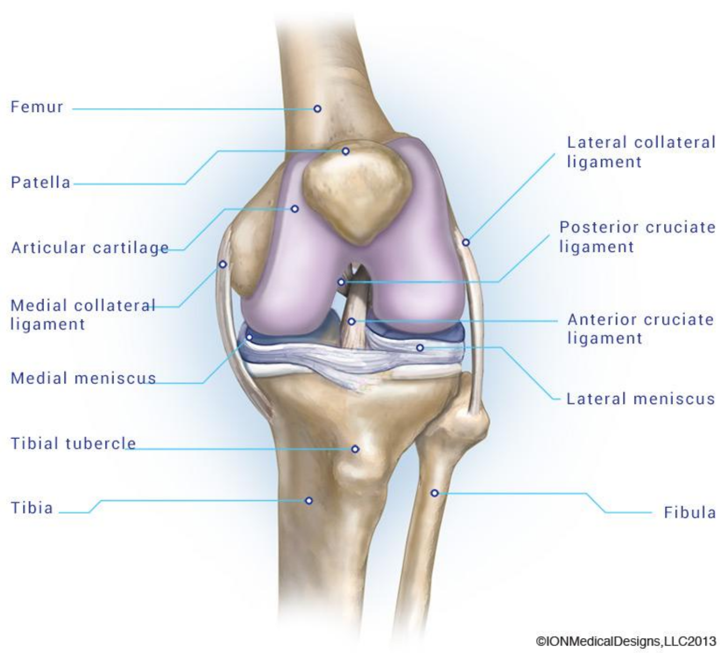

Figure 2.1 The knee joint
Adapted from www.josephbernmanmd.com

Most previous studies on knee biomechanics primarily aimed to determine the role of each knee component and how the load is transferred and distributed in the form of pressure in addition to the possible contact zones. Then in the last few years, mathematical and numerical models with different degrees of precision were augmented to complete the experimental methods.

Computer models present an effective way of evaluating knee joint mechanics during the design phase and provide an indication of expected clinical performance. They are more effective and less expensive than laboratory experiments. Still we refer to experimental data to validate the numerical model.

In the last 15 years, considerable progress has been carried out in the domain of numerical modelling of the knee, as detailed in Hefzy and Cooke [4] and Kazemi et al [5] who presented a detailed review of recent advances in computational mechanics of the human knee joint.

Early models started with two dimensional (2D) models that was transformed afterwards to three dimensional (3D). Moeinzadeh et al. [6] created a two-dimensional model of the knee that included ligament resistance and specified a force and moment on the femur. Later, there was noticeable progress to improve the technique developed by Moeinzadeh [6], Engine and Tümer [7], and Abdel-rahman et al. [8-10] developed more advanced algorithms to transform the 2D model into a 3D model. In the 3D models of Hefzy et al. [4] the thighbone and tibia were considered as rigid bodies and the ligaments were modeled as nonlinear elastic springs (cannot resist forces in compression). They were able to determine the ligaments forces and the contact forces. The 2D model developed by Tümer and Engine [11] is a three-body segment model of the knee, which consisted of 3 bodies (thighbone, tibia and patella) including both contacts (the tibio-femoral and the patello-femoral) to predict the dynamic response of the knee. They studied the movement of bending the knee between 0 and 55 degrees. Blankevoort and Huiskes [12] developed and experimentally verified a 3D knee model.

Several studies represented knee joint models that includes both patellofemoral and tibiofemoral joints, for example the model presented by Wang et al [13] who constructed finite element knee model to study stress associated with kneeling and standing positions. This study provided a comparison of the stress distribution on the knee joint cartilage between the two activities. Another study by Ho et al [14] presented a finite element knee joint model to evaluate patella bone strain and compare values between healthy subjects and those with pain. Another study presented by Adouni et al [15] which presented a tibiofemoral and patellofemoral knee joint model used to determine muscle forces in the stance (standing) phase of gait (walking pattern). In addition to the studies presented by Pena et al. [16] who investigated the combined role of ligaments and menisci in load transmission and joint stability and Ramaniraka et al [17] who evaluated the biomechanical effects of the posterior cruciate ligament reconstruction.

Other studies represented only one part of the knee joint, for example studies that focused on the patello-femoral joint such as Heegaard et al. [18], Hefzy et al. [19-20], and Mathews et al. [21] which focused on determining the patello-femoral joint contact force and its pressure distribution. Others focused on patellar movements during the bending of the knee (patellar trajectory) like Hirokawa et al.

[22], Reithmeir et al. [23] and Van Eijden et al. [24]. The experimental determination of the characteristics of the patello-femoral contact depended on measuring the region of the contact, then determining the average contact pressure via the contact forces. Most of the models developed investigating this joint in previous studies were 2D, such as those developed by Van Eijden et al. [24] and Yamaguchi et al. [25]. There were few 3D models studies done; amongst these models are those developed by Hefzy et al. [26], Blankevoort et al. [27], Mommersteeg et al. [28], and Heegaard et al. [29].

From the studies that focused on the tibiofemoral joint, the study conducted by Oshkour et al [30] which studied knee joint stress in standing, the study of Sylvia et al [31] which developed a tibiofemoral joint finite element model to investigate the effect of obesity on joint contact pressure and the study conducted by Moglo et al [32] which investigated the coupling between the anterior and posterior cruciate ligaments and the role of the posterior cruciate ligament in the knee joint at different flexion angles and under anterior femoral force.

From the studies which focused on investigating the meniscii, those conducted by by Fithian et al. [33], Shoemaker et al. [34], Newton et al. [35] and Tissakht et al. [36], which determined the menisci non-linear properties in tension and how it varies through the whole menisci. In another study, Tissakht et al. [37] also studied the properties of the fibres of the collagen that reinforces the menisci in the radial and circumferential directions by modeling the menisci as composite-reinforced bulk material.

Many studies focused on the menisci intact situations while there were very few studies that investigated the meniscectomy cases. For example the experimental study conducted by Deri et al. [38] investigated contact mechanics in partial meniscectomy and the study conducted by Mononen et al. [39] investigated the effect of radial tears in partial meniscectomy. These studies did not include a full comparison between partial and total meniscectomy. Pena et al. [40] developed a 3D finite element model to test the effect of total and partial meniscectomy under compressive loading at full extension only and did not include flexion. Another study presented by Bendjaballah et al. [41] investigated the effect of mensicii removal on the contact stresses on knee cartilages under axial loading.

Studies which investigated the landing from a jump showed many non-numerical approaches to measure the effect of the jump impact on the rupture of Anterior Cruciate Ligaments (ACL) rupture. Beutler et al. [42] used a qualitative movement screen to assess the jump-landing characteristics of a group of young individuals at high risk for musculoskeletal injury. They determined whether anthropometric factors (e.g. body mass index) and lower-extremity muscle strength contributed to observed differences in landing patterns which affects ACL injuries. Subjects in this study performed jumping from a 30 cm high box onto a force plate and then immediately rebounding back up in a maximal jump-landing quality and was assessed by analyzing videotapes of the jump-landing task in the sagital and frontal planes; t-testing was used to determine the significance.

Another study by Louw et al. [43] used six high-speed Vicon 370 cameras and biomechanical software to analyse landing patterns of two groups (healthy basketball players which acted as a control group and others with previous knee injuries). A strain gauge force plate, synchronised with the Vicon system, was used to measure the ground reaction forces as the subjects performed 10 "jump-shots", landing on each foot 5 times on the force plate while being captured on video then analyzed. Parameters of interest were: difference in peak flexion angles and peak joint moments resulting from the two groups in addition to other subjective data collected from subjects (discomfort rating scores). The literature suggests that more knee flexion during the landing phase will reduce the chances of injury due to lower ground reaction forces and better shock absorption. Another study conducted by Beillas et al. [44] investigated the knee behaviour when a ground reaction force is imposed and developed a finite element model for the lower limb.

Most of the previous studies focused on investigating the ACL tear as a result of jump impact; however those studies lacked a detailed analysis of the forces acting on the knee's other components, for example: the contact forces impacting the menisci, tibial cartilages, patellar cartilage and patellar tendon, which will be presented in this study. From the limitations of previous studies, it was very difficult to measure and calculate ligament and contact forces on various knee parts experimentally. Alternatively 3D Finite Element modeling and computer simulation techniques can estimate such parameters in a non-invasive way. This limitation will be covered in our present study. Experimental testing of real-life situations in order to understand the injury mechanism could be extremely dangerous for subjects plus it would not be ethical. One must therefore get as close to a real-life situation as possible without compromising human safety. It is difficult to perform direct measurements of essential variables such as ligament forces under experimental settings.

The experimental studies published have never performed the test at the threshold of the related injury. But a numerical model, once validated, can simulate the situation over the capacity of the components and then can determine the injury of each component. Finite element models have long been recognized and trusted as reliable means in the analysis of human joints (knee joint, elbow joint). An advantage of these numerical studies lies in precise control of loading, motions, boundary conditions and structural alterations in parametric studies of the joint response. A model study should consider the basic features of the knee such as the joint complex 3D geometry, articular surfaces, menisci, articular cartilage layers, articulations between menisci and cartilage layers with large relative displacements, as well as the main muscles of the knee.

The proposed study focuses on building a complete 3D model of the knee joint (including both tibio-femoral and patello-femoral joints) with biological properties and performing a finite element analysis to study multiple applications that were not discussed before in the literature. The present study will provide full comparison of unilateral and total meniscectomy with respect to the menisci intact and its impact on the knee joint in both full extension and flexion. In addition to investigating the effect of the landing impact on the knee joint injury and determine the region at which injury happens at various knee components, and whether it corresponds to the maximum ground reaction force (GRF) impact force or not, results of this analysis are then used to propose new landing techniques to reduce knee injury.

CHAPTER 3

KNEE JOINT ANATOMY AND BIOMECHANICS

3.1 Anatomy and Main Roles

The knee joint is considered the largest and most complex joint in the human body. It supports large loads while undergoing finite displacements. Due to these loads and motions, it is common place for various disorders and injuries to occur. In some sports or exercises, these loads and displacements may exceed the failure limits of its components causing serious dislocations, sprains, ruptures and degenerative processes. Effective prevention, evaluation, and treatment programs require an adequate knowledge of the role of various components and their interactions on knee joint biomechanics under various loading conditions.

The knee joint, shown in Figure 3.1 consists of three bony structures (tibia, femur, and patella), the articular cartilage layers, menisci, ligaments: Lateral collateral ligament (LCL), Medial collateral ligament (MCL), Anterior cruciate ligament (ACL) and posterior cruciate ligament (PCL), patellar tendon (PT) and the quadriceps muscles.

3.1.1 The femur (thigh bone)

The femur is the most proximal (closest to the body) bone of the leg in vertebrates; its main role is enabling walking or jumping. The femur is the longest and the strongest bone in the human body which extends from the hip to the knee. The femur articulates on the tibia via the articular cartilages.

3.1.2 The tibia and fibula

The tibia bone is larger and stronger than the femur bone. It is considered the second largest bone in the body. The fibula is a smaller and thinner bone attached to the tibia. Both bones connects the knee with the ankle bones. Both bones contribute to stabilizing the ankle and support lower leg muscles. The tibia is considered the most weight supporting bone.

3.1.3 The patella

The patella is a small bone in front of the femur and articulates with it. It rests between the femur and the tibia. It is also known as the knee cap. The patella protects the knee and connects the quadriceps muscles to the tibia.

3.1.4 The cartilage

The cartilage is a thin, smooth, slippery tissue surface that protects the bone and makes certain that the joint surfaces can slide easily over each other without causing bone damage. Cartilage ensures supple knee movement. There are two types of joint cartilage in the knee: fibrous cartilage (the meniscus) and hyaline cartilage. Hyaline cartilage covers the surface along which the joints move. Cartilage will wear over the years and has a very limited capacity for self-restoration.

3.1.5 The menisci

The menisci are crescent in shape, anchored outwards and inwards on the tibial plateau. They surround the femoral condyles and guide it through it. Menisci are specialized fibro cartilaginous structures that play a crucial role in the maintenance of knee stability, load distribution, joint lubrication, and shock absorption. They have a semicircular shape with a wedge-shaped cross-section that adapts the curvature of the femoral condyles to the flatter tibial plateau. The tibial surface of the meniscus is flat while the femoral surface is convex. Their shape increases the tibial plateau contact area, thereby decreasing the contact stresses significantly in the knee. The meniscus sits between these cartilaginous surfaces of the bones (femur and tibia). It distributes the weight evenly in the joints.

The meniscus also provides stability between the femur and tibial plateau. The semicircular shape and the meniscal attachments help keep the femoral chondyles in the correct location by providing resistance. This aids the other ligaments in the stability of the joint by reducing motion. The movement of each meniscus is restricted by the ligamentous anterior and posterior horns connecting the meniscus substance to the tibial plateau. The meniscus also serves as a limited shock absorbing medium and aids in lubrication of the joint. These functions come from the composition of the meniscus and the ability of the tissue to allow fluid to flow through the extra-cellular matrix. The smooth surface of the meniscus in the presence of the synovial fluid is nearly frictionless, allowing unrestricted motion in the knee. Permeability of the tissue allows fluid to leave during compression, reducing the hydrostatic pressure within the matrix. This mechanism allows the meniscus to be a natural shock absorber. The medial meniscus rests on the medial tibial plateau. The medial tibial plateau is the upper end of the bone making up the inner part of the knee. The lateral meniscus serves the same purpose and is located on the outside of the knee. The menisci help to distribute body weight across the knee joint. Without the meniscus present, the weight of the body would be unevenly applied to the bones in the legs (the femur and tibia). This uneven weight distribution would cause increased wear and tear on the cartilage covering the bones, leading to early damage of these areas. The presence of the menisci cartilage is necessary for a healthy knee.

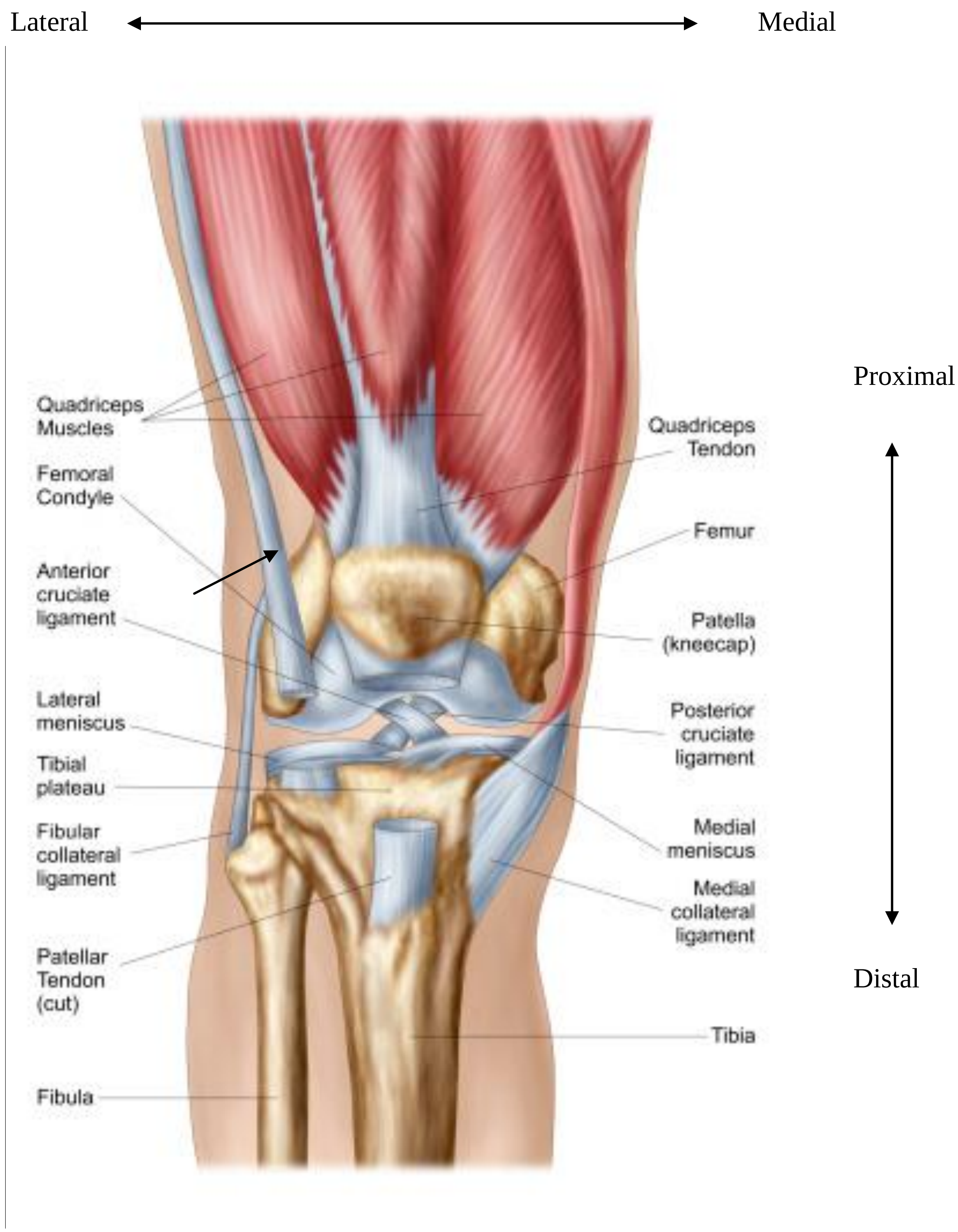

Figure 3.1: Right knee anatomy showing quadriceps muscles
Adapted from Anatomy of human knee joint
www.gettyimages.se/detail/illustration/anatomy-of-human-knee-joint-royaltyfria-illustrationer/188058334.com

3.1.6 Ligaments

The ligaments surrounding the knee joint offer stability by limiting movements and, together with menisci protect the articular capsule. In addition to stabilizing the joint, their inner (medial) and outer (lateral) sides prevent the femur and the tibial plateau from bending outward or inward under normal conditions. The anterior and posterior cruciate ligaments provide additional stabilization so that the tibial plateau is also anchored in place to prevent it from slipping too far to the front or back. There are four major sets of ligaments in the knee joint. These can be categorized into two groups: Intracapsular and Extracapsular.

3.1.6.1 Intracapsular

As mentioned above, the knee is stabilized and anchored in place by a pair of cruciate ligaments. They are divided into two types:

- ***The anterior cruciate ligament (ACL)***

The anterior cruciate ligament is one of the four main ligaments of the knee, it is composed of dense connective tissues that connect the distal femur and the proximal tibia [45]. The ACL originates on the medial surface of the lateral femoral condyle and inserts into the central tibial plateau [45] These attachments allow the ACL to resist anterior translation and medial rotation of the tibia, in relation to the femur. The ACL is critically important because it prevents the femur from being pushed posteriorly (backwards) relative to the tibia. It is often torn during twisting or bending of the knee.

- ***The posterior cruciate ligament (PCL)***

The PCL is a very strong ligament, much stronger than the ACL. This strength relates to its large cross-sectional area. The PCL is the primary restraint to tibial posterior draw. PCL have different patterns of tightening and slacking as a result of knee flexion (bending) or extension (straightening) [46].

The PCL gets its name by attaching to the posterior portion of the tibia. The PCL stabilizes the femur and the tibia during movement. It originates from the lateral edge of the medial femoral condyle then stretches, at a posterior and lateral angle, toward the posterior of the tibia. The PCL consists of two functional bundles, anterolateral and posteromedial which exhibits different tensioning patterns through the arc of the knee flexion [47].

The function of the PCL is to prevent the femur from sliding off the anterior edge of the tibia and to prevent the tibia from displacing posterior to the femur. Similar to the anterior cruciate ligament, the

PCL connects the femur to the tibia. Injury to this ligament is uncommon.. Common causes of injuries are direct hits to the flexed knee, hyper-flexion or hyper-extension [48].

3.1.6.2 Extracapsular

- ***The patellar ligament* (The patellar tendon)**

The patellar tendon attaches the bottom of the kneecap to the top of the tibia. The patellar tendon ligament is strong and flat and connects the two bones together. This strong ligament helps give the patella its mechanical leverage and also functions as a cap for the condyles of the femur. The patellar tendon is of high clinical significance as it can be used in the repair of other ligaments, like ACL [49].

- ***The medial collateral ligament (MCL)***

The medial collateral ligament is on the medial (inner) side of the knee joint. It stretches from the medial epicondyle of the femur to the medial tibial condyle. It resists forces that would push the knee medially. It protects the medial side of the knee from being bent open by a stress applied to the lateral side of the knee (a valgus force).

- **The lateral collateral ligament (LCL)**

The lateral collateral ligament runs along the outside of the knee. It connects the femur to the fibula. It specifically stretches from the lateral epicondyle of the femur to the head of fibula. It is separate from both the joint capsule and the lateral meniscus. It protects the lateral side from an inside bending force (a varus force).

3.1.7 Quadriceps muscle

Quadriceps muscle consists of three main bundles, the rectus femoris, the vastus lateralis and the vastus medialis.They originate from the top of the femur and attach to the front of the tibia. The primary role of the quadriceps is to extend and straighten the leg outwards. Weakened quadriceps can have negative effects on leg posture and the correct movement and positioning of the knee.

3.2 Biomechanics

Mechanically, the knee is considered as a biological organ that acts like a motion transmission coupler (connector between two moving parts to relay the motion). The ligaments of the knee, then, play the role of the communicator for motion transmission between the femur and the tibia. The articular cartilages and menisci are considered as the support bearings, which allow a contact without friction between the thigh bone (femur) and the tibia on the one hand and the tibia and the fibula on the other. This biological system has six degrees of freedom in space: three translations and three rotations as shown in Figure 3.2.

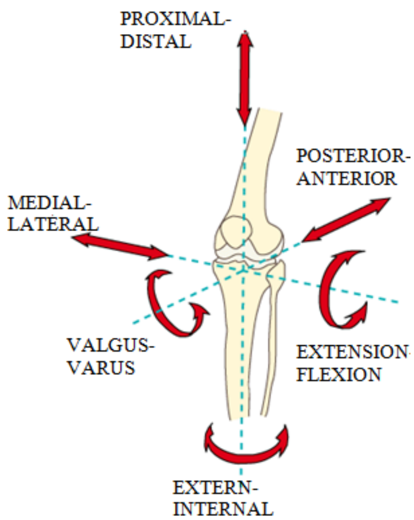

Figure 3.2: Knee joint anatomical axes showing its 6 degrees of freedom [50]

\

CHAPTER 4

OBJECTIVES AND FINITE ELEMENT METHOD

4.1 Objectives

The degree of complexity of the proposed model is that it includes both the tibio-femoral and patello-femoral joints in addition to the quadriceps muscles. The main objectives of this thesis are to create a 3D model from MRI images and validate a tibio-femoral and patello-femoral joints finite element model and to predict various forces on knee cartilages, ligaments and tendons. This complex model will be used to simulate and test the following scenarios:

1) The impact of unilateral and total meniscectomy on various knee components and compare them to menisci intact condition to determine the worst condition.

2) The impact from a jump landing on various knee parts and determining the region of injury at each part. Based on results, we will recommend better landing techniques to reduce joint injury.

Modeling the full knee joint and conducting simulations under large quadriceps forces increases the sophistication of the model. However, it is our objective to make this significant contribution to the field in an effort to better understand the full image of the knee biomechanics as close as possible to a real situation.

The presented 3D finite element model of the knee joint is developed based on converting 3D image data obtained from medical imaging and magnetic resonance imaging (MRI) into numerical meshes suitable for finite element analysis. The goal of this research study is to increase our knowledge with regards to meniscectomy procedures and determine the most impacting scenario on the knee function, also the injury zones due to jump impact on the knee joint.

4.1.1 Three specific aims will be addressed in this research study

1) Development of knee joint model:

- This is to construct a preliminary model is constructed based on medical images (MRI), using Mimics software and SolidWorks software.
- In the second stage, the preliminary model is exported to SolidWorks in order to convert it to computer aided design CAD format that enables Abaqus (a finite element software) to assign properties in addition to smoothing the model parts' surface for better meshing.
- In the third stage, a final model is obtained by assigning material properties to various assembled knee parts, apply meshing and boundary conditions that mimics the biological behaviour.

2) Validating the developed model kinetically and kinematically. Another validation testing was conducted to compare ACL forces during flexion with experimental results in the literature.

3) Using the obtained model to proceed to finite element analysis of the knee for the simulation of two applications that were not investigated in previous literature:

1. Meniscectomy investigation

(a) Impact of total meniscectomy on tibial plateau, femoral cartilage and cruciate ligament forces in passive knee flexion. At this stage only the tibio-femoral joint is considered since it is passive knee flexion which means the quadriceps muscle and the patello-femoral joint have no effect.
(b) The effect of unilateral meniscectomy versus the total meniscectomy on posterior cruciate ligament forces under femoral anterior displacement at full extension.

2. Landing from a jump investigation

In order to specify the region at which injury occurs (at this stage the full knee joint model incorporating both tibio-femoral and patello-femoral joints in addition to the quadriceps muscles is analyzed). New results will be obtained for various knee parts that were not studied in previous literature (parameters of interest include contact forces and contact area in all knee cartilages and menisci in addition to patella tendon forces).

4.2 The Finite Element Method

The Finite Element method is a numerical technique used to obtain the approximate solution of boundary value problems. It divides a complex problem into simpler parts (finite elements) so we can have simple equations that represent them. Then these simpler equations are assembled into a larger system of equations that represents the original complex problem. Dividing a bigger problem into simpler parts have many advantages, among which accurate representation of complex geometries, safe simulation of hard or potentially dangerous load conditions in addition to fast calculation time for most applications.

As it is an approximation, it involves assumptions and simplifications. The goal is to approximate the exact solution as closely as possible to a real life situation. Quality and accuracy of the solution depends on many factors like specifying the correct element type, mesh size, analysis type, type of behaviour expected and the accuracy of the results in comparison with previous literature.

4.2.1 Basic 3 Steps in the finite element method

- **Pre-processing:** involves importing the preliminary model created via Mimics and smoothed via SolidWorks to Abaqus and defining the material properties, element type, loading and meshing technique.

- **Solution:** Solves the system of equations for unknown variables.

- **Post processing:** Results of the parameters of interest are presented.

4.2.2 Sources of analytical error in finite element analysis

- **Idealization errors:** element type and geometry or applied boundary conditions.

- **Discretization errors:** due to approximation and mesh density.

- **Manipulation errors:** computer errors due to round-off.

4.2.3 Error diagnosis in finite element static and quasi-static analysis

- **Singularity**: This means there are more unknowns than equations and the matrix is singular (no inverse for it and solution can not be obtained). Constraints have to be applied to obtain a solution.

- **Rigid body motion**: This means the model is not sufficiently constrained. The model must be sufficiently constrained so the system of equations can be solved.

4.2.4 Potential benefit of using finite element model in the study

- Laboratory tests simulating real-life situations in order to understand the injury mechanism could be extremely dangerous for subjects and may risk their injury

- Previous experimental studies published never performed the test at the threshold of the injury level.

- Finite Element model allows the researcher to get as close to a real-life situation as possible without compromising human safety.

- The model, once constructed can simulate even more scenarios and can be useful for other research applications.

- Finite Element models provides a guideline for experimental testing, they represent a virtual testing to narrow down physical test matrix.

- Finite element analysis can solve extremely complex problems in a timely manner which may be very hard and time consuming to achieve by hand calculations.

CHAPTER 5

METHODS

5.1 Solid Model Development

5.1.1 MRI Segmenting Using Mimics

Mimics (Materialise's Interactive Medical Image Control System) is Materialise's software for processing medical images and creating 3D models. Mimics uses 2D cross-sectional medical images such as from computed tomography (CT) and magnetic resonance imaging (MRI) to construct 3D models, which can then be directly linked to rapid prototyping, computer aided design CAD, surgical simulation and advanced engineering analysis.

To process data in Mimics, a set of stacked 2D cross-sectional images is first imported. These 2D images come from medical scanning equipment. Once the stacked images are imported, they can be viewed and edited using the various tools available in Mimics. The Mimics screen is broken up into four main views: coronal, axial, sagital, and 3D as shown in Figure 5.1. Engineers can think of coronal as a front view, axial as a top down view, and sagittal as a right view. The axial view comes from the imported stack of images. To obtain the coronal and sagittal views, Mimics transposes the axial images into their respective positions. The 3D pane is where 3D models are visualized. This enables a more comprehensive 3D feel of the 2D data.

The key to converting anatomical data from images to 3D models is a process called segmentation. During segmentation the part of interest is indicated in the sliced image data. This information is then used to recreate a 3D model from the segmented structures. To describe the outer surface of the 3D model, Mimics uses the stereo-lithography STL format. STL is considered ideal format as it can accurately describe very complex geometries (anatomical geometries) [51]. This is necessary, since anatomical data is in general very intricate. Mimics translate CT and MRI scanner data into full 3D models, finite element meshes or rapid prototyping data STL in a short period of time. Since the models constructed via Mimics accurately match patient data, the models allow engineers to test and investigate many scenarios on actual patient data prior to testing them on actual patients. Mimics is used to simulate surgical procedures, to prepare data for finite element analysis and to export medical data to CAD. Mimics provides a bridge from CT and/or MRI data to 3D computer models, optimized surface meshes, finite element analysis, physical 3D models, device and implant design and traditional CAD.

In the present study, MRI images in the form of 2D data were obtained from a healthy adult male volunteer for the right knee. Digital images were separated at intervals of 4 mm in the sagittal, coronal and axial planes with the knee at 0^{o} degree flexion as shown in Figure 5.2. Although the MRI image is widely spaced, meniscii and cartilages were captured via Mimics and missing frames were interpolated using SolidWorks as will be detailed later. Mimics was used to segment the MRIs and construct 3D geometry of each individual bone and soft tissue structure (menisci and cartilages). The bones included in the model are the distal head of the femur, the proximal head of the tibia and fibula, and the patella. The final model also includes the four main stabilizing ligaments of the knee: the posterior cruciate ligament (PCL), the anterior cruciate ligament (ACL), the medial collateral ligament (MCL) and the lateral collateral ligament (LCL) in addition to the patellar tendon and quadriceps muscles. The medical images of the knee joint obtained from the MRI scans consist of gray-scale information. Based on the gray values within these images, the preliminary model is constructed. A gray value is a number associated with an image pixel defining the shade (white, gray, or black) of the pixel. There is a direct association between material density of the scanned object and the gray value assigned to each pixel in the image data. By grouping together similar gray values, the image data was segmented and the initial model was created as detailed later. This type of segmentation is called thresholding. Thresholding is process used by Mimics to select pixels that fall within a user defined region of the gray scale.

The user can create a mask to identify boundaries or regions of interest. After thresholding, masks are edited to create boundaries around the anatomical structure. Mimics then stacks the masks drawn on the 2D images and develops the 3D surface model as shown in Figure 5.2 and Figure 5.3. For the cruciate and collateral ligaments, they were only identified on a single MRI, thus there was an insufficient number of masks to produce a 3D geometry. The ligaments' insertion points were identified and marked on the bones, then these ligaments were manually constructed using spring elements as detailed later.

The software has predefined quality options for the quality of the 3D model created. Low and medium quality have short calculation times but may produce a more approximated model. By selecting the option of High quality, it can give a smoother, more accurate model, which was used in constructing our model. The highest quality setting was selected to calculate the 3D model as shown in Figure 5.3 and Figure 5.4. Noise produced in the data due to segmentation resulted in uneven and rough surfaces on the model. This was smoothed out using Mimics tools; a smoothing factor of 0.9 was selected after several trials. The smoothed 3D model was then surface processed in SolidWorks.

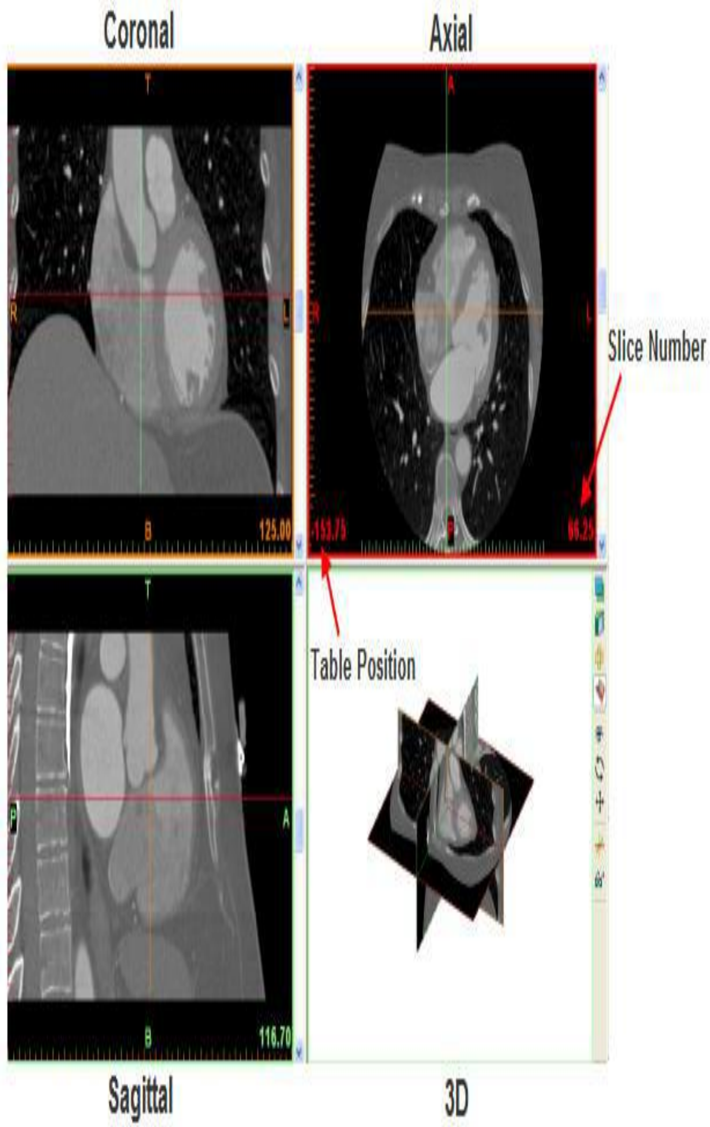

Figure 5.1 Sample screen display of Mimics and slice information

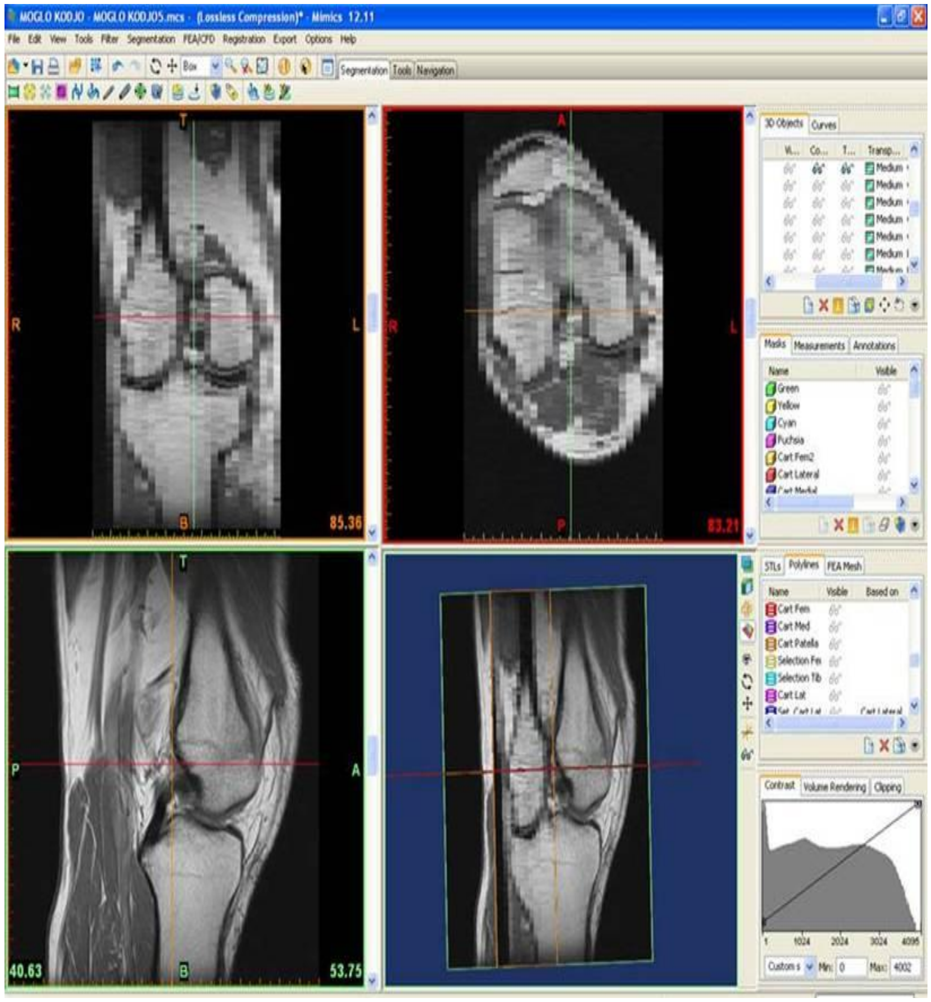

Figure 5.2. MRI of the right knee showing coronal, axial and sagittal planes (before creating coloured threshold masks to separate each part).

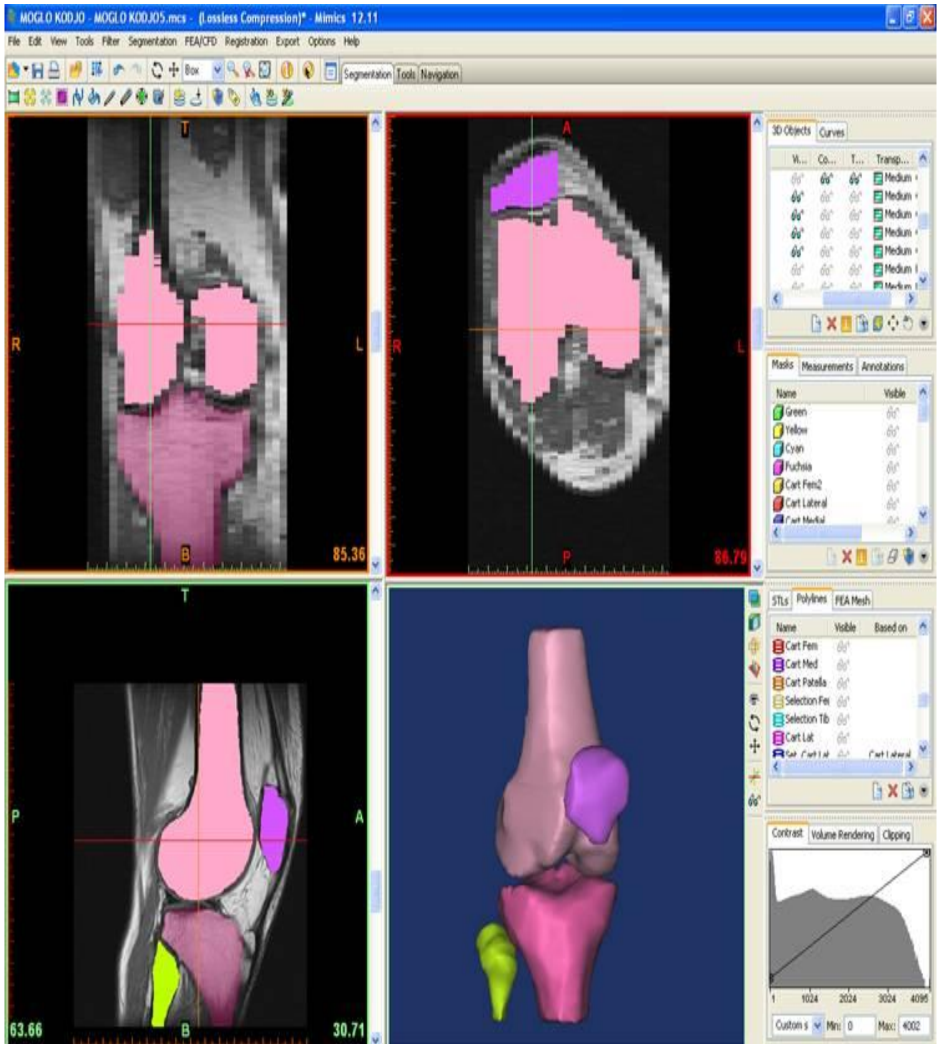

Figure 5.3: Segmentation to extract 3D version of Bones-Mimics-
Fourth image shows 3D colored bones

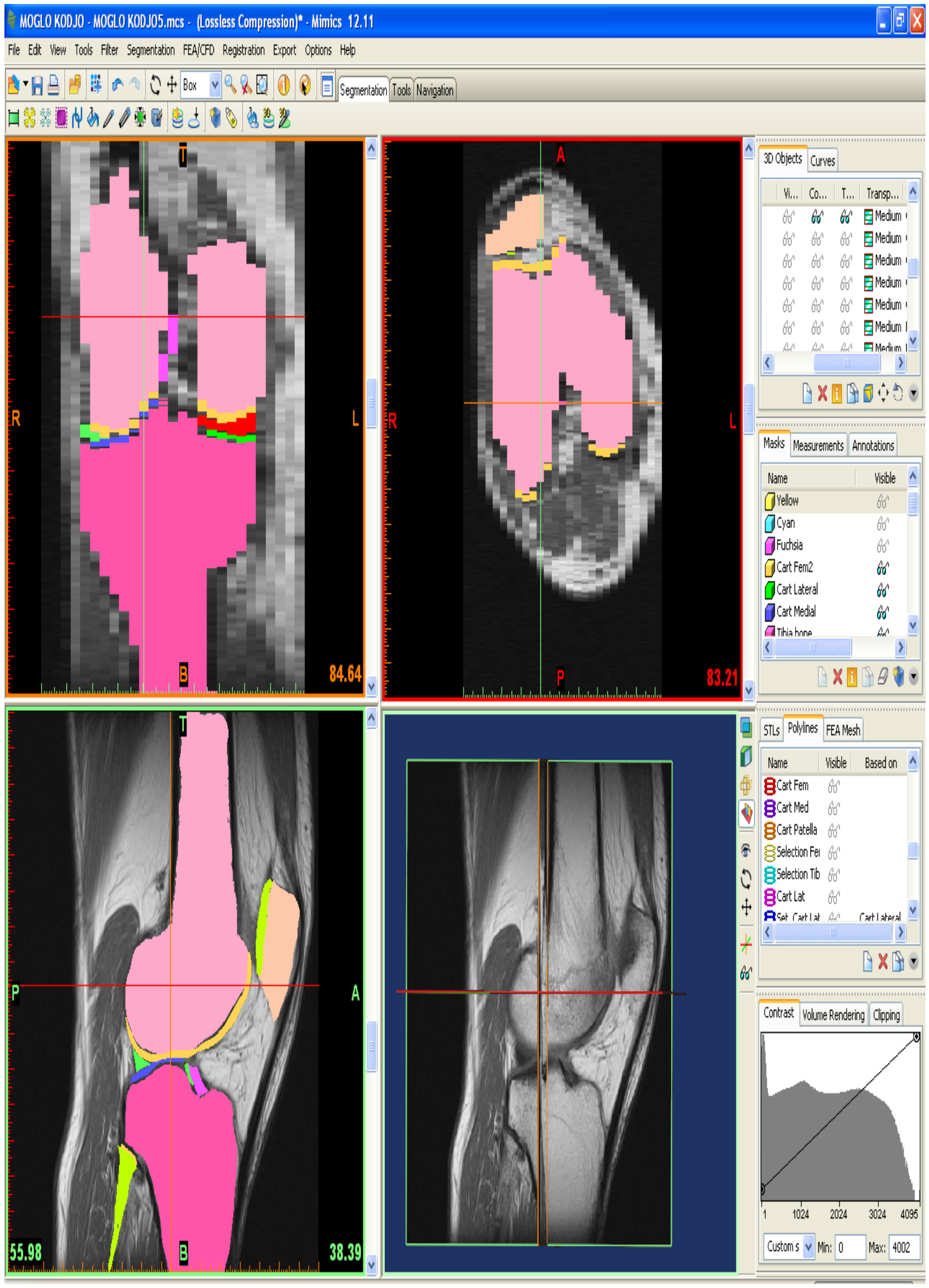

Figure 5.4 Extracting cartilages, and menisci

5.1.2 Surface Processing using SolidWorks

SolidWorks transfers the part into CAD format which makes it easier to control and to assign material properties to different layers or sections independently.

The smoothed 3D model is exported from Mimics as STL files to SolidWorks for surface processing. Another local smoothing is processed to remove any sharp edges. Some parts had missing frames due to spatial resolution in the original MRI image. SolidWorks is used to interpolate missing frames as shown in Figure 5.5. Using SolidWorks, the part that has missing frames is sliced using multiple planes to capture the entire part contour as shown in Figure 5.5.

For the present model, missing frames existed in femoral cartilage and the lateral meniscus. Multiple planes were used (8 planes for the femoral cartilage and 11 planes for the lateral meniscus) to divide the parts into sections and to interpolate the missing frames. The intersection between these planes and the part results in spline curves that uniquely defines the geometry of this specific frame. Thus the missing frame's spline curve geometry can be interpolated using the information from its previous and following frames. The surface of the bone is used as a guide to ensure the fixed part accurately assemble to the bone contour without overlapping. This interpolation procedure performed in SolidWorks is essential to reconstruct missing frames and take control of the limitation of working with MRI images that are sliced widely and missing frame information. Finally, solid parts were assembled based on their relative positions and a surface inspection was processed to fix any surface errors and trim overlapping regions.

The final model was then converted to a CAD file before transferring it to Abaqus. The importance of converting the model to CAD lies in the complete control it enables the user to manipulate the model and be able to control each part separately (applies specific material property, mesh type or concentrated load). The locations of the ligaments, tendon and muscles insertion sites were identified from the MRI by Mimics then defined and constructed via SolidWorks.

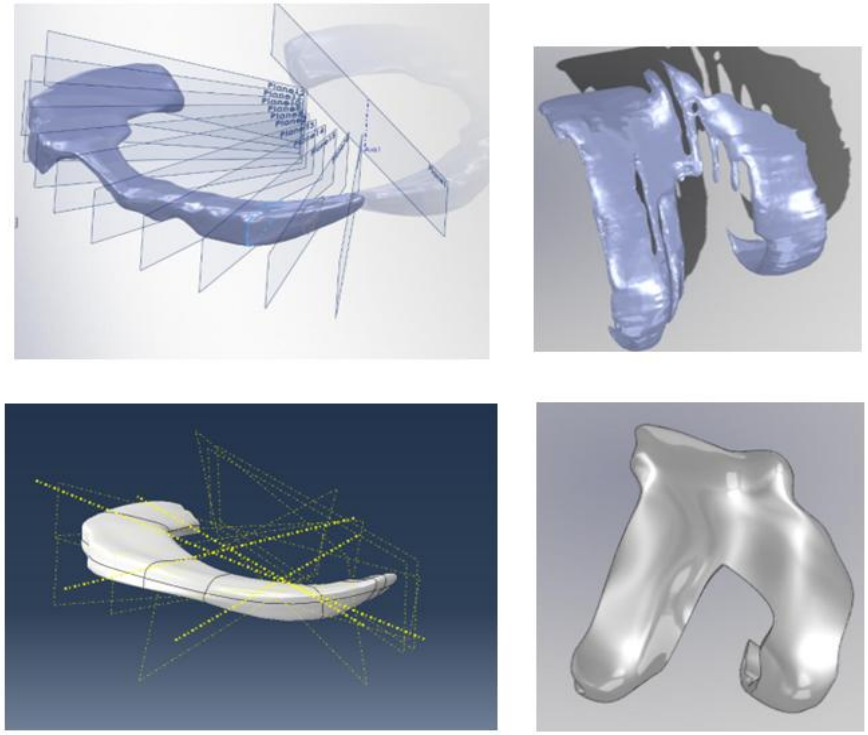

Figure 5.5 Fixing low resolution parts by interpolating missing frames to reconstruct original geometry

5.1.3 Finite Element Mesh Using Abaqus

Abaqus is a highly sophisticated, general purpose finite element program, designed primarily to model the behaviour of solids and structures under externally applied loading. Abaqus includes the following features (advantages):

- Capabilities for both static and dynamic problems
- The ability to model very large shape changes in solids, in both two and three dimensions
- A very extensive element library, including a full set of continuum elements, beam elements, shell and plate elements, among others.
- A sophisticated capability to model contact between solids.
- An advanced material library, including the usual elastic and elastic-plastic solid, models for foams, concrete, soils, piezoelectric materials, and many more.

5.1.3.1 Mesh development of hard biological tissues:

Each bony structure is meshed in Abaqus using free quad elements. Each bone is represented by a primary node (Reference Point RP) as shown in Figure 5.6. These nodes with 6 degrees of freedom control the whole kinematics of each bone as rigid body. All rigid bodies were meshed with free quad-elements shape of element type R3D4 (a 4-node 3D rigid quadrilateral element) as shown in Figure 5.6. This element allows both translation and rotation degrees of freedom. Bony structures were modeled as rigid bodies due to their much greater stiffness compared to cartilages and menisci.

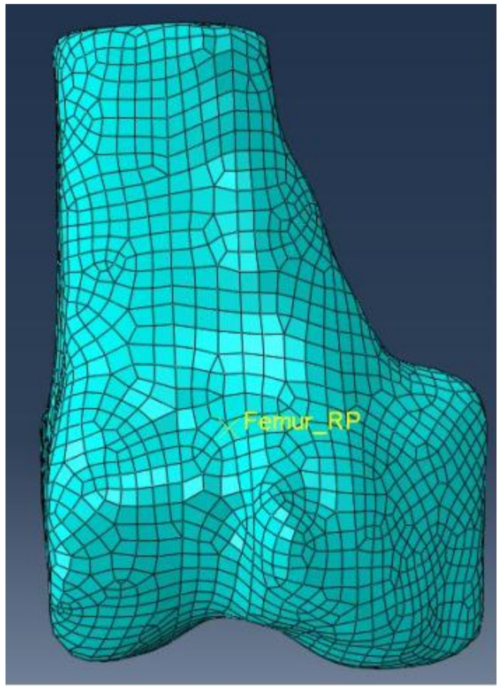

(a)
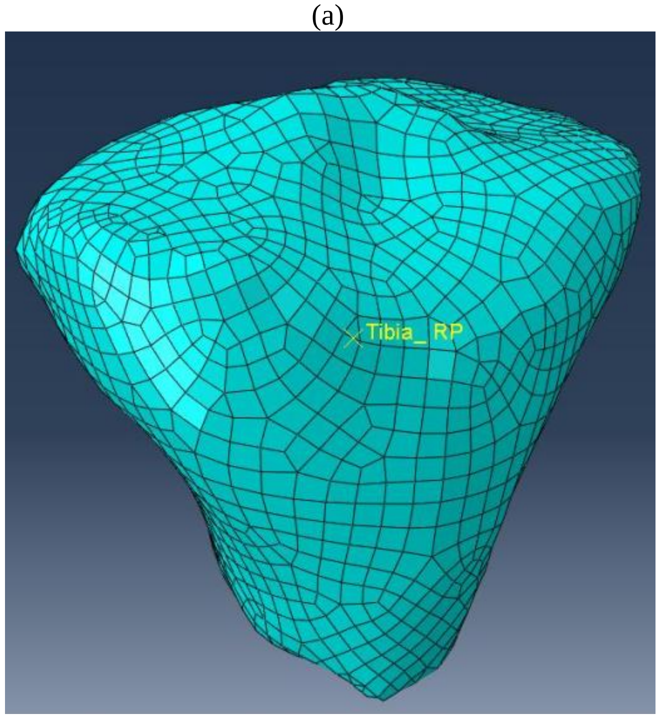

(b)

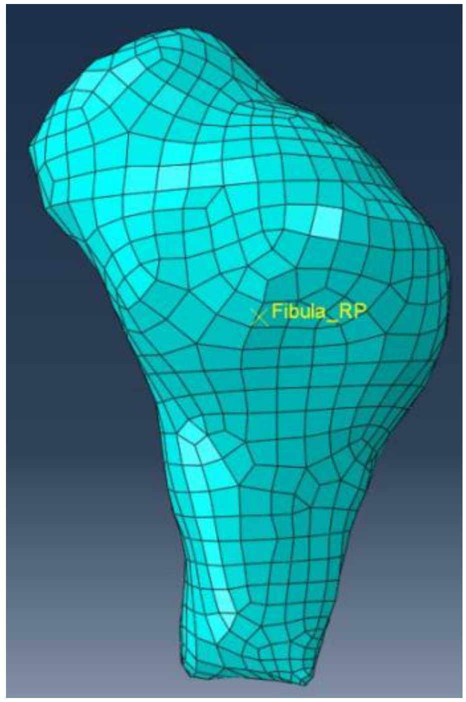

(c)

Figure 5.6 Free quad -meshed (a) femur, (b) tibia and (c) fibula showing reference node

5.1.3.2 Mesh development of soft biological tissues:

Soft tissues (meniscii and cartilages) were meshed using hexahedral elements. Hexahedrals are often preferred as they are flexible solid elements

A challenge was faced while performing the hexahedral-meshing for the soft tissues since their geometry is not extrudable. In order to overcome this, each part is partitioned into several partitions to create virtual four sided blocks within the part and hence allowing the hexahedral-mesh to be swept across the body as shown in Figure 5.7. All these soft tissues were hexahedral-meshed with element type C3D20R, a reduced integration 20 node-quadratic brick element; this element was chosen as it has more nodes than the C3D8R (only has eight nodes) which increases the accuracy of the results as shown in Figure 5.8, Figure 5.9 and Figure 5.10.

The choice of this element type was determined from a convergence study (outlined in Appendix A) plotting the number of nodes for different element types versus stress results produced for each. Element types with low stress values were eliminated as the mesh was not fine enough to produce accurate results. When the stress curve saturates approaching the real solution, the element type with the fewest number of nodes and which produces a near real solution stress value was selected.

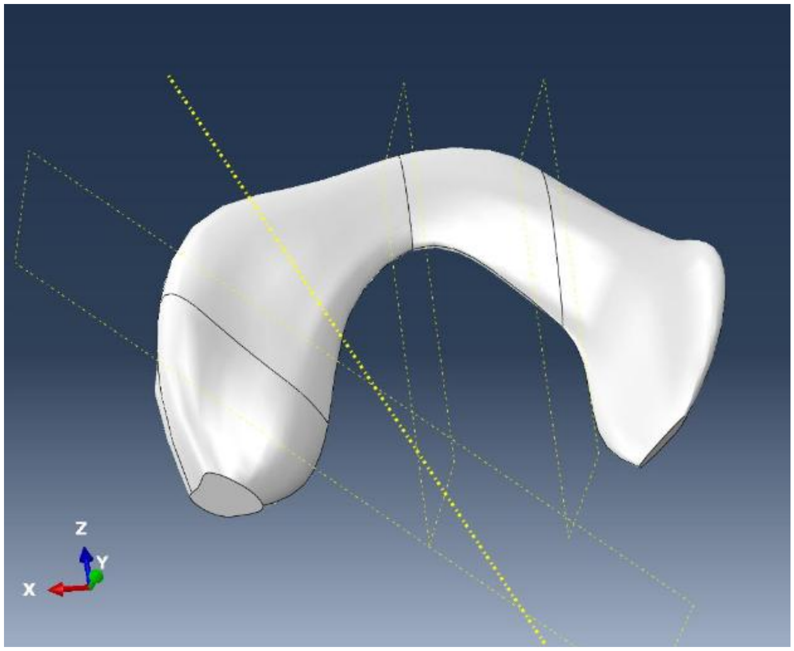

(a)

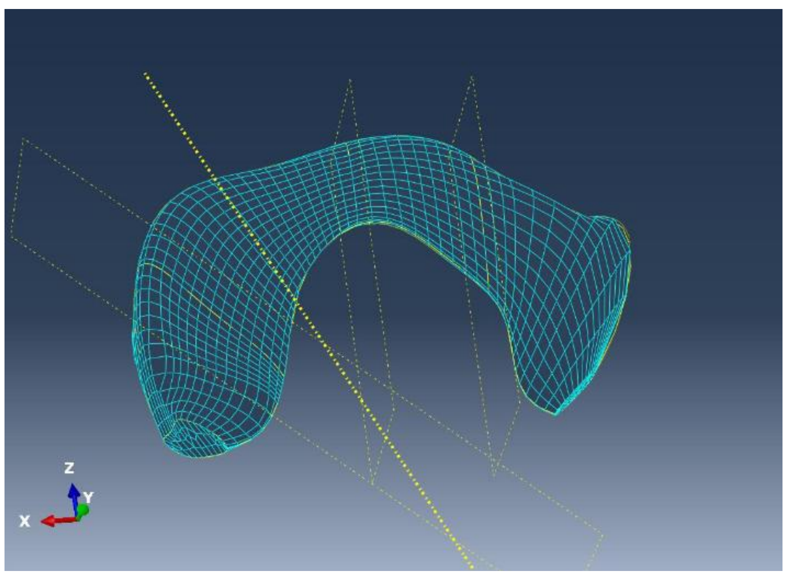

(b)

Figure 5.7: (a) Partitioning the part into four sided sections to prepare for hexahedral-meshing, (b) Menisci hexahedral-meshed

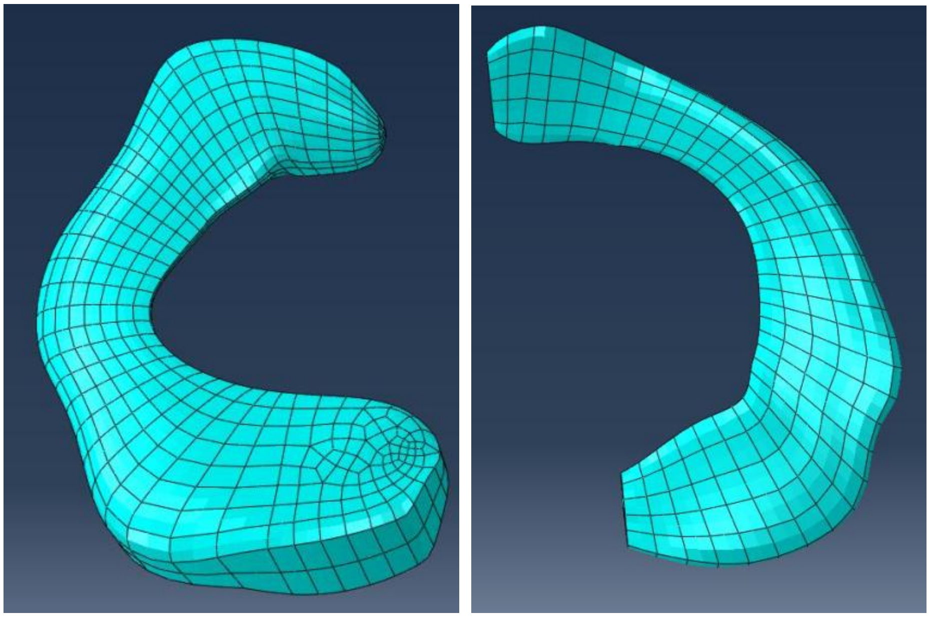

(a) (b)

Figure 5.8 Hexahedral-mesh (a) Medial menisci , (b) Lateral menisci

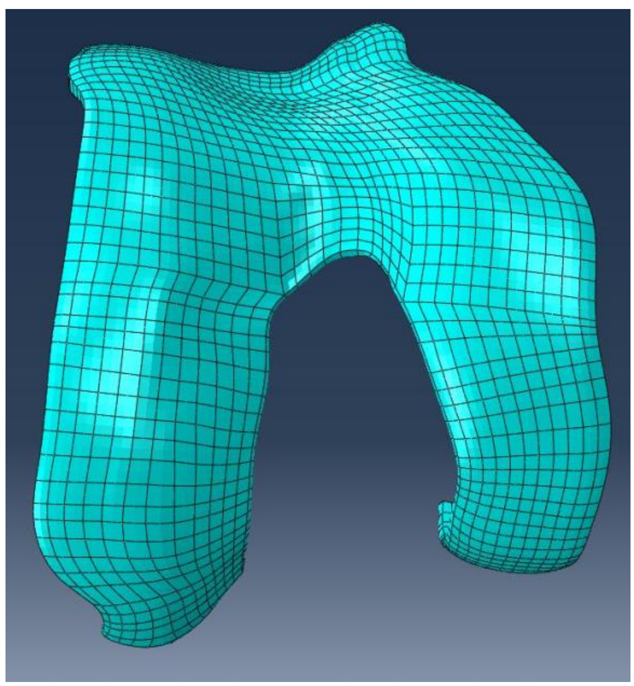

Figure 5.9 Hexahedral-mesh of femoral cartilage

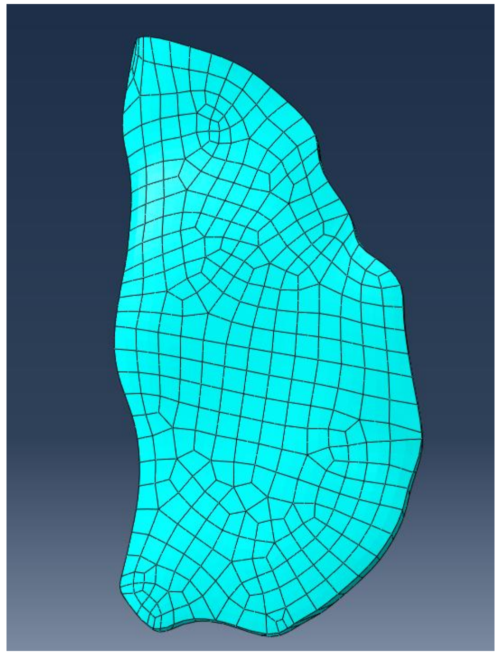

(a)

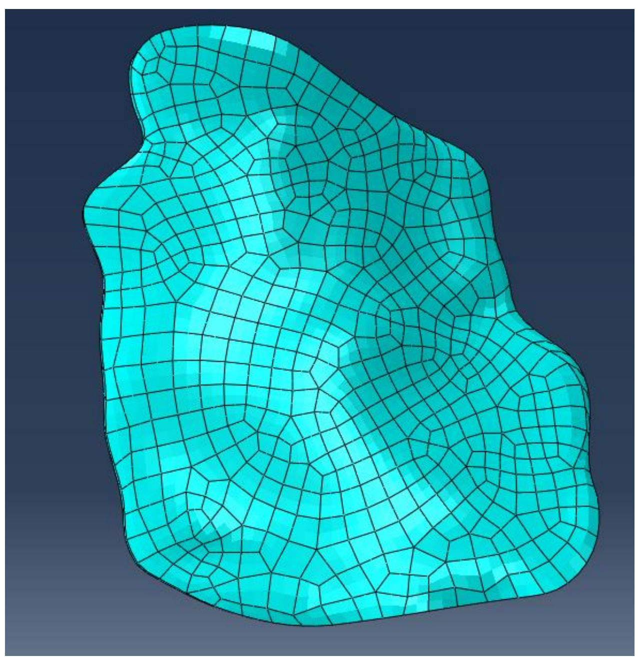

(b)

Figure 5.10 Hexahedral-mesh (a) Medial cartilage , (b) Lateral cartilage

Meshed parts are then assembled as shown in Figure 5.11 which shows a meshed assembly of the completed model with the four ligaments and patellar tendon. Ligaments, tendon and quadriceps muscle modeling are detailed in the following section. Mesh validation was performed via Abaqus to ensure no meshing errors in any of the parts

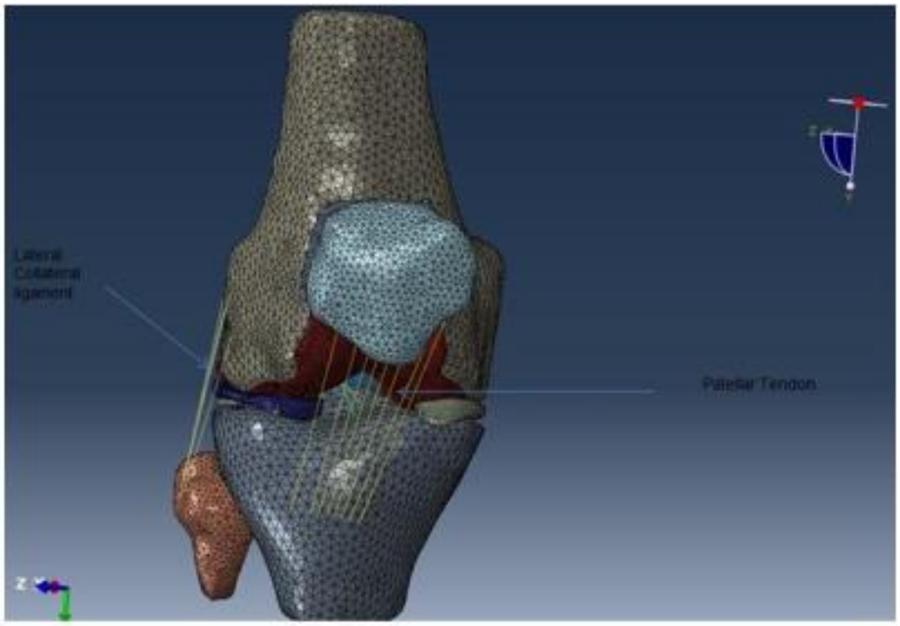
Lateral
Collateral
ligament
Patellar Tendon

(a)

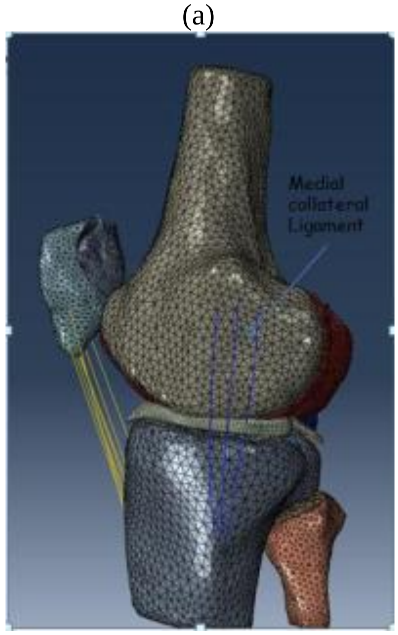
Medial
collateral
Ligament

(b)

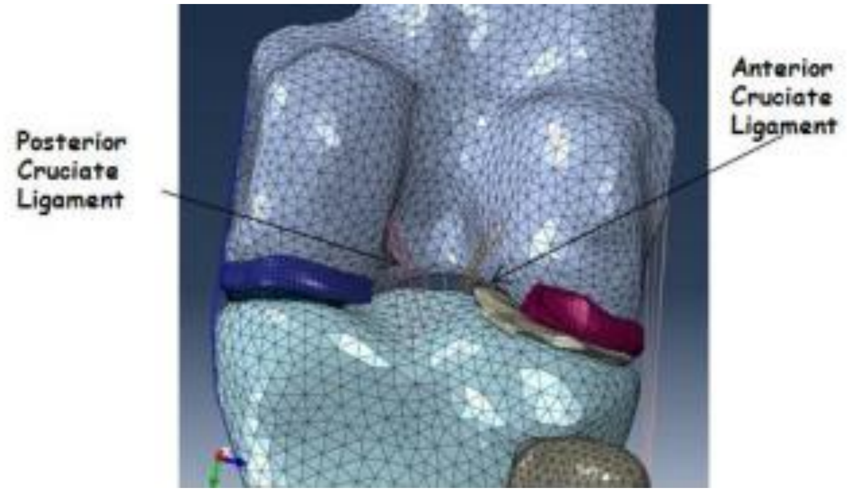

(c)
Figure 5.11 Knee model mesh in Abaqus showing main four ligaments and tendons

5.2 Material Property Assignment

The bony structures were modeled as 3D shell rigid bodies due to their much greater stiffness as compared with joint soft tissues. This is a very common approximation used in finite element analysis and does not affect results, Shirazi et al. [52-53]. It also helps decrease computational time since stresses and deformation are not calculated. 3D shell elements were chosen since they allow loading types (force and moment) and nodal degrees of freedom (translational and rotation), which is needed in this analysis.

The articular cartilage was considered to behave as linear elastic, homogenous and isotropic material with an elasticity modulus of E =5 MPa and Poisson ratio of ν=0.46, Pena et al. [54]. Menisci were also assumed to be linear elastic and isotropic material with elastic modulus of E =59 MPa, Pena et al. [55]. Pena reported this value of elasticity modulus is good enough to predict short term cartilage response, this will be needed in our impact analysis. The poisson ratio of chosen for the Menisci was ν =0.49 as reported by LeRoux and Setton [56].

For modeling the quadriceps muscle, three axial connectors were used to represent three main bundles:

1. Vastus Lateralis (VL).
2. Rectus Femoris-Vastus Intermidus Medialis (RF-VIM).
3. Vastus Medialis Obliqus (VMO).

Quadriceps muscles are modeled as axial non-linear spring connectors to behave as close as possible to the biological behaviour. The proximal and distal ends of the connector elements are assigned kinematic coupling constraint to the femur and patella bone reference node respectively. This constraint restricts the motion of the coupled nodes to the rigid body motion of the single reference node. Three connectors are used to model the muscle and the force value is distributed among them based on the cross-sectional area of each muscle. Loading is distributed according to the ratios of their physiological cross-sectional areas as reported in a previous study by Sakai et al [57] as represented in equation (5.1).

$$VMO : RF : VL = 2 : 3 : 2.5 \tag{5.1}$$

For example, a quadriceps load of 100 N will be distributed on various muscle bundles as follows:
VMO= 26.7N, RF=40N, and VL=33.3N.

Muscle orientations and insertions were adapted from the study of Sakai et al. [57] as shown in Figure 5.12. Sakai et al. was selected as he presented a detailed anatomical model of the quadriceps muscles orientation in his study. While anatomy of various subjects differ, the anatomical model of Sakai is used as an acceptable approximation of the muscle orientation of average male subjects and which was cited in other literature studies.

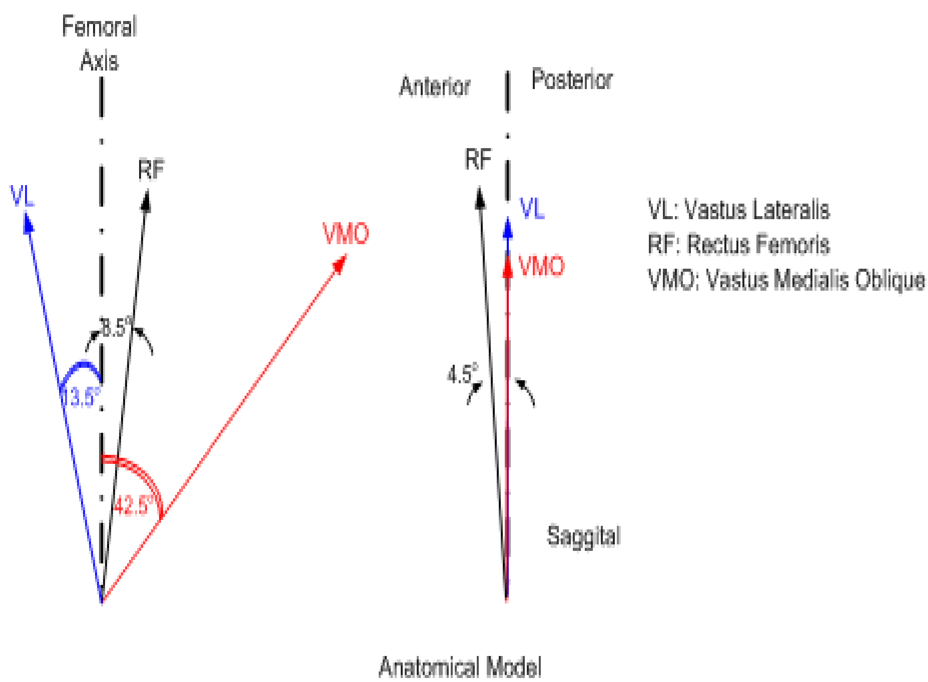

Figure 5.12: Quadriceps muscle orientation adapted from Sakai et al. [57]

When modeling ligaments, the ligament body and its insertion were considered in the model. Ligament bundles were modeled as elastic nonlinear axial springs represented by connectors whose properties follow the stress-strain curves shown in Figure 5.13 and Figure 5.14 for ligaments and patellar tendon, respectively, in order to mimic their exact biological behaviour.

The spring itself is a type of element where the nodes are located at its ends. Springs only resist axial load. Force versus displacement data for each ligament or tendon was extracted from its corresponding stress-strain curves reported in previous study by Mesfar et al. [58] and was fed into the property table of each connector. The cross-sectional area of each ligament, as shown in Table 5.1, was divided equally by the number of connectors used to represent the ligament bundle. Table 5.2 presents a summary of each structure element type, material type and properties.

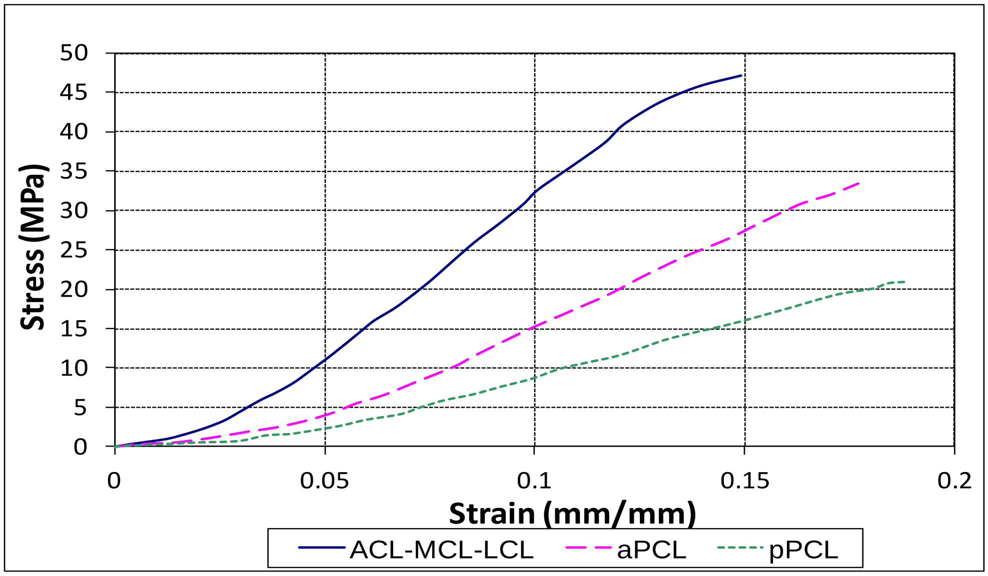

Figure 5.13: Stress-strain curves for knee joint ligaments [58]

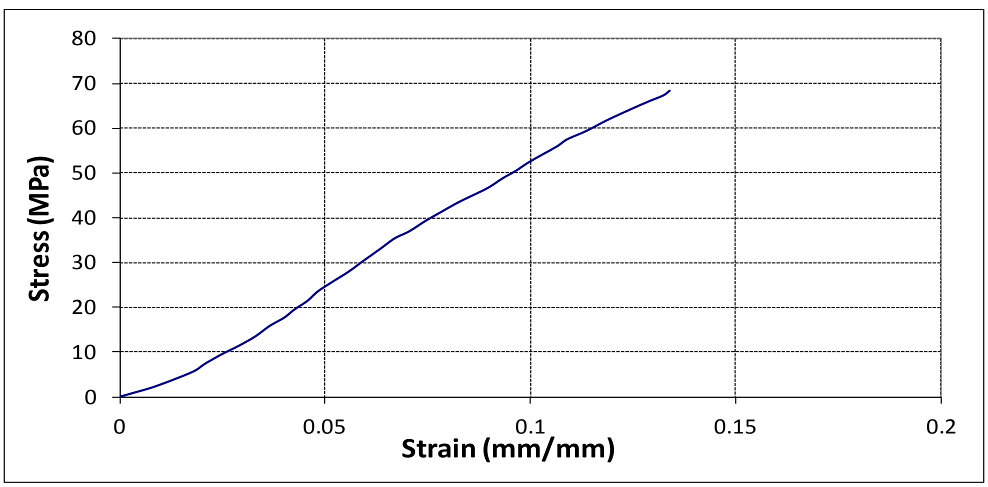

Figure 5.14: Stress-strain curves for knee joint patellar tendon [58]

Table 5.1: Ligaments and Patellar tendon cross-sections [59]

Ligament	**Average cross-sectional area (mm^2)**
ACL	42
PCL	60
LCL	18
MCL	25
PT	99

Table 5.2: Element type, material type and material properties assigned to bones, cartilages and meniscii

Part	**Element Type**	**Material Type**	**Material Properties**
Bone *Tibia, Femur, Fibula and Patella*	Shell	Rigid Body	--
Cartilage *Femoral, Lateral and Medial tibial*	3D Hexahedral C3D20R	Linear Elastic Isotropic	E =5 MPa ν =0.46
Menisci *Medial and Lateral*	3D Hexahedral C3D20R	Linear Elastic Isotropic	E =59 MPa ν =0.49

The final meshed model with the quadriceps muscles, four main ligaments and patellar tendon is shown in Figure 5.15.

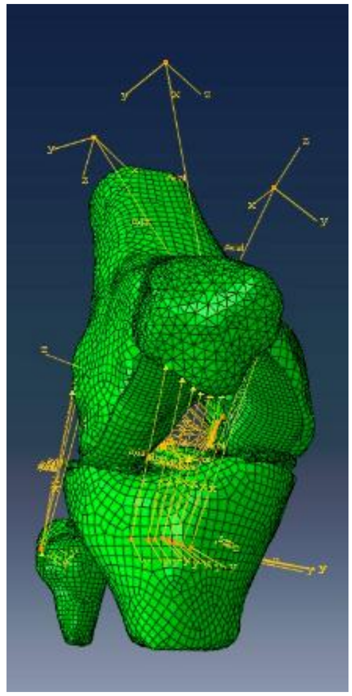

(a)

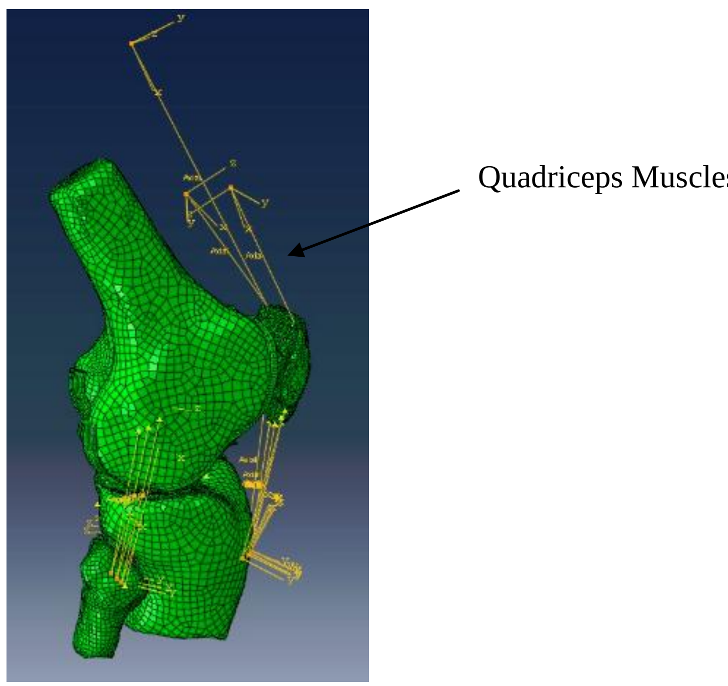

(b)

Figure 5.15: Final model of knee joint with the quadriceps muscles (a) Frontal view, (b) side view

5.3 Contact Interactions, Loads and Boundary Conditions

Hard contact interactions were defined for all the articulations (contact pairs) as frictionless, surface to surface contact between the following surface pairs: the femoral cartilage and each of the superior surfaces of the medial and lateral menisci (2 contact pairs); the femoral cartilage and each of the superior surfaces of the medial and lateral tibial cartilages (2 contact pairs); the medial tibial cartilage and the distal surface of the medial menisci (1 contact pair); the lateral tibial cartilage and the distal surface of the lateral menisci (1 contact pair) and finally the femoral cartilage and the patellar cartilage (1 contact pair).

Frictionless contact was chosen to mimic the biological behaviour of the synovial fluid in the articular joint. The seven contact pair zones identified above are shown in Figure 5.16.

Boundary conditions were defined to mimic the anatomical orientation and biological behaviour as follows: each of the horns of the menisci (both ends) was attached to the tibia plateau through coupling with the tibia reference node so that there is no relative motion between them which represents reality as the meniscii horns are attached to the tibial plateau so that no relative motion between them. The lower surfaces of both the medial and lateral cartilages were also attached to the tibia through coupling with the tibia reference node. The internal surface of the femoral cartilage was attached to the femur through coupling it with the femur reference node, this represents reality as biologically they both move as one part (no relative motion between them).

The same procedure was done for the patella bone-patellar cartilage and the fibula bone-fibular cartilage. Ligaments were attached to the nearby bone at their proximal and distal ends through coupling with the reference node of the corresponding nearby bone in which they are inserted. The motion of each bone was controlled by the six degrees of freedom of its reference node. Both tibia and fibula bones are fixed and load is applied to the femur. Figures showing contact interactions and boundary conditions are illustrated in Appendix B.

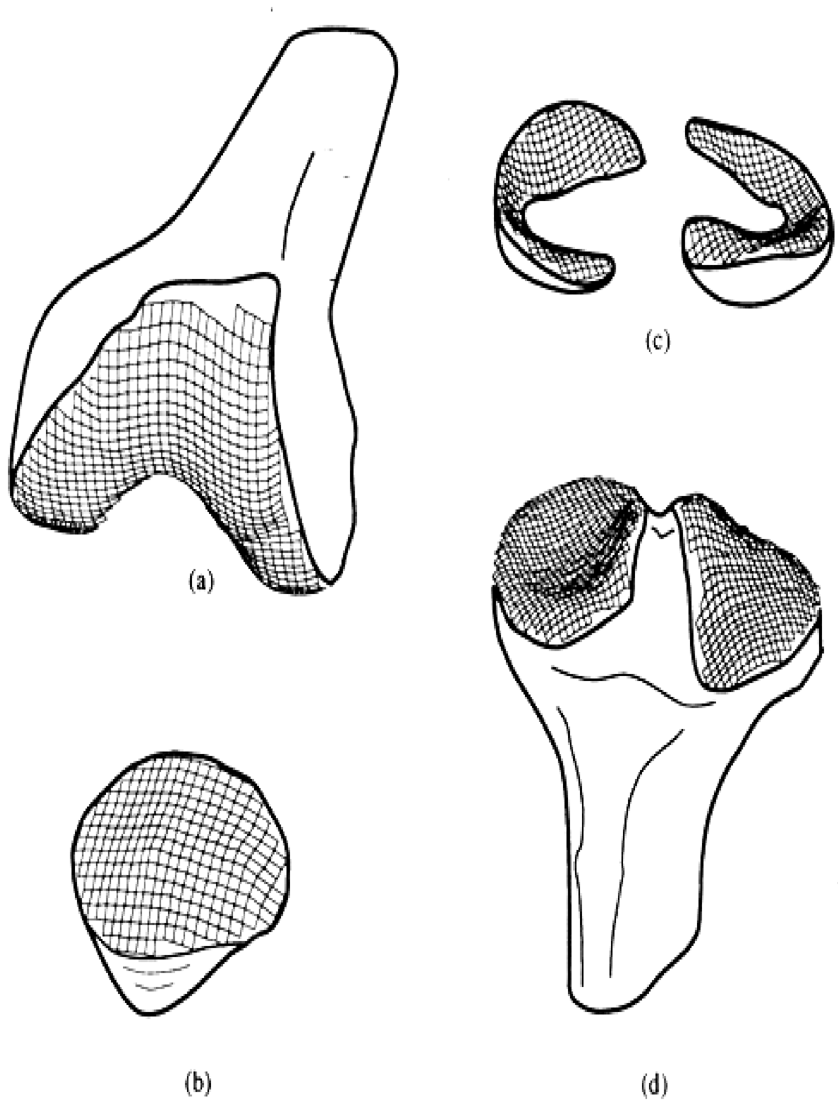

Figure 5.16: Contact pair zones defined in the model –(a) Femur (b) Patella (c) Menisci (d) Tibia and tibial cartilages.[50]

5.4 Model Validation:

5.4.1 Equilibrium Check:

To check for equilibrium in the present model, the vertical reaction force at the tibia was calculated versus the total vertical contact force corresponding to it. The boundary conditions were to fix the tibia and fibula, apply a small flexion (rotational displacement) of 5 degrees, then compute the R_F (reaction force at the tibia) and compare it with the corresponding vertical contact forces resulting on the tibial plateau as shown in the Figure 5.17. R_F was found to be 54 N and the total vertical contact and cruciate ligament forces were found to be 53 N, which is acceptable for computational approximation.

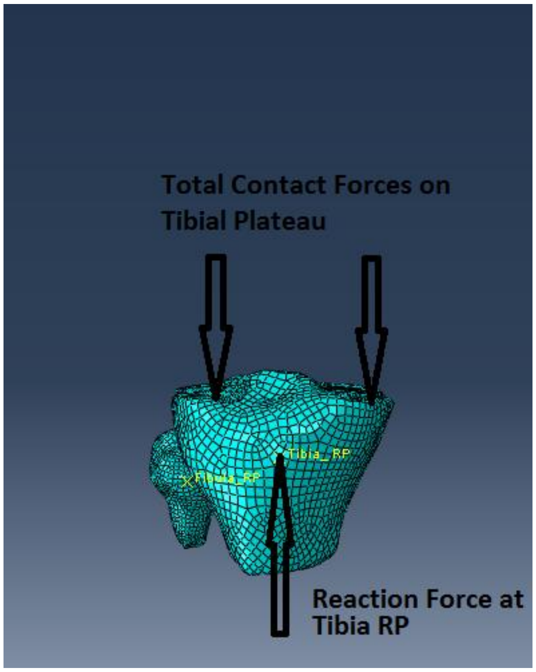

Figure 5.17 Equilibrium check

5.4.2 Kinetic Validation:

The model was validated kinetically against previous studies under the same boundary conditions as reported in Im et al. [60] where the subject was lying supine (on his back) and performed cycles of different flexion angles while keeping muscle force constant. Some studies reported results till 50 degrees knee flexion and others extended to 80 degrees flexion as shown in Figure 5.18. The ratio between the patella tendon forces (FPT) and the quadriceps forces (FQ) versus the knee flexion angle was plotted as shown in Figure 5.18. The results of the present model lie within range with those reported by previous studies Im et al. [60] , Van Eijden et al. [24], Ward et al. [61] and Yamaguchi et al. [25]. This validation proves that the patella tendon joint does not act as a perfect pulley as the ratio between the patella tendon forces and the quadriceps forces during flexion was not equal to 1.

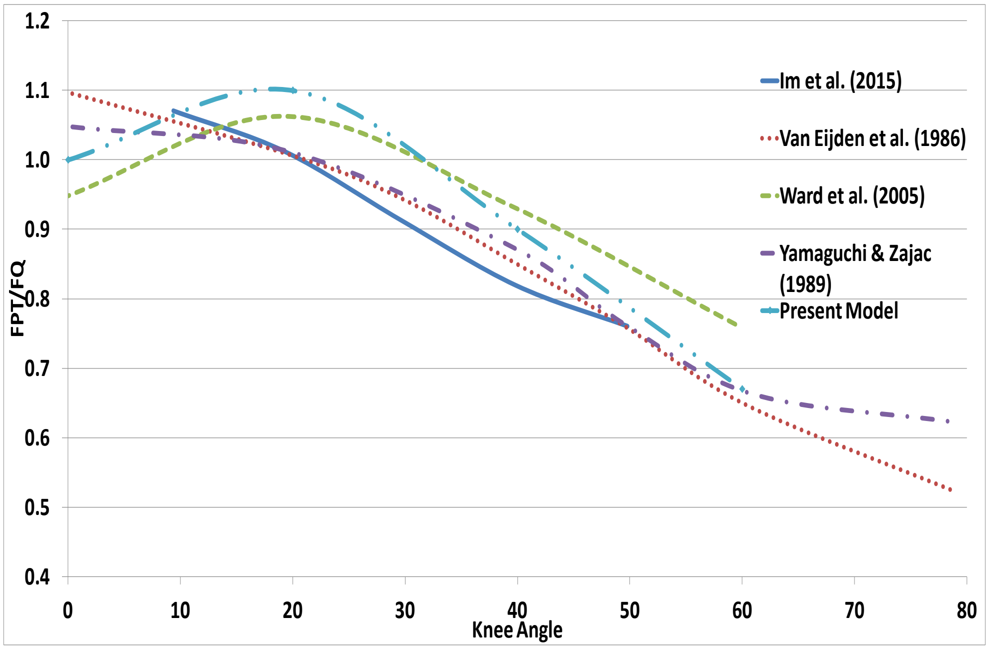

Figure 5.18 Kinetic validation of presented model versus previous studies

5.4.3 Kinematic Validation:

To validate the model kinematically, the presented model is tested under the same boundary conditions reported in the experimental study conducted by Markolf et al. [62]. A 500N axial load was applied with femoral flexion of 50 degrees; the valgus rotation (a condition in which a bone or joint is twisted outward from the center of the body) of the tibia with respect to the femur was computed as shown in Figure 5.19.

The present model resulted in the same valgus angle as the experimental study at flexion angle of 30 degrees and was within acceptable range in further flexion. Internal-external rotation was found to be 8 degrees at 50 degrees flexion angle.

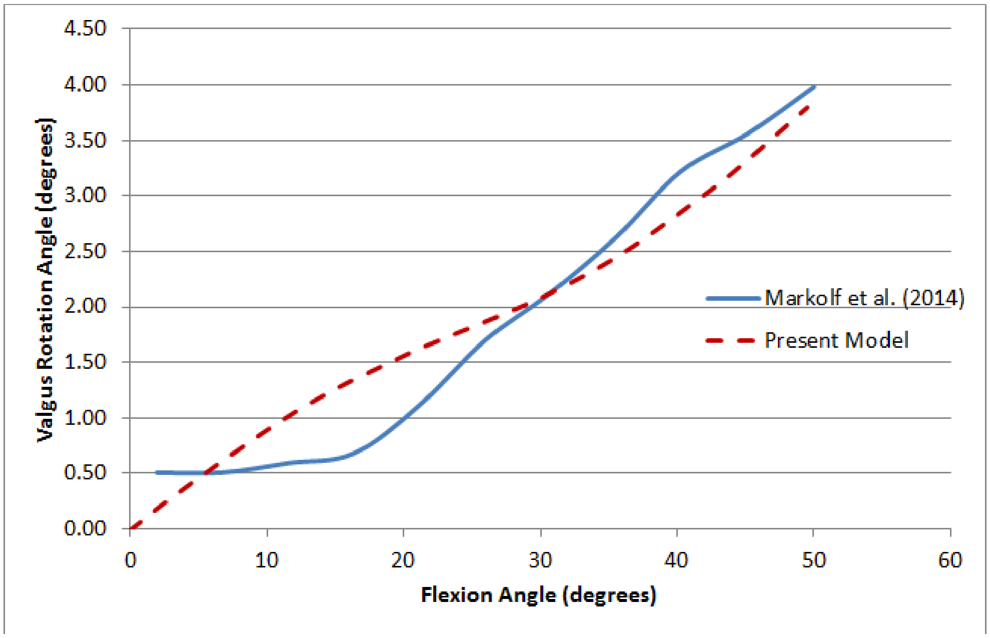

Figure 5.19 Kinematic validation of present model

5.4.4 Additional Validation:

Another validation is conducted using a vertical compression loading. This analysis applies excessive loading that tends to flex the knee without applying real flexion.

At the initial step, the system is stabilized (constrained) by creating the following boundary conditions: tibia and fibula were fixed by applying a boundary condition directly to their reference nodes. The boundary conditions for the loading scenario used to simulate passive knee flexion for the femur and tibia were set as shown in Table 5.3.

Table 5.3: Simulation scenario for the compressive loading

Femur						
	U_X	**U_Y**	**U_Z**	**UR_X**	**UR_Y**	**UR_Z**
Load step1	free	550N (compression)	free	free	free	0
Tibia						
Load step1	Fixed	Fixed	Fixed	Fixed	Fixed	Fixed

It is noticed that the tibia is fixed in all degrees of freedom while the femur is free.Vertical compression loading is applied as a concentrated force to the femur reference node in the proximal-distal direction. Contact pressure on the menisci were recorded and results were compared with data from previous studies under the same conditions of loading.

Contact pressure results are shown in Figure 5.20. A Maximum contact pressure of 1.3 MPa resulted at the horns and the middle of the internal circumference of the lateral menisci due to the contact zones with the femoral condoyle. Maximum contact pressure resulted on the medial menisci was 0.9 MPa under a loading of 550 N, which agrees in values with G. Papaioannou et al. [63]. The highest contact pressure took place in the posterior region of the medial meniscus, with a maximum of 0.9 MPa, and in the horns and middle section of the inner circumference of the lateral meniscus, with 1.19 and 1.3 MPa respectively.

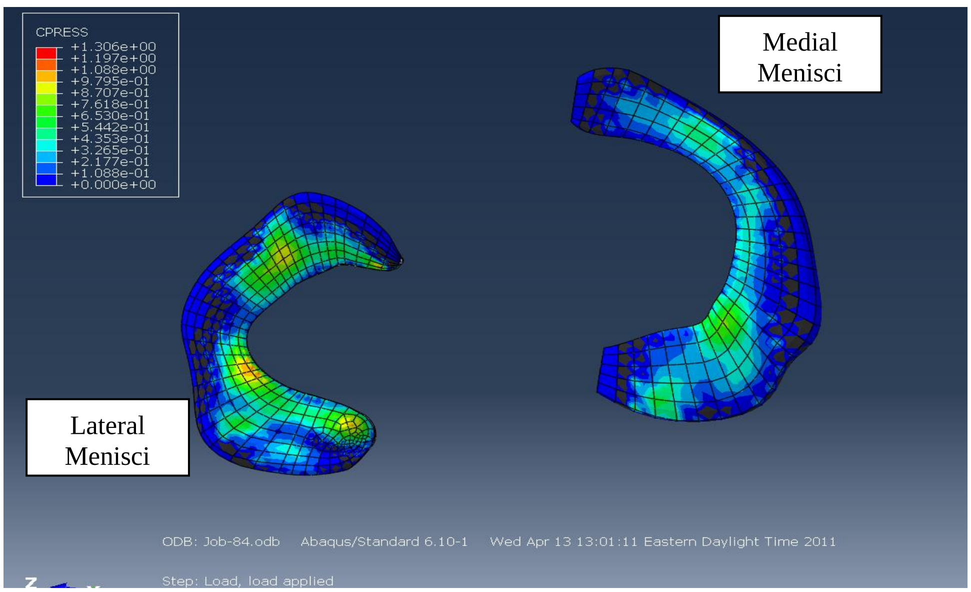

Figure 5.20 Contact pressure resulted on menisci due to loading of 550 N

Another model validation testing was conducted by plotting the results of ACL forces versus flexion angle in passive knee flexion, as compared to similar results in previous studies, Mesfar et al. [58] and Markolf et al. [64] under the same boundary conditions. The model results had the same curve trend and values within range with the compared studies as shown in Figure 5.22. MCL and LCL values for the present model were 25 N and 150 N respectively.

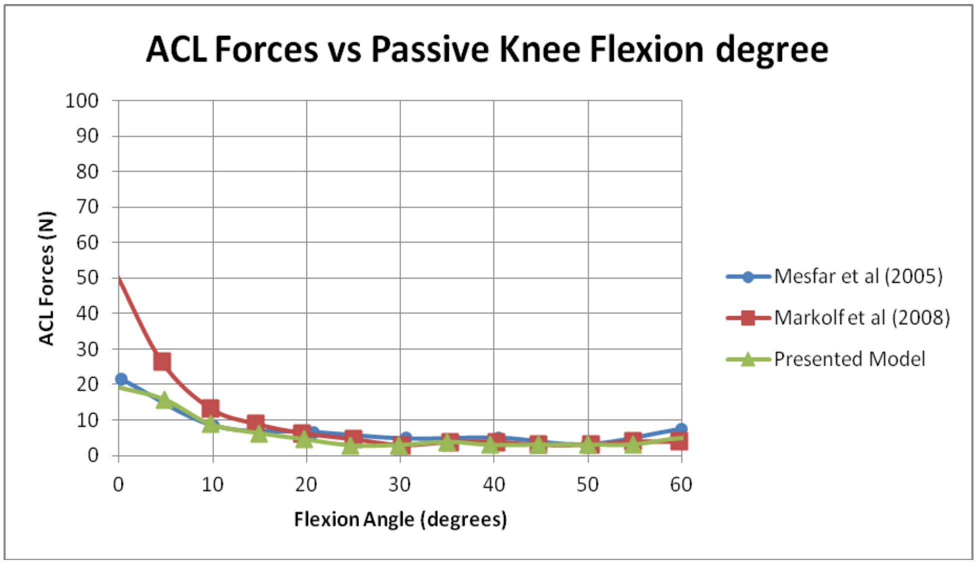

Figure 5.21: ACL forces versus flexion angle in Passive knee flexion for presented model versus previous studies.

CHAPTER 6

APPLICATIONS AND RESULTS

6.1 Meniscectomy Application

6.1.1 Investigating unilateral and total meniscectomy

Cartilage degeneration in the knee joint is mainly caused by elevated stress levels and high contact forces resulting from total meniscectomy procedures [65]. Statistics show that among patients who had meniscectomy surgeries, 14.1% of men and 22.8% of women over 45 years show symptoms of osteoarthritis (OA) the treatment of which costs around $185.5 billion annually in the USA [66].

PCL injuries account for about 20% of knee ligament injuries; however, the PCL is seldom discussed because these injuries are often left undiagnosed. Knee joint cruciate ligaments become more vulnerable to injury specifically when the meniscii are torn or removed. The loss of part or the entire meniscus severely alters the mechanics of the knee function, leading to overloading on the knee ligaments and cartilage degeneration which leads to osteoarthritis [67]. When a meniscus is injured, the standard protocol is complete removal. Partial or total meniscectomy associated with anterior cruciate ligament (ACL) failure was studied excessively [67]; however very little research was directed to meniscectomy associated with posterior cruciate ligaments (PCL).

Most authors agree that total meniscectomy leads to progressive articular wear after a few years due to the fact that the global biomechanics of the knee is altered and articular instability increases resulting in a progressive and degenerative arthrosic pathology [68]. Several researchers have reported higher stress and decrease in shock absorbing capability after total meniscectomy [69]. Few studies used the finite element method to study meniscectomy; Pena used the finite element method to investigate the effect of meniscal tears and meniscectomies under a compressive load at zero flexion (full extension position) [40]. The presented study uses the finite element approach to investigate meniscectomies not only at full extension, but also flexion. The objective of this study is to use the constructed 3D knee model to provide full comparison between menisci intact and menisctomized knee joint of the same subject in order to evaluate the impact taking place on patients undergoing unilateral and full meniscectomy procedures. Two sub-applications studies were conducted under the main meniscectomy application:

1) Impact of the total meniscectomy
2) Impact of partial or unilateral meniscectomy on knee function during passive flexion.

6.1.1.1 Impact of total meniscectomy on tibial plateau, femoral cartilage and PCL forces in passive knee flexion

Boundary conditions and loading were set to fix the tibia and fibula in all degrees of freedom. Flexion was applied as rotational displacement to the femur in the range of 0-60 degrees in both the menisci intact and meniscectomy cases. To simulate meniscetomy, both medial and lateral menisci parts were removed from the model and contact pair was defined directly between the femoral cartilage and both tibial cartilages.

Frictionless contact was defined for all articulations. Frictionless contact was chosen to mimic the biological behaviour of the synovial fluid in the joint that aims to reduce friction between the articular cartilage of the knee joint during movement. For this study, in the case of intact menisci (control) six contact pair interactions were defined: femoral cartilage and both menisci (2 pairs), femoral cartilage and both tibial cartilages (2 pairs), both menisci and tibial cartilages (2 pairs). In the total meniscectomy case, only two contact pair interactions were defined between the femoral cartilage and both tibial cartilages (2 pairs), as menisci were removed. Parameters of interest are Von Mises (VM) stress, axial contact force, contact pressure and cruciate ligament forces, In this study, the same passive knee joint model was analyzed under two boundary condition scenarios: (1) Menisci intact (control), and (2) total meniscectomy during passive knee flexion (0-60 degrees) using quasi static analysis.

6.1.1.2: Unilateral versus total menisectomy effect on PCL forces under anterior femoral drawer in full knee extension

In this testing, four different cases were studied and compared:

(1) Unilateral lateral meniscectomy,

(2) Unilateral medial meniscectomy,

(3) Total meniscectomy,

(4) Menisci intact.

Similar to previous application, frictionless hard contact was defined for all articulations. For this study, in the case of unilateral meniscectomy, only four contact pairs were defined: femoral cartilage and the considered meniscus (1 pair), femoral cartilage and both tibial cartilages (2 pairs), the considered meniscus and its corresponding tibial cartilage (1 pairs). In the case of total meniscectomy, only two contact pair interactions were defined between the femoral cartilage and both tibial cartilages (2 pairs). Boundary conditions and loading were set to fix the tibia and fibula in all D.O.F. A femoral anterior displacement of 3 mm was applied to the four cases detailed above under free and fixed femoral axial rotation (internal-external rotations). The parameter of interest was PCL forces.

6.2 Meniscectomy Results

6.2.1 Impact of total meniscectomy on tibial plateau, femoral cartilage and PCL forces in passive knee flexion

Higher load-bearing was noticed on the medial compartment in an intact model while it shifted to the lateral compartment in the meniscectomy model due to the internal axial rotation of the femur (screw-home meschanism). Results of axial contact forces on the tibial plateau in the menisci intact versus meniscectomy cases are shown in Table 6.1. Menisci Intact results are divided to two zones, uncovered (tibial cartilage part not covered by menisci) and covered (tibial cartilage part covered by menisci) as illustrated in Figure 6.1. In the case of meniscectomy, predicted results showed a substantial increase in the axial contact forces on the tibial plateau compared with the menisci intact case, as shown in Figure 6.2. Higher Von Mises stress level values on the femoral cartilage resulted in the case of meniscectomy. At 15 degrees of flexion, a minor difference was noted; however the stress level started to increase at 30, 45 and 60 degrees flexion as shown in Table 4 and Figures 6.3-6.5. For cruciate ligaments forces, in the case of meniscectomy, much higher PCL forces were noted compared to the menisci intact case Figure 6.6. Model-predicted results of PCL forces in meniscectomy were 42N, 144N, 250N and 424N at 15, 30, 45 and 60 degrees flexion, respectively. ACL forces in the case of the meniscectomy were almost twice the value of the intact model between 0 and 15 degrees flexion; then both values matched at higher flexion angles as shown in Figure 6.7. ACL values were zero at higher flexion angle as the ACL is completely slack at deeper flexions when there is no anterior tibial displacement. Maximum contact pressure values on femoral cartilage were 3, 3.3 and 5.2 MPa (intact) versus 4.6, 6.4 and 7 MPa (meniscectomy) at 30, 45 and 60 degrees flexion, respectively.

Table 6.1: Contact forces on tibial plateau and VM stress on femoral cartilage versus flexion angle in both cases mensci intact and meniscectomy

Flexion (Deg)	Axial contact force on medial cartilage (N)			Axial contact force on lateral cartilage (N)			VM stress on femoral cartilage (MPa)	
	Uncovered	Covered	Meniscectomy	Uncovered	Covered	Meniscectomy	Intact	Meniscectomy
30	313	100	915	190	95	1360	1.2	1.7
45	365	80	1040	140	60	1588	1.3	2.2
60	278	40	800	100	45	1618	1.68	2.2

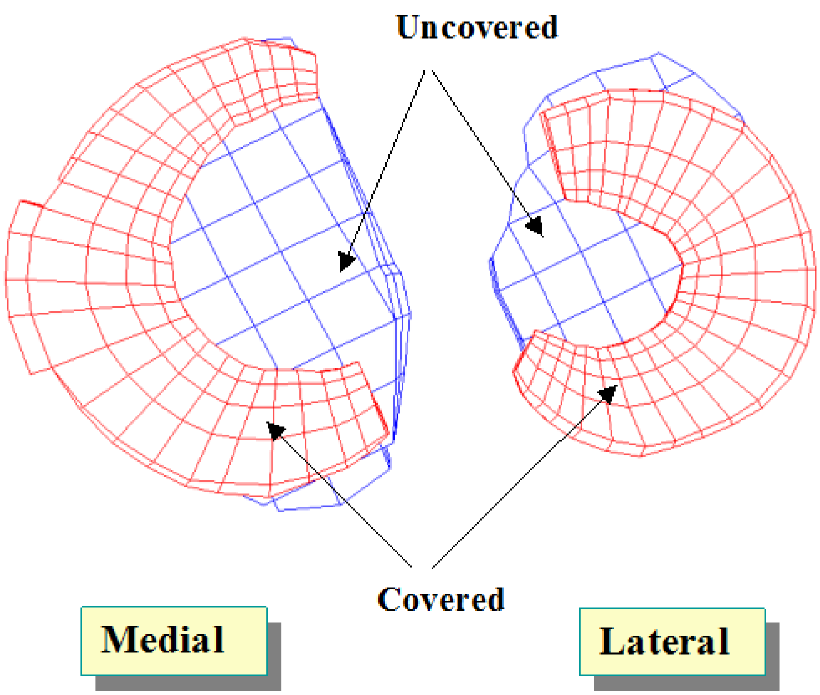

Figure 6.1 Covered and uncovered zones [32]

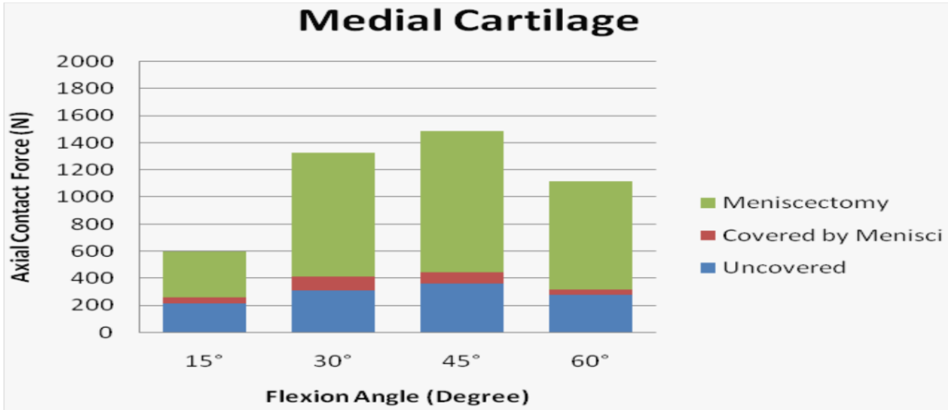

(a)

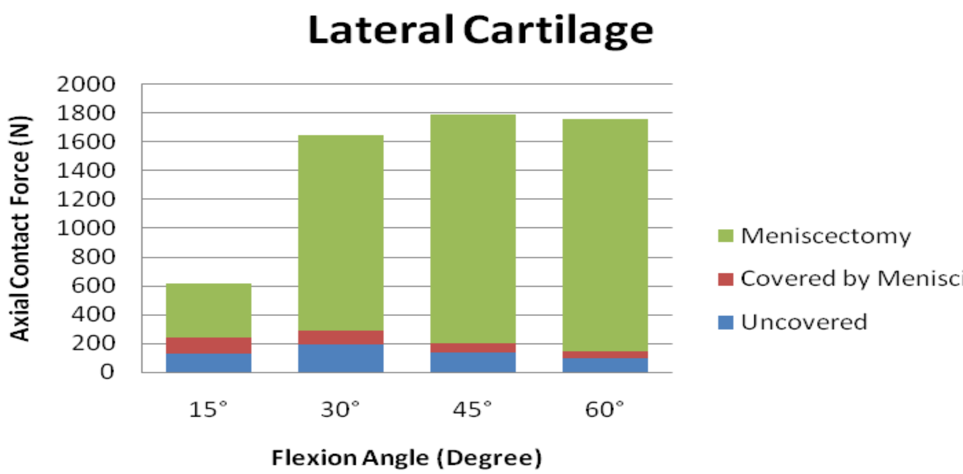

(b)

Figure 6.2 Axial contact forces on tibial plateau for (a) medial cartilage and (b) lateral cartilage versus flexion angle

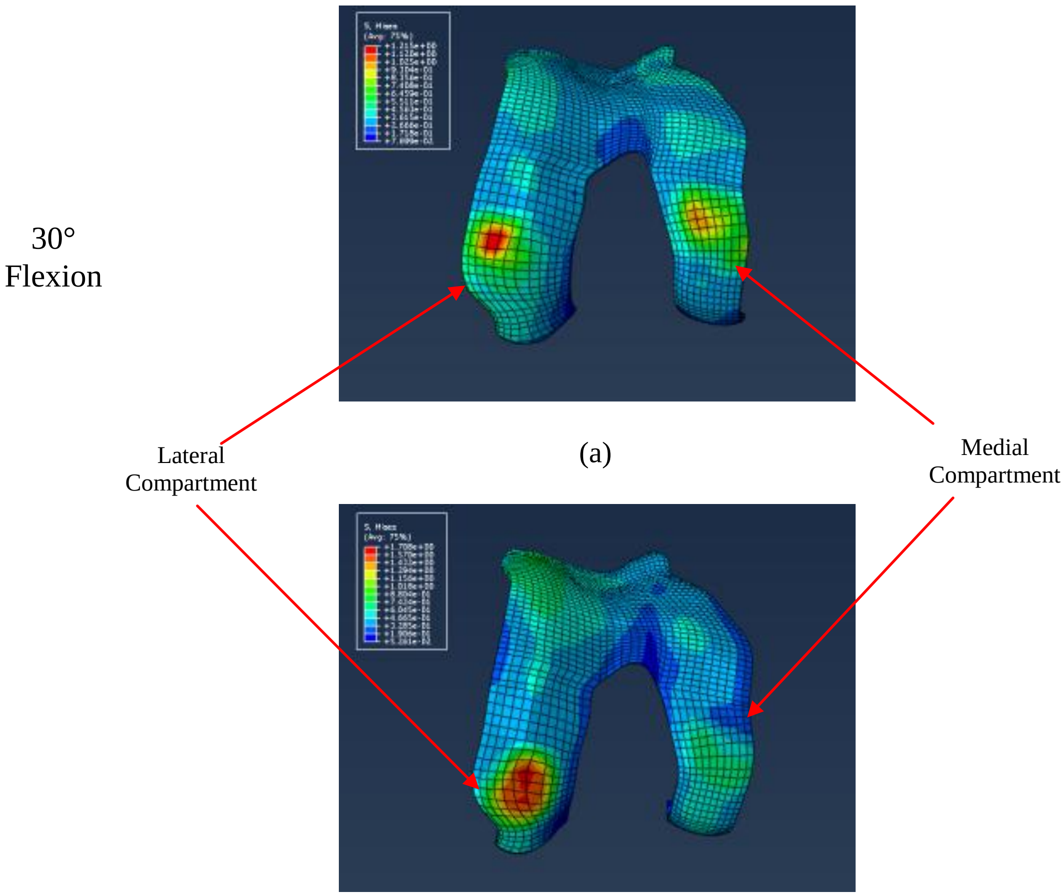

(b)

Figure 6.3 VM stress (MPa) on lateral (L), medial (M) femoral-compartments vs flexion angle (a) menisci intact. (b) meniscectomy for 30^{o} flexion.

45°
Flexion

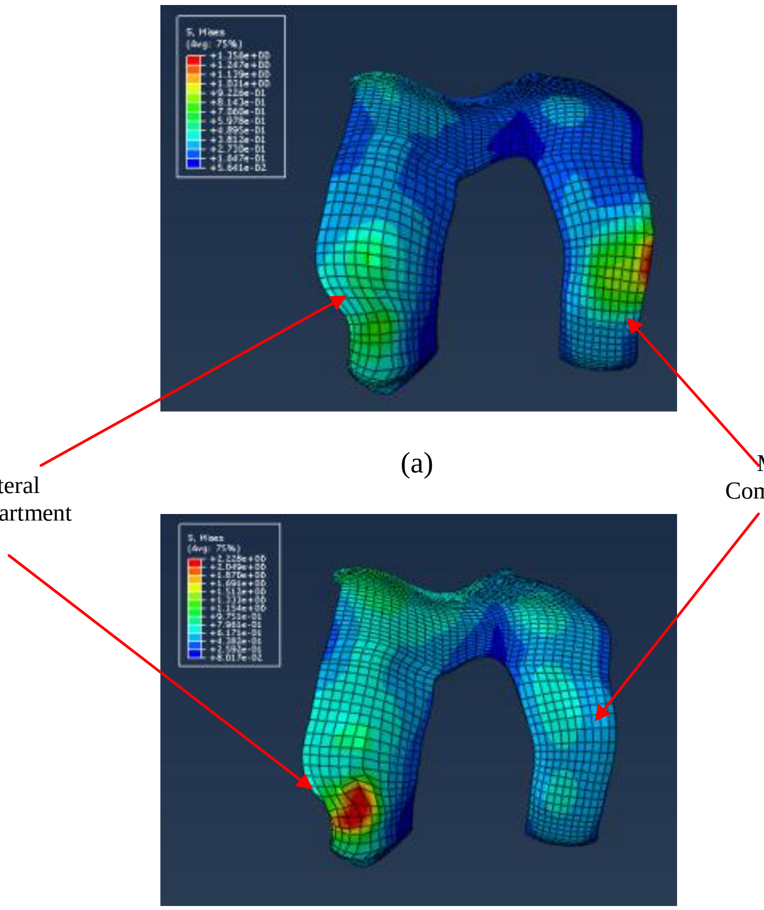

(a)

(b)

Figure 6.4 VM stress (MPa) on lateral (L), medial (M) femoral-compartments vs flexion angle (a) menisci intact. (b) meniscectomy for 45^{o} flexion.

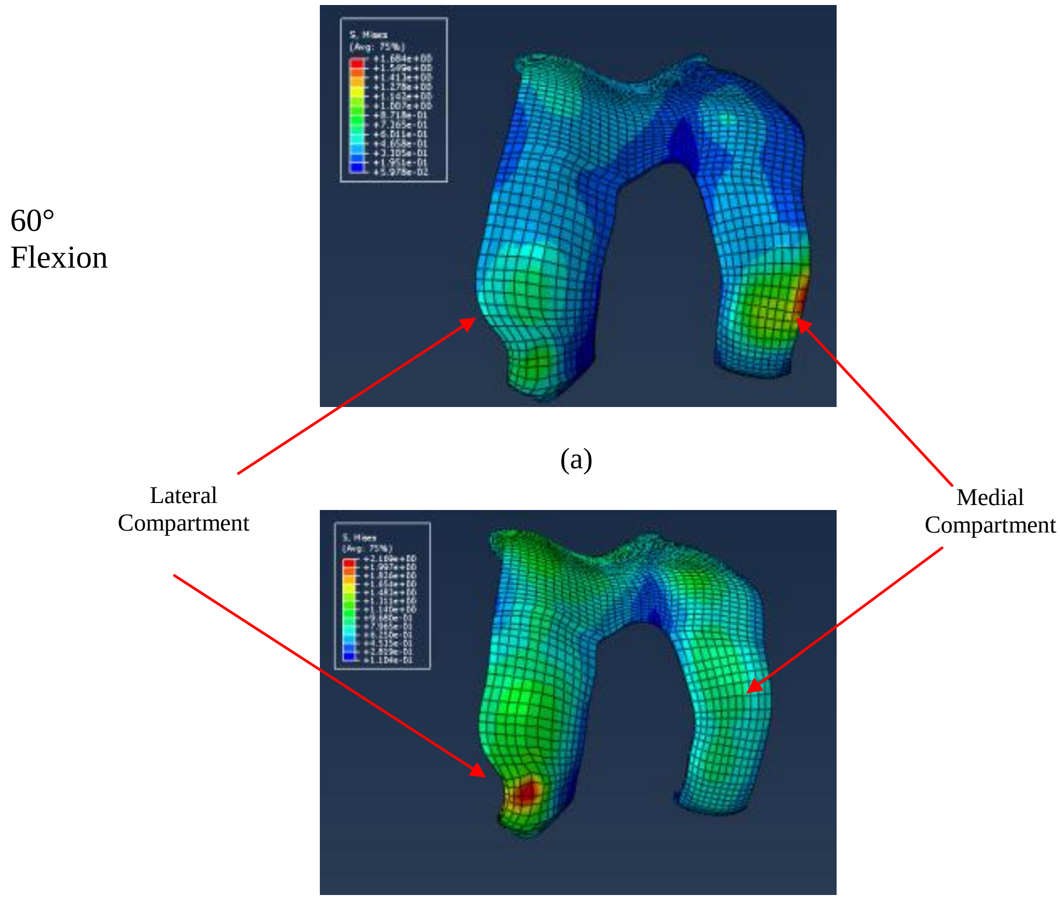

(b)

Figure 6.5 VM stress (MPa) on lateral (L), medial (M) femoral-compartments vs flexion angle (a) menisci intact. (b) meniscectomy for 60^{o} flexion.

.

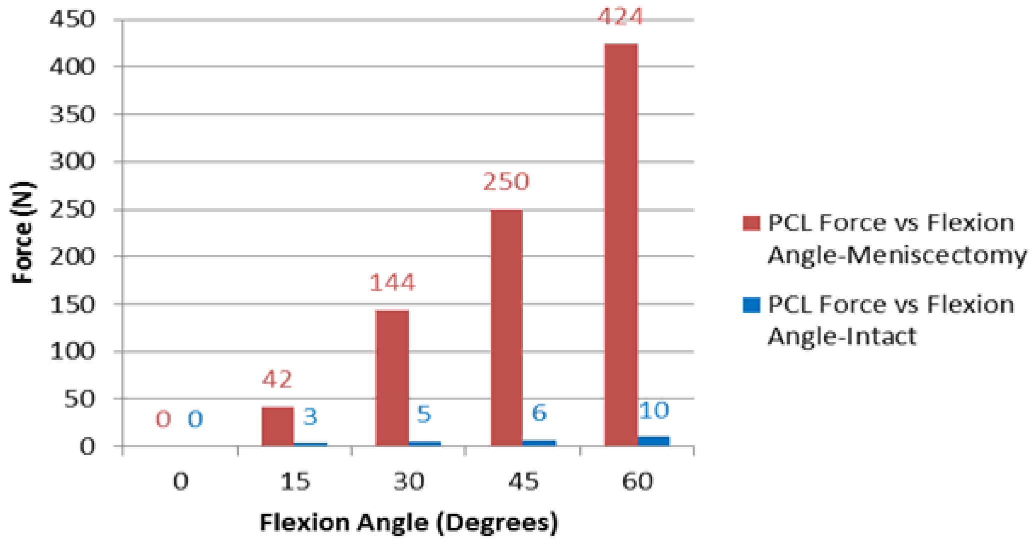

Figure 6.6 PCL forces versus flexion angle-intact and meniscectomy

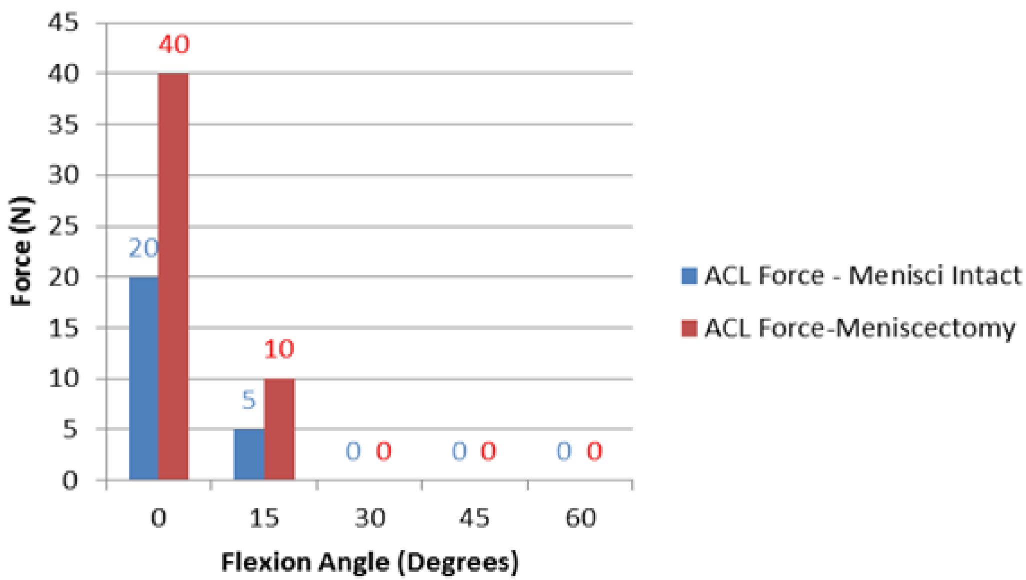

Figure 6.7 ACL forces versus flexion angle-intact and meniscectomy

6.2.2 Unilateral versus total menisectomy effect on PCL forces under anterior femoral drawer in full knee extension

In this application, unilateral medial and lateral meniscectomy were compared versus total meniscectomy as shown in Figure 6.8. The left image shows lateral meniscectomy (lateral menisci removed), the middle image shows medial meniscectomy (medial menisci removed) and the right image shows total meniscectomy (both meniscii removed). At fixed femoral axial rotation, higher PCL forces were noticed in the case of medial meniscectomy compared to lateral meniscecotmy at displacements greater than 1 mm as shown in Figure 6.9. PCL forces were 70N and 88N at 2 mm displacement, 127N and 155N at 3 mm displacement for lateral and medial meniscectomy, respectively.

It was noted that PCL forces resulting from medial meniscectomy were the next highest value to those resulted from total meniscectomy. Total meniscectomy resulted in the highest PCL forces in all conditions. At free femoral axial rotation, lower PCL forces resulted due to the extra degree of freedom applied as less resistance to femoral drawer was noted. Predicted results of PCL forces for the medial meniscectomy were relatively higher than for lateral meniscectomy. Both maintained higher PCL forces than the intact case. However, a substantial increase of PCL forces resulted in total meniscectomy as shown in Figure 6.10. Predicted PCL forces were 13.5N and 18N at 2 mm anterior displacement, 20N and 24N at 3 mm anterior displacement for lateral and medial menisectomy respectively.

ACL remained slack in all cases. Contact pressure on tibial cartilages were twice as high in the case of medial menisectomy 0.9MPa and 1.02MPa than lateral menisectomy 0.5MPa and 0.52MPa in free and fixed axial rotation, respectively. It was noted that contact pressure resulting from medial menisectomy was close in value to that resulting from total meniscectomy in both conditions as shown in Table 6.2.

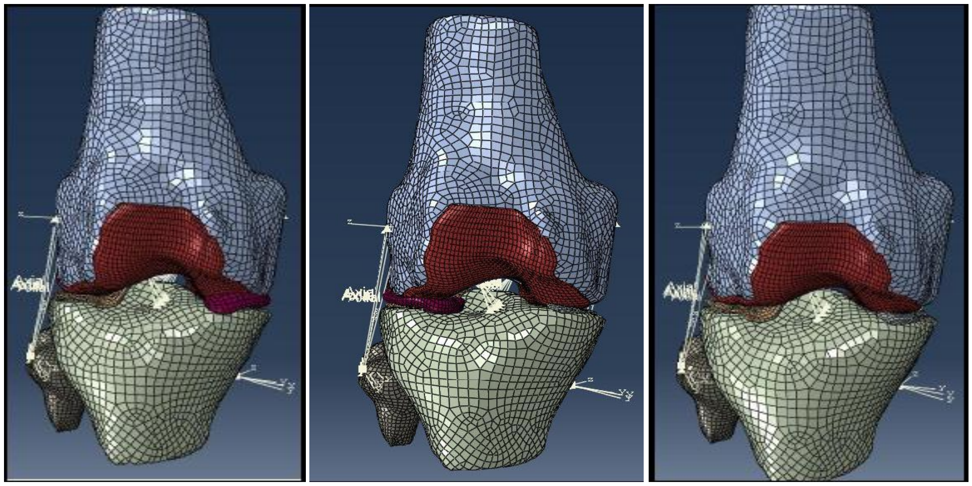

Figure 6.8 Unilateral versus total meniscectomy: Lateral meniscectomy (left), Medial meniscectomy (middle) and Total meniscectomy (right)

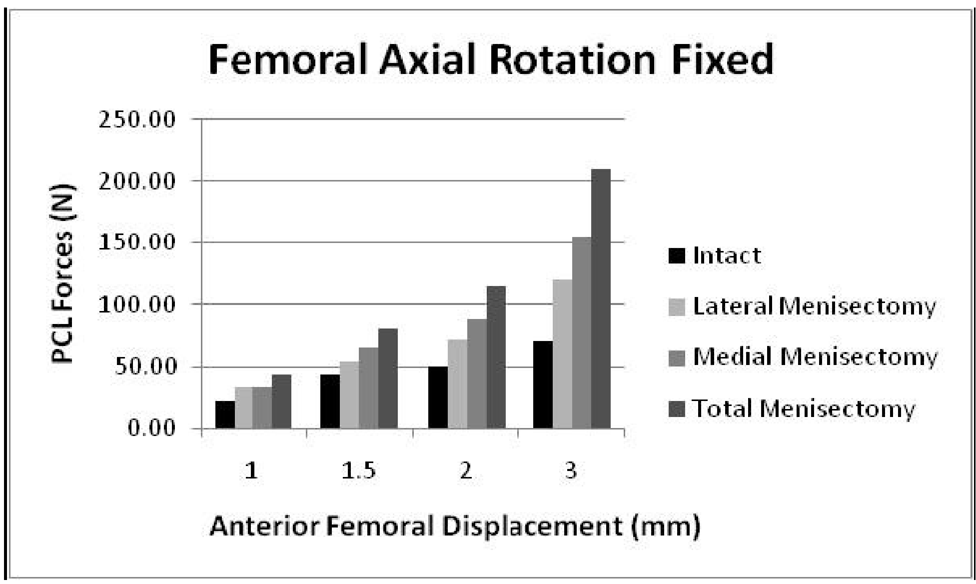

Figure 6.9 PCL forces versus anterior femoral displacement at full extension, for unilateral and total meniscectomy-fixed axial rotation.

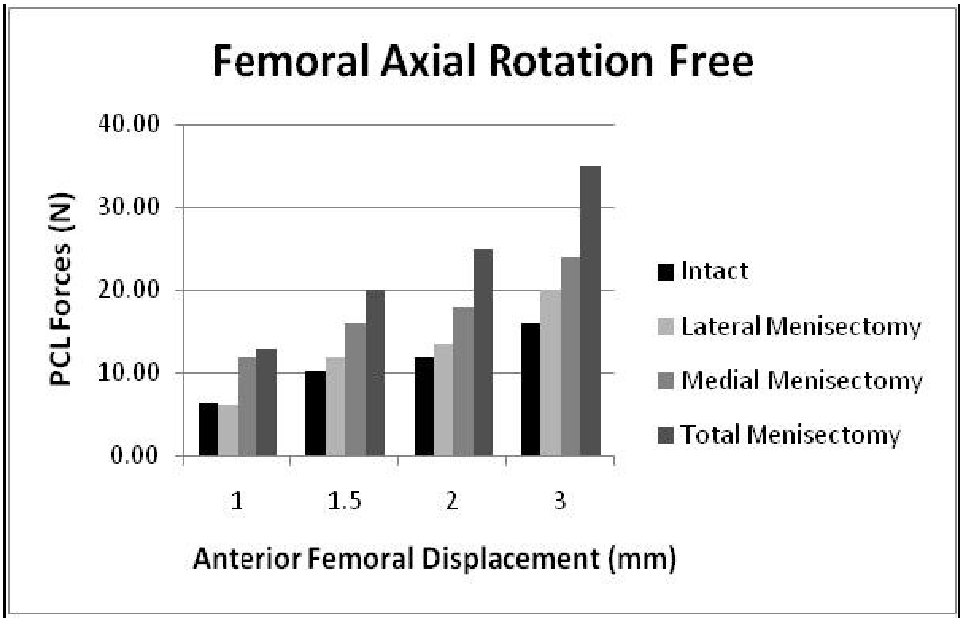

Figure 6.10 PCL forces versus anterior femoral displacement at full extension, for unilateral and total meniscectomy-free axial rotation

Table 6.2: Contact Pressure (MPa) on tibial cartilages at 3 mm drawing in unilateral meniscectomy versus total meniscectomy

	Intact	Lateral Meniscectomy	Medial Meniscectomy	Total Meniscectomy
Free Axial Rotation	0.56 MPa	0.5 MPa	0.9 MPa	1.15 MPa
Fixed Axial Rotation	0.5 MPa	0.52 MPa	1.02 MPa	1.18 MPa

Contact pressure contour plots of the femoral cartilage in all four tested cases are shown in Figure 6.11, Figure 6.12, Figure 6.13 and Figure 6.14. In Figure 6.11, in case of menisci intact maximum contact pressure resulted on the lateral compartment of the femoral cartilage is 0.6 MPa in both conditions (fixed and free axial rotation), while maximum contact pressure resulted on the medial compartment of the femoral cartilage is 0.45 MPa. In case of lateral meniscectomy (Figure 6.12), more load bearing is noticed on the medial compartment of the femoral cartilage with a maximum contact pressure value of 0.47 MPa and maximum contact pressure value of 0.3 MPa on the lateral compartment of the femoral cartilage (at fixed axial rotation). At free axial rotation, maximum contact pressure value on the medial compartment increased to 0.51 MPa while the contact pressure dropped to zero on the lateral compartment, this is attributed to the external rotation of the femur due to the absence of the lateral menisci which concentrates more pressure on the medial menisci.

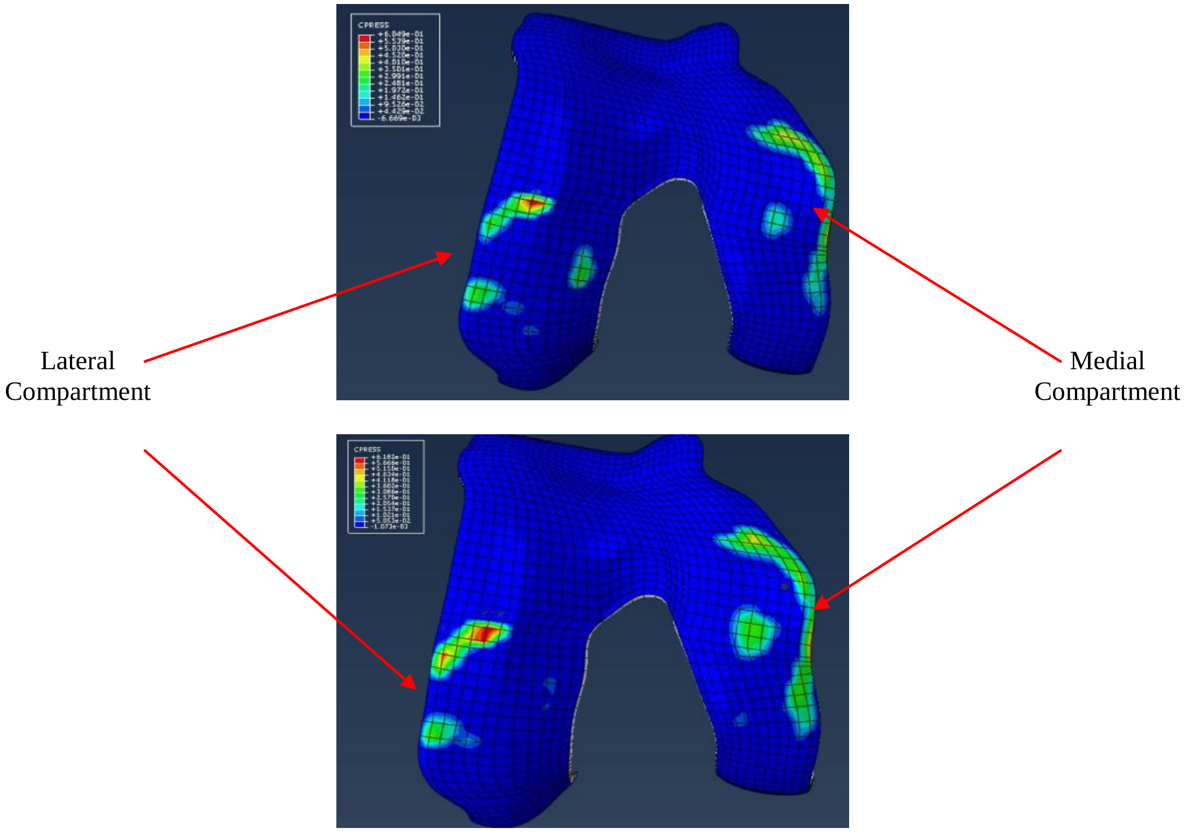

Figure 6.11 Contact Pressure (MPa) values on femoral cartilage in case of menisci intact

(Top=Fixed rotations; Bottom=Free rotations)

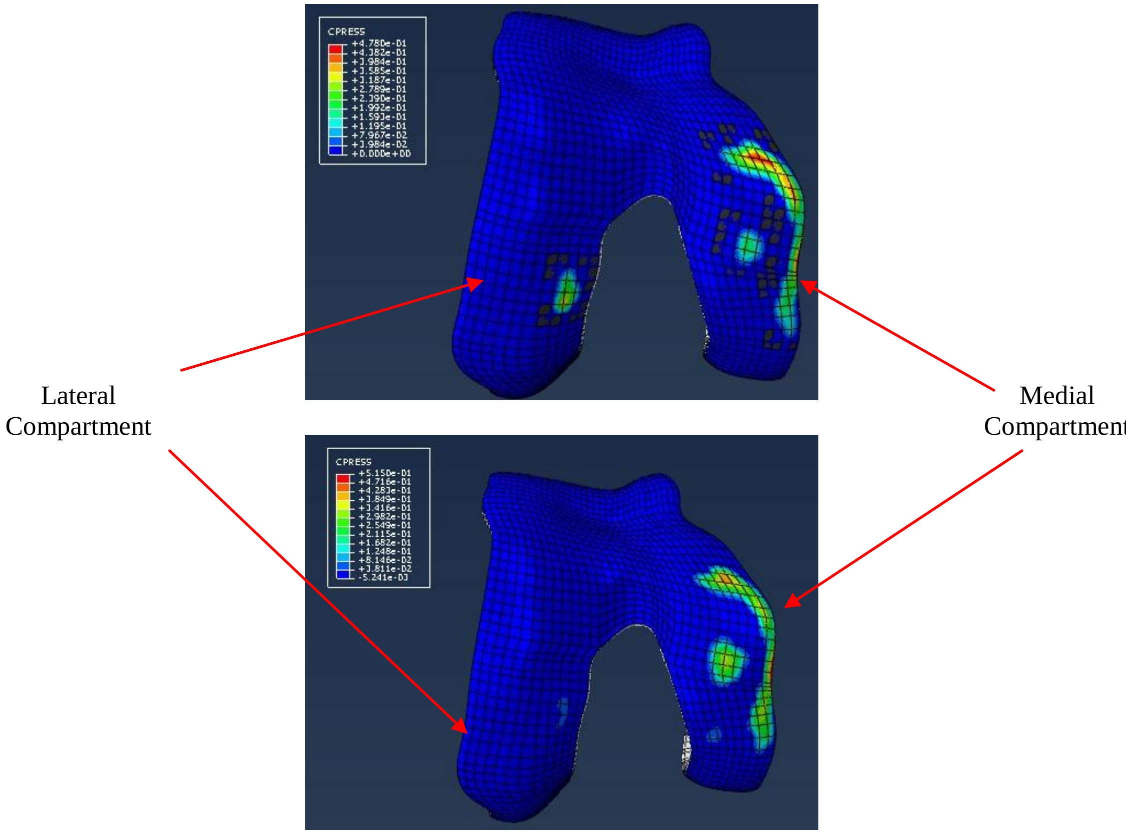

Figure 6.12 Contact Pressure (MPa) values on femoral cartilage in case of lateral meniscectomy

(Top=Fixed rotations; Bottom=Free rotations)

In case of medial meniscectomy (Figure 6.13), maximum contact pressure values on both the lateral and medial compartments of the femoral cartilage are 0.9 MPa in both fixed and free axial rotations. This shows that medial meniscectomy has a higher impact on the knee cartilages when compared to lateral mensicectomy. In case of total meniscectomy (Figure 6.14), maximum contact pressure values resulted are the highest of all cases studied. Maximum contact pressure values on both lateral and medial compartments of the femoral cartilage are 1.17 MPa in fixed axial rotation. In case of free axial rotation, maximum contact pressure on lateral compartment of the femoral cartilage dropped to 7.88 MPa while maximum contact pressure value on the medial compartment slightly increased to 1.18 MPa. This again indicates external rotation of the femur and more load bearing on the medial compartment.

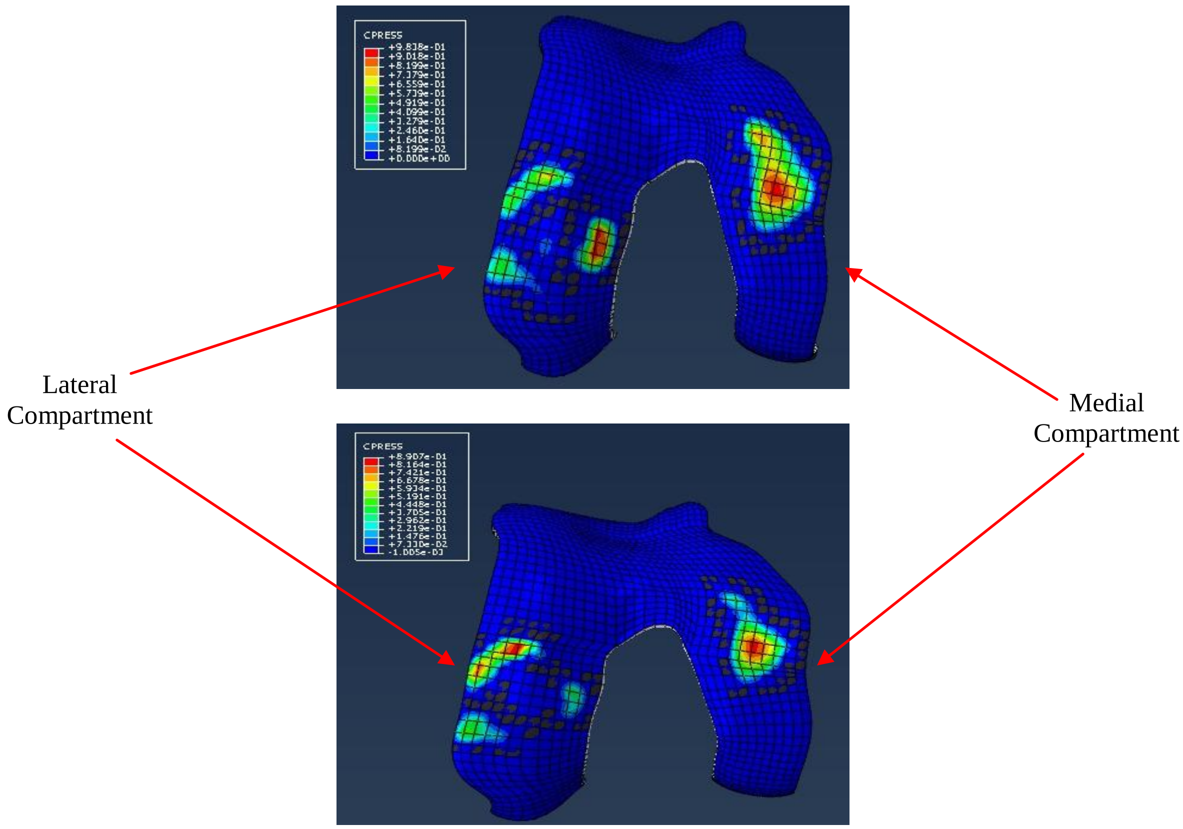

Figure 6.13 Contact Pressure (MPa) values on femoral cartilage in case of medial meniscectomy

(Top=Fixed rotations; Bottom=Free rotations)

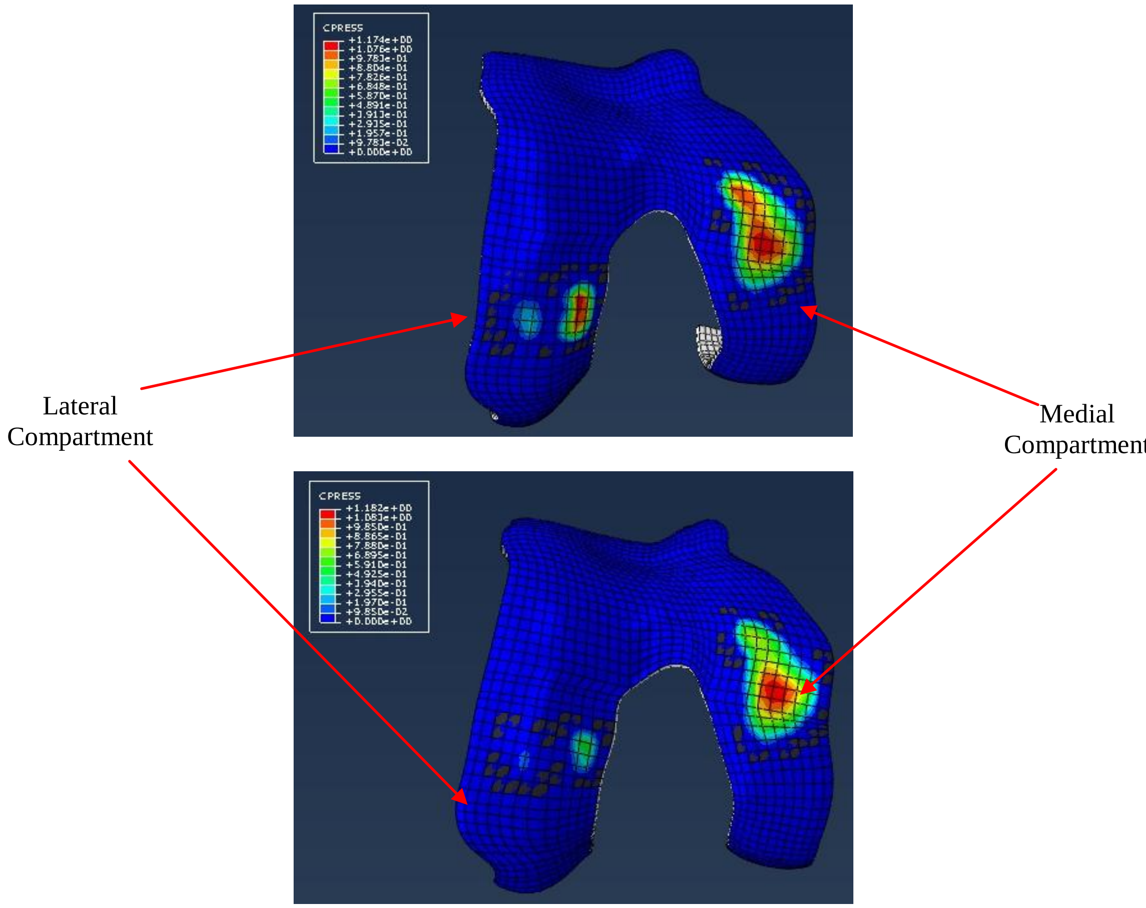

Figure 6.14 Contact Pressure (MPa) values on femoral cartilage in case of total meniscectomy

(Top=Fixed rotations; Bottom=Free rotations)

6.3 Jump Impact Application

6.3.1 Impact of landing from a jump on tibial plateau, femoral cartilage, menisci and patellar tendon during active knee joint flexion:

Previous experimental studies have provided a lot of insight in the area of joint kinematics [70-71], joint kinetics [70-73], landing style [71] and muscle activation patterns [72]. Most of the previous studies focused on investigating the ACL tear as a result of jump impact. However, those studies lacked a detailed analysis of the forces acting on the other components of the knee, for example, the contact forces impacting the menisci, tibial cartilages, patellar cartilage and patellar tendon.

To evaluate the internal forces of the knee joint during impact, it is difficult to measure the ligament forces or contact forces experimentally which is a major limitation. As an alternative, 3D finite element modeling and computer simulations provide us with approximate estimates for such parameters in a non invasive way [74-77]. The goal of this study is to measure the ligament forces, contact forces on menisci and cartilages in addition to the patellar tendon joint at five different points during landing from a jump. Each point is at a different combination of quadriceps loading and flexion angle to simulate the effect of the ground reaction force at the measured instant. Results will be compared to determine the zone of injury of each part.

Previous studies lacked an investigation of the injury zone that can take place during the landing motion which will be presented in this study. In addition, a recommended landing technique will be simulated to determine if it decreases the forces acting at the knee. The 3D knee joint model that was constructed will be used for this application analysis, this time incorporating the quadriceps muscles and the patello-femoral joint.

In this application, the patello-femoral joint in included in the analysis. Contact was defined as frictionless hard contact. For this study, seven contact pair interactions were defined: femoral cartilage and both menisci (2 pairs), femoral cartilage and both tibial cartilages (2 pairs), both menisci and tibial cartilages (2 pairs) in addition to femoral cartilage and patellar cartilage (one pair).

Boundary conditions were set to fix the tibia and fibula in all degrees of freedom. Ligament insertion nodes were coupled to the reference nodes of the corresponding bone. Femoral cartilage and tibial cartilage were tied to the femur and tibia bone respectively. Menisci ends (horns) were tied to the tibia to mimic the real biological behavior. The landing parameters of the vertical ground reaction force curve reported by Pflum et al. [78] was sectioned at five separate frames and data was collected at each time frame. Both the knee flexion angle and the corresponding quadriceps load that correspond to each frame was entered into our 3D model as a combination of boundary conditions which is equivalent to the effect of the vertical ground reaction force component at that frame that was reported in the model results of Pflum et al [78]. Five different combinations of quadriceps loading and flexion angles were used at five different points on the vertical ground reaction force (GRF) as shown in Figure 6.15 and summarized in Table 6.3. Parameters of interest are contact pressure, contact area and patella tendon forces at each point measured.

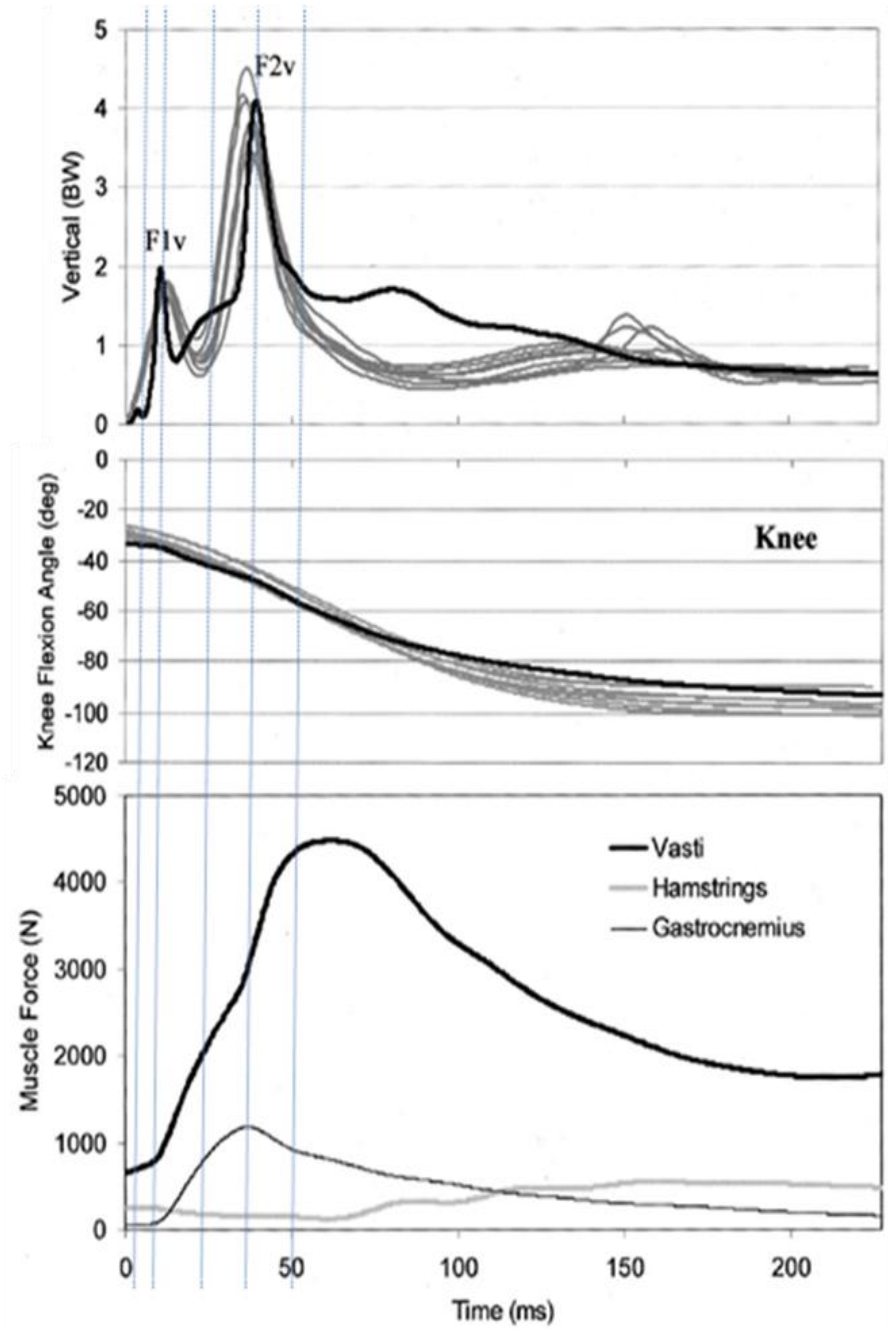

Figure 6.15 Landing parameters adapted from Pflum et al [78] and the five selected points in the presented study

Table 6.3: Boundary condition scenarios showing the various combinations of femoral flexion angle and quadriceps loading at the five measured points

Point Measured	**Femoral Flexion Angle (Deg)**	**Quad. Load (N)**	**Time (ms)**
Point before first peak: P1	30	625	3
First Peak (ground reaction force due to toe landing F1V): P2	33	800	11
Point between two peaks: P3	40	2000	25
Second Peak (ground reaction force due to heel strike F2V): P4	46	3700	40
Point after second peak: P5	50	4000	47

6.4 Jump Impact Results

6.4.1 Contact and Ligament Forces

6.4.1.1 At first point (P1)

The first point measured P1 was selected before the first peak of vertical ground reaction force curve as illustrated in Figure 6.15 at time approximately 3 ms. The landing parameters at this point was a flexion angle of 30 degrees and quadriceps loading of 625N. Contact forces and ligament/tendon forces results for each measured part are summarized in Table 6.4. At this point, more load bearing resulted on the lateral compartment of the knee joint (lateral cartilage and lateral menisci) when compared with the medial compartment. For the patellar tendon joint, the resulting patellar tendon forces F_p was 732 N. The resultant contact forces at the patella cartilage R was 703 N. Resultant contact forces at the patella are directly output from the analysis, and can be calculated as shown in equation (6.1), which simplifies the patella joint as a pulley in behavior.

$$R=\sqrt{\left(F_Q\ \cos\alpha+F_P\cos\beta\right)^2+\left(F_Q\sin\alpha-F_P\sin\beta\right)^2} \qquad (6.1)$$

where,

R is the resultant contact force at the patella.

F_Q is quadriceps force

α is the angle between F_Q and the line of motion of the patella.

F_P is patella tendon force

β is the angle between F_P and the line of motion of the patella.

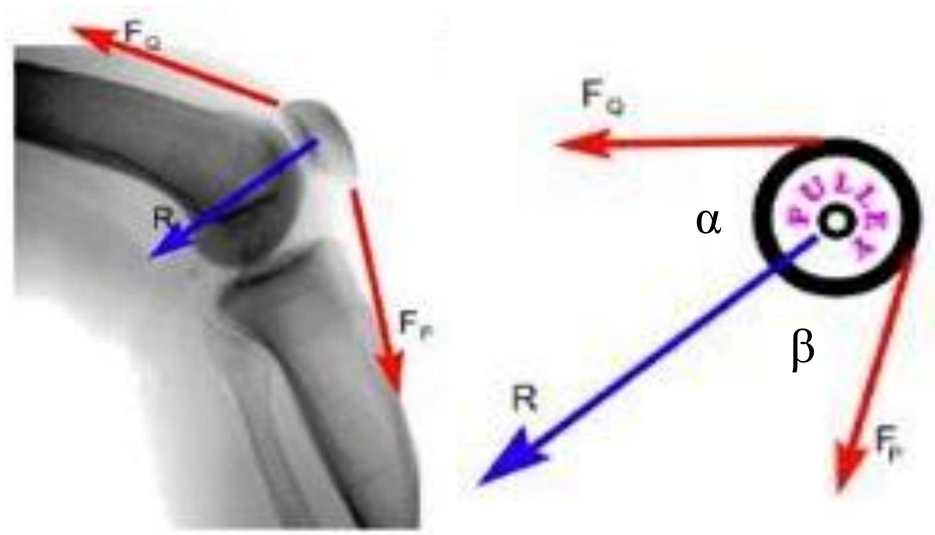

(a)

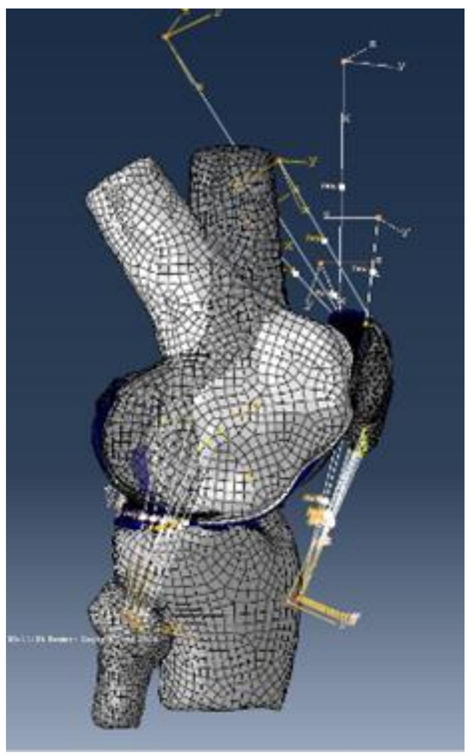

(b)

Figure 6.16 (a) Illustration of the patellofemoral joint resultant forces

Fq= Quadriceps load, Fp=Patella tendon, R=Resultant forces acting at the patella

(b) Superimposed deformed (after flexion) and non-deformed (before flexion) knee joint

Table 6.4: Ligament and Contact force results at P1

Part Instance	Ligament/Tendon/Muscle Forces (N)	
LCL	10	
MCL	5	
PCL	1240	
ACL	0	
F_p	732	
Contact Pair	**Contact Forces (N)**	**Contact Area (mm^2)**
Femoral Cartilage/Medial Cartilage	1200	200
Femoral Cartilage/Lateral Cartilage	1700	225
Femoral Cartilage/Medial Menisci	35	9
Femoral Cartilage/Lateral Menisci	250	65
Patella Cartilage (Resultant contact forces at the Patella Cartilage)	703	240

6.4.1.2 At second point (P2)

The second point measured P2 was selected as the first peak of vertical ground reaction force curve F1v as illustrated in Figure 6.15 at time approximately 11 ms, which corresponds to the forefoot impacting the ground (toe-landing). The landing parameters at this point were a flexion angle of 33 degrees and quadriceps loading of 800 N. Contact forces and ligament/tendon forces results for each measured part are summarized in Table 6.5. At this point, a similar pattern to the previous point P1 was noticed. More load bearing resulted on the lateral compartment of the knee joint (lateral menisci, lateral cartilage and LCL) due to external rotation of the femur with respect to the tibia (screw-home mechanism). The resultant contact force at the patellar cartilage is 885 N. Imposed non-deformed (before flexion) and deformed (after flexion) image of the knee joint at zero and 33 degrees respectively is shown in Figure 6.17.

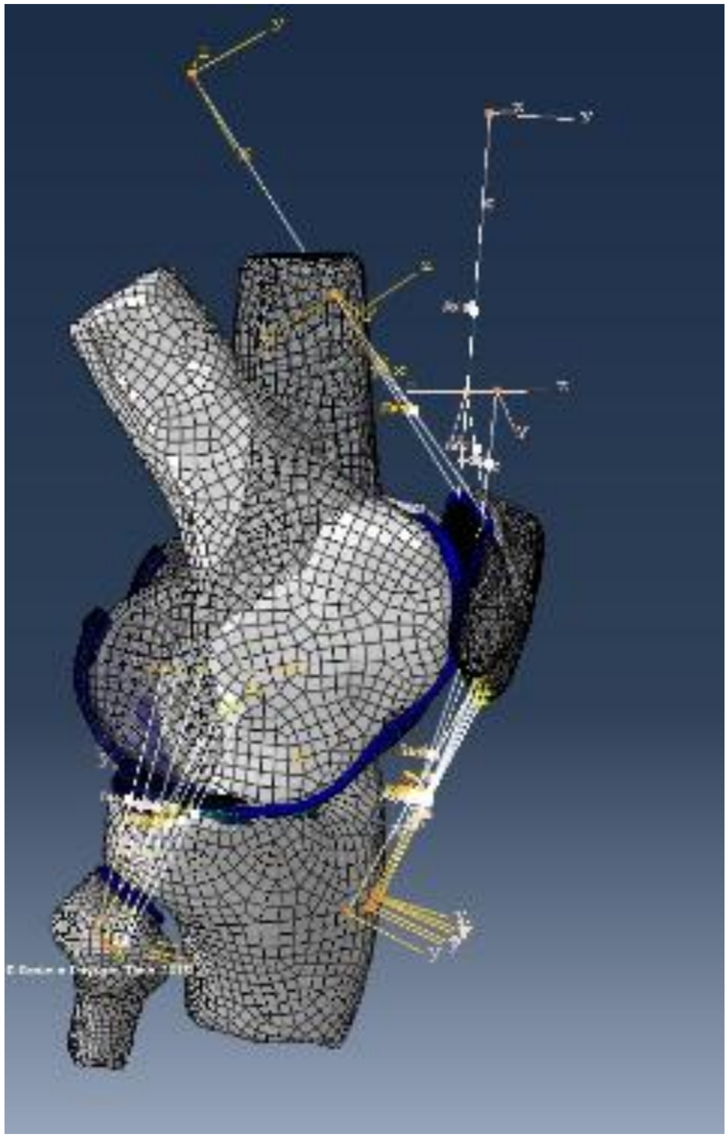

Figure 6.17 Imposed before and after flexion at 33 degrees

Table 6.5: Ligament and Contact forces results at P2

Part Instance	Ligament/Tendon Forces (N)	
LCL	18	
MCL	5	
PCL	1568	
ACL	0	
F_p	907	
Contact Pair	**Contact Forces (N)**	**Contact Area (mm^2)**
Femoral Cartilage/Medial Cartilage	1100	200
Femoral Cartilage/Lateral Cartilage	1750	225
Femoral Cartilage/Medial Menisci	25	10
Femoral Cartilage/Lateral Menisci	300	75
Patella Cartilage (Resultant contact forces at the Patella Cartilage)	885	280

6.4.1.3 At third point (P3)

The third point measured P3 was selected between the first peak of vertical ground reaction force curve F1v at time approximately 11 ms which corresponds to the forefoot impacting the ground and the second peak of vertical ground reaction force curve F2v at time 40 ms, which corresponds to the heel impacting the ground as illustrated in Figure 6.15. The landing parameter at this point was a quadriceps loading of 2000 N at 40 degrees flexion angle as shown in Figure 6.18. Contact forces and ligament/tendon forces results for each measured part are summarized in Table 6.6. At this point, a substantial load bearing was concentrated on the lateral compartment of the knee joint compared to previous points measured. The patella tendon force result 1805N and the resultant contact force acting on the patella 1934N.

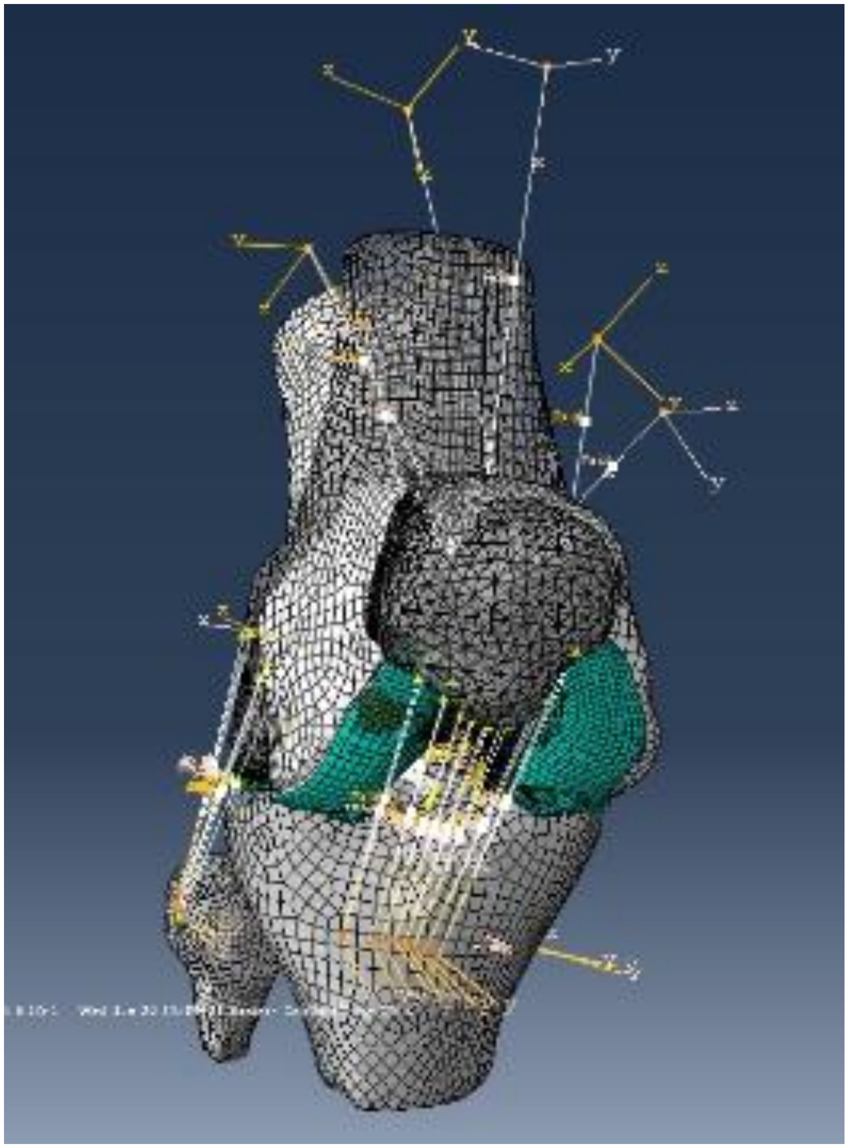

Figure 6.18 Imposed before and after flexion at 40 degrees

Table 6.6: Ligament and Contact forces results at P3

Part Instance	**Ligament/Tendon Forces (N)**	
LCL	45	
MCL	5	
PCL	1863	
ACL	0	
F_p	1805	
Contact Pair	**Contact Forces (N)**	**Contact Area (mm^2)**
Femoral Cartilage/Medial Cartilage	580	120
Femoral Cartilage/Lateral Cartilage	1500	175
Femoral Cartilage/Medial Menisci	18	5
Femoral Cartilage/Lateral Menisci	270	98
Patella Cartilage (Resultant contact forces at the Patella Cartilage)	1934	310

6.4.1.4 At fourth point (P4)

The fourth point measured P4 was selected at the second peak of vertical ground reaction force curve F2v at time 40 ms which corresponds to the heel impacting the ground as illustrated in Figure 6.15. The landing parameters at this point was a quadriceps loading of 3700 N and 46 degrees flexion angle. Contact forces and ligament/tendon forces results for each measured part are summarized in Table 6.7. At this point, it was noticed that the medial collateral ligament (MCL) contributed more to load bearing than previous cases, MCL ligament forces were 50 N compared to 5 N in previous cases and it approached the load value contributed by the lateral collateral ligament (LCL) of 60N in the current case. More load bearing is concentrated on the lateral compartment of the knee joint (menisci and cartilages). The lateral and medial tibial cartilages contact forces were 1250 and 200 N, respectively and the lateral and medial menisci contact forces were 205 N and 20 N, respectively. The patellar tendon force results after flexion was 2851 N, and the resultant contact force at the patella cartilage was 3854 N. Imposed plot of the femur before and after flexion is shown in Figure 6.19.

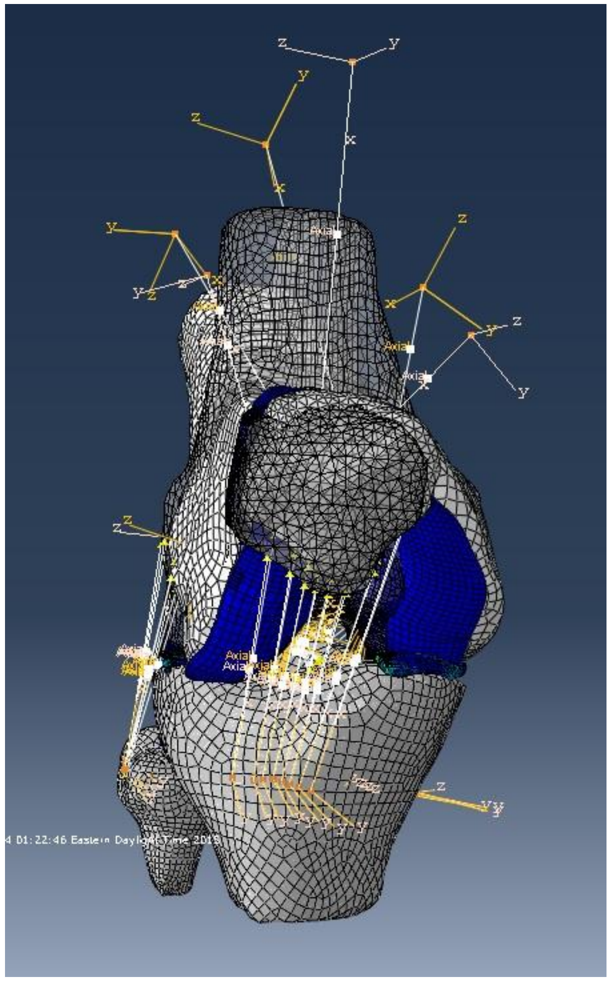

Figure 6.19 Femur before and after flexion at 46 degrees

Table 6.7: Ligament and Contact force results at P4

Part Instance	Ligament/Tendon Forces (N)	
LCL	60	
MCL	50	
PCL	1917	
ACL	0	
F_p	2851	
Contact Pair	**Contact Forces (N)**	**Contact Area (mm^2)**
Femoral Cartilage/Medial Cartilage	200	92
Femoral Cartilage/Lateral Cartilage	1250	138
Femoral Cartilage/Medial Menisci	20	7
Femoral Cartilage/Lateral Menisci	205	75
Patella Cartilage (Resultant contact forces at the Patella Cartilage)	3854	333

6.4.1.5 At fifth point (P5)

The fifth point measured P5 was selected after the second peak of vertical ground reaction force curve F2v at time 47 ms, as illustrated in Figure 6.15. The landing parameters at this point were a quadriceps loading of 4000 N at 50 degrees flexion angle. Contact force and ligament/tendon force results for each measured part are summarized in Table 6.8. At this point, it was noticed that the load bearing shifted totally to the lateral compartment. Lateral and medial menisci contact forces were 140N and 0N, respectively. Contour plots of the contact pressure on the femoral cartilage shows contact at the lateral compartment and at the patellar cartilage while so small or no contact pressure was detected on the medial compartment. LCL and MCL forces were 85N and 50N, respectively. The patellar tendon forces results after flexion was 3357N;

the resultant contact force at the patella was 4042 N. Imposed plot of the femur before and after flexion is shown in Figure 6.20.

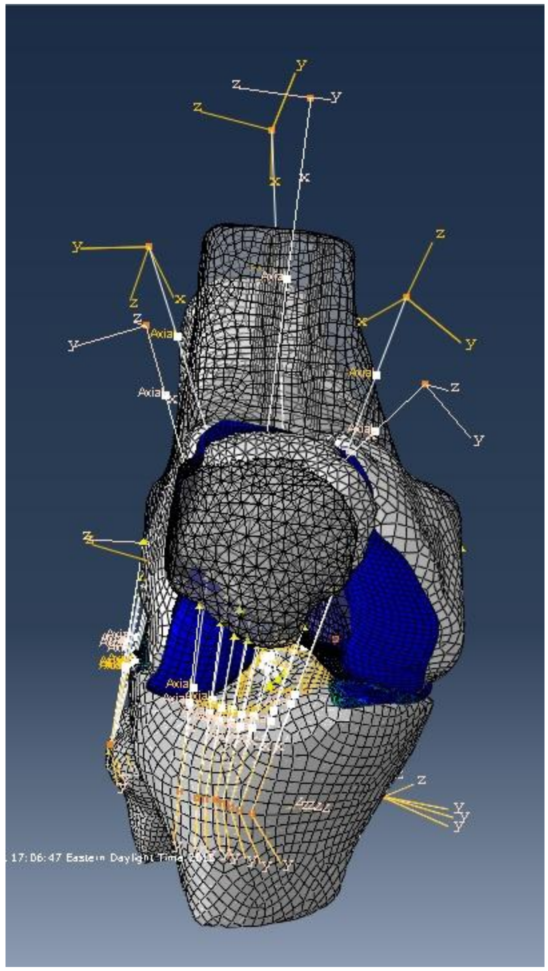

Figure 6.20 Femur before and after flexion at 50 degrees

Table 6.8: Ligament and Contact forces results at P5

Part Instance	Ligament/Tendon Forces (N)	
LCL	85	
MCL	52	
PCL	1925	
ACL	0	
F_p	3357	
Contact Pair	**Contact Forces (N)**	**Contact Area (mm^2)**
Femoral Cartilage/Medial Cartilage	5	40
Femoral Cartilage/Lateral Cartilage	1200	135
Femoral Cartilage/Medial Menisci	0	0
Femoral Cartilage/Lateral Menisci	140	60
Patella Cartilage (Resultant contact forces at the Patella Cartilage)	4042	267

Contact force and ligament force results at the five measured points were plotted on one curve versus the Quadriceps loading as shown in Figure 6.21 and Figure 6.22. Comparing the results at each of the selected time increments will determine the specific zone at which injury occurs to the ligaments, menisci and articular cartilages.

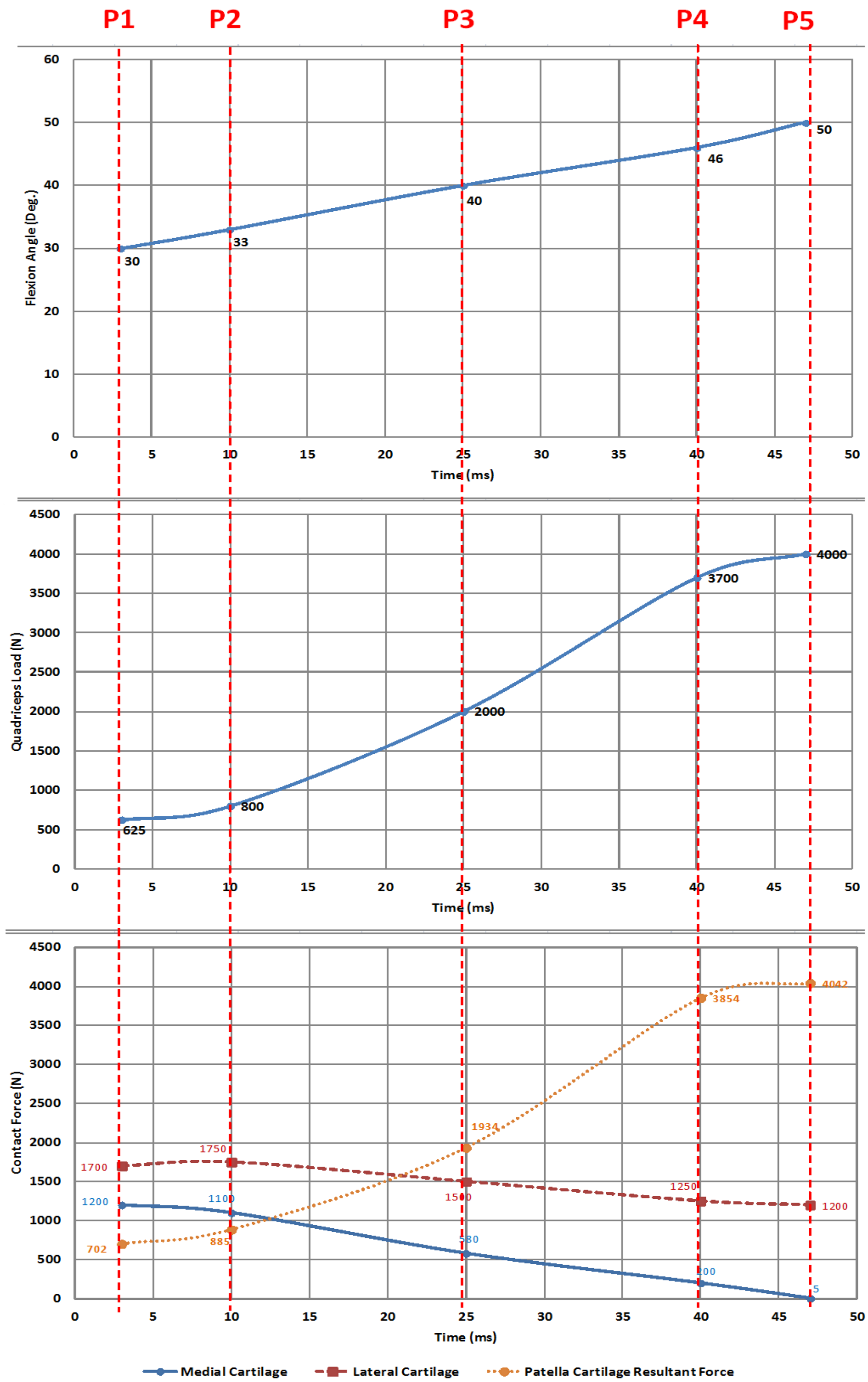

Figure 6.21 Contact Force results for Cartilages versus quadriceps loading and flexion angle

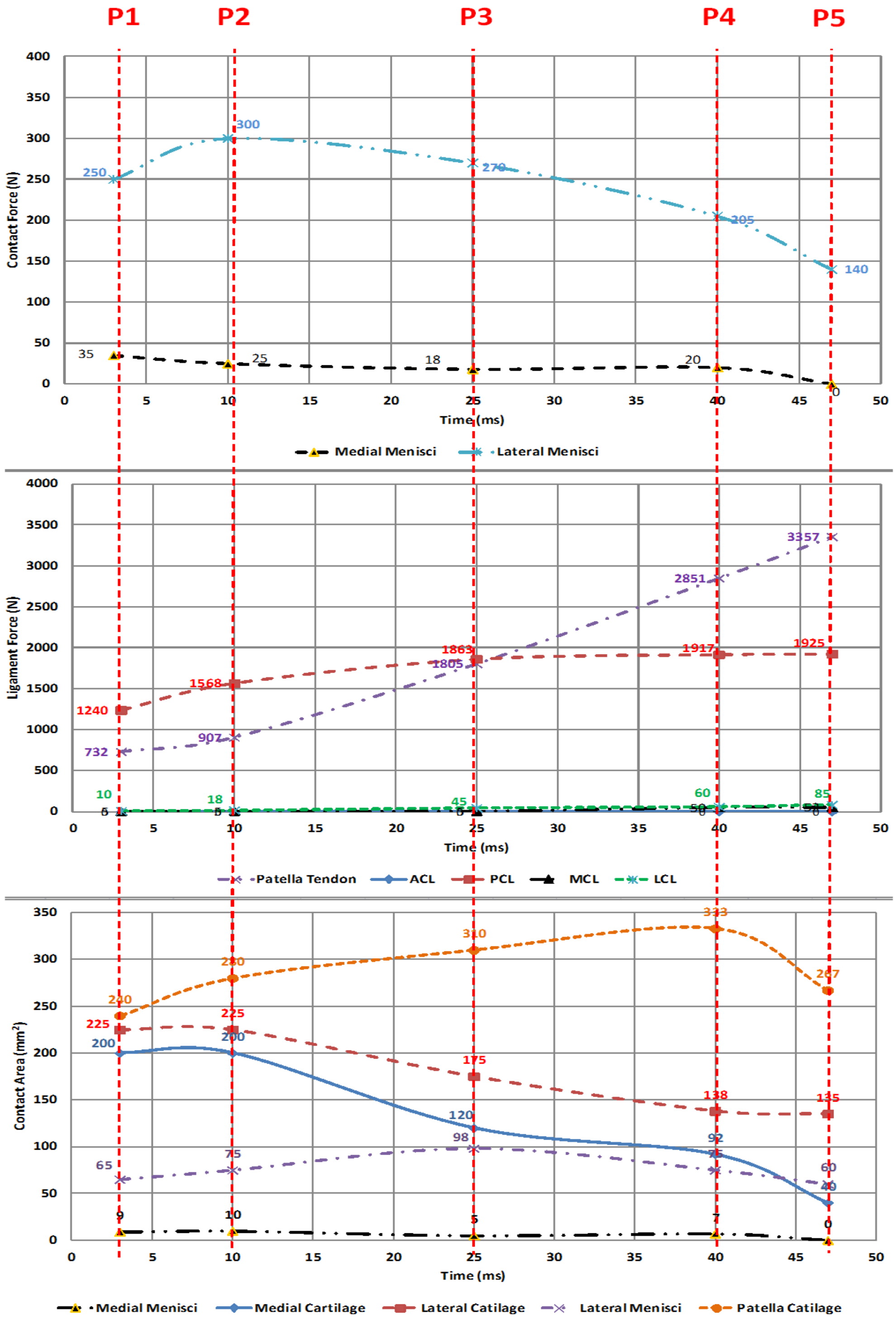

Figure 6.22 Contact Forces results for meniscii, patellar tendon and ligaments forces and contact area at the same five points

6.4.3 Contact Pressure Results

Contact pressure at points P1, P2, P3, P4 and P5 are shown in Figures 6.23, 6.24, 6.25, 6.26, and 6.27 respectively. In Figure 6.23 at P1, maximum contact pressure of 11.4 MPa resulted on the lateral compartment of the femoral cartilage while on the medial compartment and the patella contact zone (shows contact interaction between the patella cartilage and the femoral cartilage), a maximum contact pressure of 7.6 MPa is indicated. This shows more load bearing on the lateral compartment which indicates an internal rotation of the femur.

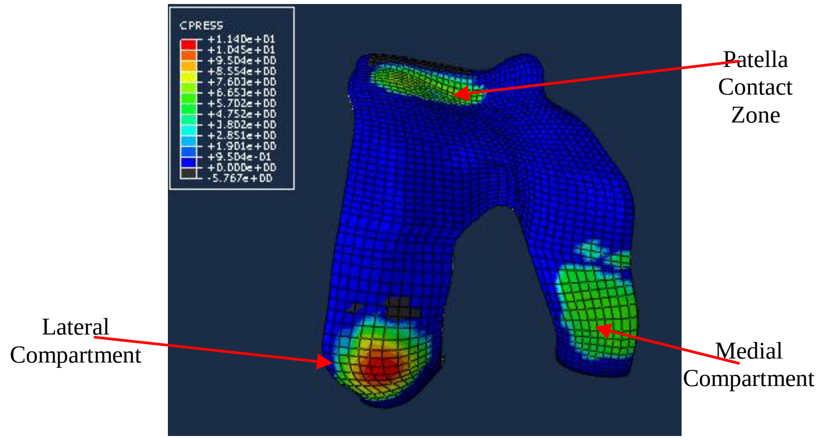

Figure 6.23 Contact pressure (MPa) contour plot at P1

In Figure 6.24 at P2, similar contact pressure values to that of P1 resulted at the same locations.

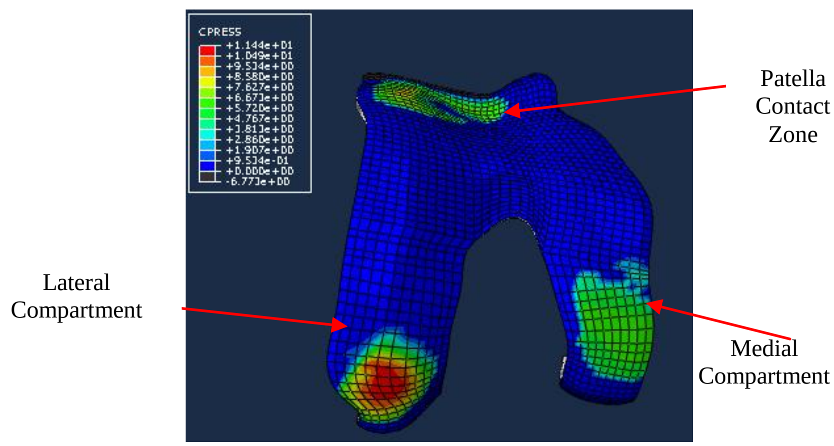

Figure 6.24 Contact pressure (MPa) contour plot at P2

In Figure 6.25 at P3, maximum contact pressure of 12 MPa resulted on the lateral compartment of the femoral cartilage and some points in the patella contact zone due to more pressure as the patella slides on the femoral cartilage while flexion angle increases. Maximum contact pressure of 8 MPa is noticed on the medial compartment of the femoral cartilage. In Figure 6.26 at P4, maximum contact pressure values are 12 MPa and 5.5 MPa on the lateral and medial compartments of the femoral cartilage respectively which shows a decrease in contact pressure on the medial compartment. Maximum contact pressure of 16 MPa resulted in the patella contact zone. Finally, in Figure 6.27 at P5, there is no contact pressure on the medial compartment of the femoral cartilage as the load shifted due to internal femoral rotation to concentrate on the lateral compartment of the femoral cartilage with a maximum contact pressure of 12 MPa. Higher contact pressure values were noticed in the patella contact zone to reach a maximum of 21 MPa as quadriceps loading increase.

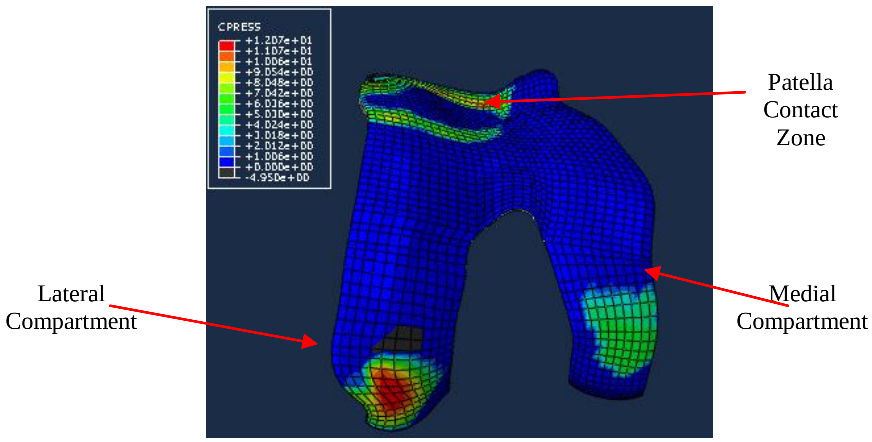

Figure 6.25 Contact pressure (MPa) contour plot at P3

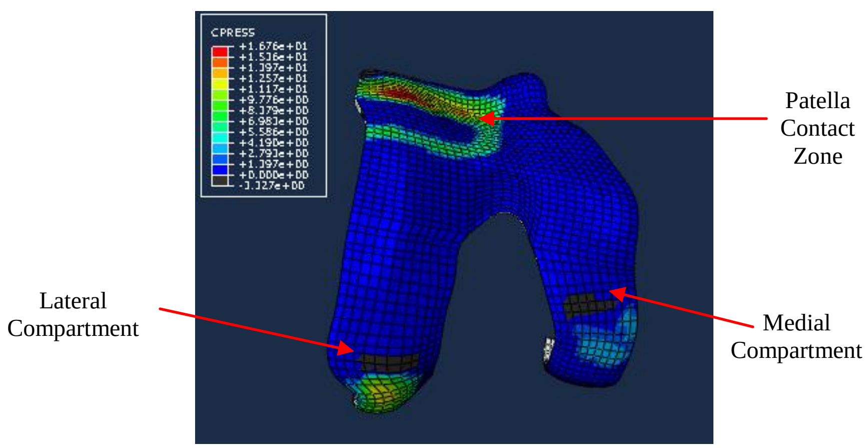

Figure 6.26 Contact pressure (MPa) contour plot at P4

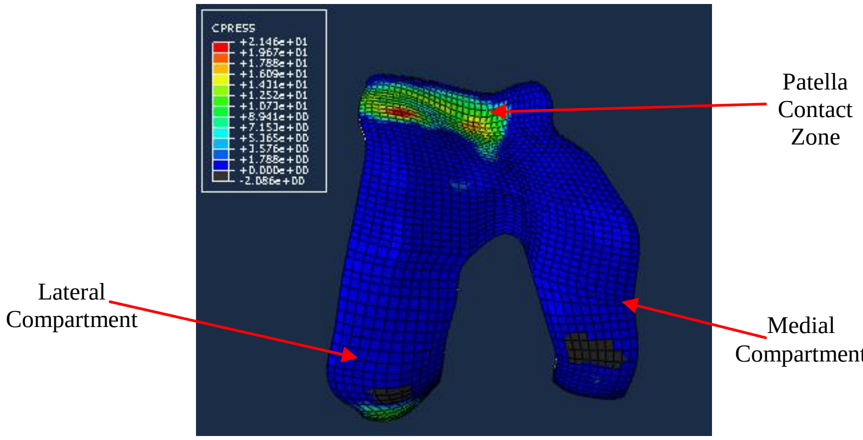

Figure 6.27 Contact pressure (MPa) contour plot at P5

Contact forces results of the previous simulations (as illustrated in tables 6.4-6.8) showed that contact forces on the articular cartilage decreased as flexion angle increased. This trend was investigated using the model constructed.

A set of simulations were conducted under the same boundary conditions (same loading) but with a deeper flexion at point P2 (toe landing point), increments of 5 degrees were added to the original flexion angle at P2 (33 degrees) and contact forces values on the femoral cartilage was recorded as shown in Table 6.9.

Results show a decrease in contact forces (as shown in Table 6.9) and contact pressure (as shown in Figure 6.28) at a flexion angle of 38 degrees when compared to results at a flexion angle of 33 degrees. As flexion angle at toe landing increased, contact forces decreased to reach its lowest value at flexion angle 48 degrees (Table 6.9) which is less than 40% of the contact force value resulted originally at flexion angle 33 degrees.

This new finding was found in agreement with a proposed landing technique in a recent study by U.C. Davis, conducted by Myers and Hawkins (2010) on injury prevention for basket ball players landing from jumps [90], instructed that landing with a deeper knee flexion and initiating the landing with toes led to reduced force at the knee when compared to landing on heals first.

The study showed that increasing the flexion angle by as little as (5 degrees) before toe landing made a substantial decrease in the forces at the knee, which agrees with the results obtained from the presented model.

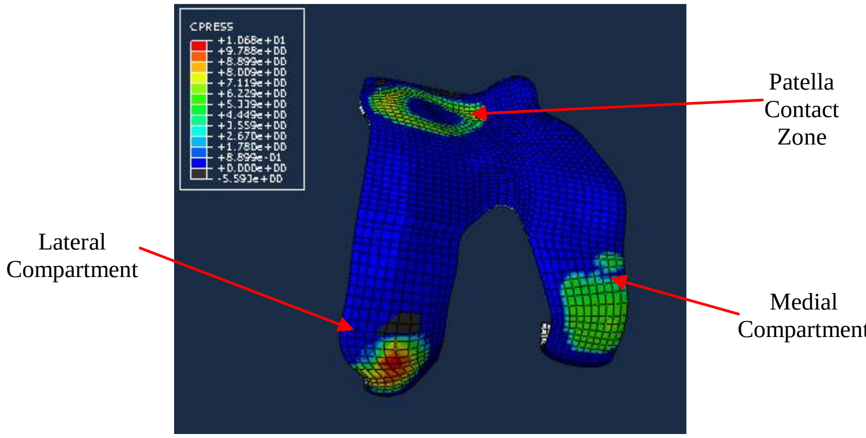

Figure 6.28 Contact pressure at the femoral cartilage when toe landing at 38 degrees at P2 instead of 33 degrees.

Table 6.9: Contact Force of the femoral cartilage at different flexion angle while toe landing

Flexion Angle (degrees) at Toe landing	33	38	43	48
Contact Force at femoral cartilage (N)	1120	940	750	440

In reality, changing the landing angle will change the corresponding quadriceps force and ground reaction force. Keeping the quadriceps force the same is a limitation of the presented model.

CHAPTER 7

DISCUSSION AND RECOMMENDATIONS

7.1 Discussion

Finite Element models have proven to be able to provide deep insights into the mechanical properties of biological tissues and the performance of living organs reducing both cost and time. They present an effective way of evaluating knee joint mechanics during the design phase and provide an indication of expected clinical performance. They are more effective, less invasive and less costly than experiments conducted on real subjects.

An appropriately developed finite element model is a powerful tool to predict the effects of the different parameters involved and to provide information otherwise difficult to obtain from experiments. It is important to note that the reliability of these models strongly depends on an appropriate geometrical reconstruction and on an accurate description of the behaviour of the biological tissues involved and their interactions with the surrounding environment which was taken into account in the model construction. In this study, a 3D finite element knee joint model is constructed to behave as close as possible to the real biological and anatomical joint behaviour. The aim of this study was to construct a full knee joint model that includes both the patello-femoral and tibio-femoral joints to serve as a powerful tool to analyze scenarios that were not discussed in depth in previous literature and to predict new results that were not presented in previous studies. Two main applications were conducted using the built model.

7.1.1 Meniscectomy applications

The first application (investigating the impact of meniscectomy procedures in meniscal tears treatment) consisted of two sub applications to simulate different scenarios of treatment surgeries, the total meniscectomy and the unilateral meniscectomy. Since menisci play a major role in the distribution of loads in the knee joint [79]. Surgical operation of unilateral and total meniscectomy is commonly used to decrease knee joint pain caused by meniscal tears as reported in many articles [80], [81]. However such procedures severely impacts the knee function as it exposes the cartilage to direct loading without the essential role of menisci as shock absorbent. Experimental studies have shown that excessive loading on the cartilage can cause damage that could lead to subsequent Osteoarthritis [82], [83], [84] and [85]. Total meniscectomy have been proven to lead to knee Osteoarthritis initian and progression [86].

Previous studies presented finite element models including the menisci [87] and [88], but they focused on the menisci intact cases and did not fully investigate unilateral and total meniscectomy. The presented study provides a full comparison between the menisci intact and fully meniscectomized knee joint. In the first application, it was found that total meniscectomy resulted in much higher cruciate ligament forces, higher contact pressure, higher stress level on femoral cartilage and higher axial contact force on tibial cartilages in all analyses processed. The elevated values of contact force and VM stress on cartilage due to full meniscectomy indicate higher cartilage degeneration risk, which promotes osteoarthritis. The role of menisci in load bearing and shock absorption was highlighted when comparing axial contact force values between menisci covered and uncovered versus meniscectomized tibial cartilages. In the meniscectomized model, a higher stress level was concentrated on the lateral compartment of the femoral cartilage due to the internal rotation of the femur.

In the second application, at fixed axial rotation, total meniscectomy resulted in the highest PCL forces in all conditions tested; the next highest impacting condition was the unilateral medial meniscectomy. This highlights that the medial compartment contributes more to load bearing as reported in previous studies. At free femoral axial rotation, noticeably less PCL forces were noticed. Contact pressure values on tibial cartilages due to medial menisectomy was very close to that resulting in total menisectomy in both conditions. Clinically, the results of this study show that unilateral medial menisectomy has a higher impact on knee joint function than lateral menisectomy and that medial meniscus should have a higher priority for preservation either by grafting or transplantation [89].

Analysis results show that total meniscectomy remains the most disruptive condition. It is clinically recognized that dealing with meniscal preservation is of paramount importance to avoid sequential failure of knee joint ligaments and cartilages. Recent approaches like prolotherapy, grafting and artificial scaffolds are recommended to treat complex meniscal tear as an alternative to total menisci excision. Prolotherapy is a treatment technique based on repeated injections of an irritating solution into the damaged menisci in order to provoke a regenerative tissue response. This procedure showed promising results in treating chronic musculoskeletal pain [90]. If the menisci is partially damaged, and has to undergo partial meniscectomy, artificial scaffolds are recommended as partial replacement. This procedure helps alleviate post partial meniscectomy knee pain and prevent further articular cartilage degeneration. Previous studies results reported by Spencer et al. [91] showed that twenty-one out of twenty-three patients had a significant improvement in knee scores and showed progression of regenerative tissue. If the menisci is totally damaged or severely torn and had to be totally removed, another procedure is recommended which is meniscal transplantation. This procedure replaces the worn or damaged meniscus by a new one from a cadaver (known as Allograft). This procedure is still under progression; currently it shows improvement of pain and function over the short and intermediate term. The effect on future joint degeneration is still unknown [92]. Future work shall consider simulating the grafting procedure and analyze results to determine effect on knee function.

7.1.2 Jump task application

The purpose of this study was to calculate the internal contact and ligament forces acting on the knee joint due to jump impact and determine the zone of injury at various knee parts. Previous studies focused on the ACL injury and rupture when landing from a jump but did not investigate the contact forces on various knee cartilages and collateral ligament forces.

From the results and the new findings presented, the lowest force value with respect to the patellar tendon (732 N) was recorded at the point before the first Peak F1V (P1), while the highest PT forces was recorded at the point after the second peak F2V (P5) with a value of 3357 N. According to the load capacity of the patellar tendon as extracted from its stress-strain curve and which was reported in Seynnes et al. [93], which reported the force elongation curve for the patella tendon. Patella tendon can withstand up till 4000 N and 6000 N for non-trained and heavy trained personnel respectively, which means in our study the patellar tendon maximum value obtained at P5 is below the maximum capacity of the untrained person and not prone to injury.

For the medial compartment, it was noticed that the maximum contact force 35N and 1200N for the medial menisci and medial cartilage, respectively resulted at P1 as it at angle 30 degrees, then the contact forces decreased as the flexion angle increased where the load shifted to concentrate more on the lateral compartment. The average contact pressure resulted on the medial compartment at all cases was 5.7MPa while for the lateral compartment, maximum contact forces was recorded at the first peak F1V (P2) for the lateral cartilage, and at P5 for the lateral menisci. Average contact pressure on the lateral compartment was 8MPa which indicates the lateral compartment is more prone to injury than the medial compartment. It was noticed from the results that the lateral compartment contributed to more load bearing as quadriceps load and flexion angle increase.

ACL values remained zero at all cases, which is expected as ACL values in flexion becomes zero when there is no posterior femoral displacement. For the PCL forces, resulted values of the first three points were below the ultimate tensile strength of 1880 N as reported in the study of Amis et al. [94] while results of points P4 and P5 slightly exceed that limit which indicates prone to injury.

For the MCL and LCL bundles, force results of all five points were within the tensile capacity reported in [94] and do not approach the injury zone. The ratio between the patellar tendon forces FPT and the quadriceps forces FQ versus the knee flexion of the presented model showed that the patella tendon joint did not act as a perfect pulley. From the results of this study, it was noticed that as the flexion angle increased, the contact forces on the femoral cartilage decreased. Using our knee model, another simulation is conducted at the first peak point P2 which corresponds to toe landing and this time increased the flexion angle by almost 5 degrees under the same previous landing conditions in order to compare both results at the two different knee flexion angles. The total contact forces resulted at toe landing with flexion 38 degrees was considerably less than landing with 33 degrees under the same quadriceps loading. The simulation was repeated by increasing increments of 5 degrees to determine if there will be a trend in contact forces decrease. Results showed considerable decrease in contact forces on the femoral cartilage.

This finding was found in agreement with a recent study by U.C. Davis, conducted by Myers and Hawkins in 2010 on injury prevention for basketball players landing from jumps [95]. This study found that landing with a deeper knee flexion and initiating the landing with toes led to reduced force at the knee when compared to landing on heals first. The study showed that increasing the flexion angle at toe landing made a substantial decrease in the forces at the knee. In the study, Hawkins recommends warm-ups that exercise the knee focusing on landing on the toes and balls of the feet aiming to reduce contact force at the tibia which in turn reduces the risk of an ACL tear.

Another point was investigated beyond P5 and which corresponds to the Vasti peak (Figure 6.14-lower image). This peak in quadriceps forces curve (4400 N) can be attributed to the subject trying to retain stability after heel strike by more squatting (flexion angle 60 degrees) and exerting more quadriceps force. Results at this point followed the same trend as previous points. Contact forces decreased significantly on the tibial plateau to reach 350 N (compared with values at P5 shown in Table 6.8) despite the increase of quadriceps load at this point. The contact forces results agree with the proposed landing technique (as flexion angle increased, the contact forces decreased), this time at a higher quadriceps load. PCL forces were higher (2200 N) which is expected as PCL forces increase with flexion angle. MCL forces increased slightly from its previous value at P5 (80 N), while LCL forces were significantly higher (450 N). This indicates more internal rotation motion of the femur as the subject tries to maintain stability. PCL values indicates an increase in the injury risk and which did not correspond to the maximum ground reaction force. Further investigation of PCL behaviour while landing using the proposed technique under various quadriceps loading is recommended.

7.2 Recommendations

The following forefoot landing technique steps is recommended in order to minimize forces at the knee and thus minimizing injury:

1. Aim to land on the toes first.

2. More knee flexion at toe landing is recommended to reduce contact forces. Increasing the flexion angle when toe landing with as little as 5 degrees showed less contact forces at the knee femoral cartilage. Flexion angle of 48 degrees at toe-landing is recommended as it resulted in lowest contact force.

3. From the ball of the foot being placed down, the heels can roll down towards the ground.

CHAPTER 8

CONCLUSIONS, LIMITATIONS AND FUTURE WORK

8.1 Conclusions

Finite element models have proven to be able to provide deep insight into the mechanical properties of biological tissues and performance of living organs reducing both cost and time. Finite element models present an effective way of evaluating knee joint mechanics during the design phase and provide an indication of expected clinical performance. They are more effective and less costly than in-vivo experiments.

A 3D finite element model is developed of the tibio-femoral and patello-femoral knee joints including hard (bones) and soft tissues (meniscii, cartilages, ligaments and muscles) and was used to analyze two differnet scenarios.

In the first scenario, the presented study provides a full comparison between the menisci intact and fully meniscectomized knee joint. As a conclusion, it was found that total meniscectomy is the worst condition resulting in higher cruciate ligament forces, higher contact pressure, higher stress level on femoral cartilage and higher axial contact force on tibial cartilages. Total meniscectomy resulted in the highest PCL forces in all conditions tested; the next worst condition was the unilateral medial meniscectomy which highlights the role of the medial meniscectomy in load bearing contribution [96]. Clinically, the results of this study show that unilateral medial meniscectomy has a higher impact on knee joint function than lateral meniscectomy and that medial meniscus should have a higher priority for preservation either by grafting or transplantation [97].

In the second scenario, a detailed insight of the internal contact and ligament forces acting on various knee parts as a result of landing from a jump is presented and the injury zone for each part is determined. The lowest force value with respect to the patellar tendon was recorded at the point before the first Peak F1V (P1), while the highest patellar tendon forces was recorded at the point after the second peak F2V (P5) with a value of 3357 N. According to the load capacity of the patellar tendon as extracted from its stress-strain curve and which was reported in previous studies [88], patella tendon can withstand up till 4000 N and 6000 N for non-trained and trained personnel respectively, which means in the presented study the patellar tendon maximum value obtained at P5 is below the maximum capacity of the untrained person and not at risk of injury. Contact forces on menisci and articular cartilages were highest at point P5 followed by P4. ACL values remained zero at all cases (no posterior femoral displacement). For the MCL and LCL bundles, force results of all five points were within the tensile capacity reported in literature [94] and do not approach the injury zone. For the PCL forces, resulted values of the first three points were below the average tensile strength of 1880 N as reported in previous studies [94] while results of points P4 and P5 exceed that limit which increase the risk of injury for PCL. From the previous results the worst condition was recorded at P5, followed by P4 in severity.

From the results of this study, it was noticed that as the flexion angle increased, the contact forces on the femoral cartilage decreased. To recommend a new landing technique, we conducted several simulations to validate this trend. By increasing the flexion angle increments of 5 degrees at toe landing and rerunning the analysis under same previous loading conditions, predicted results of the model showed substantial decrease in the contact forces acting at the knee. The predicted results obtained were found in general agreement with the available reported experimental measurements.

8.2 Limitations

From the limitations of this study, the transverse ligaments, the patellar ligaments and the hamstrings were not modeled which may have resulted in higher values of PCL forces as their load sharing was not represented.

For the proposed landing technique, keeping the same quadriceps loading is another limitation as in reality changing the flexion angle while landing will result in different quadriceps force and ground reaction force.

8.3 Future Work

- Modeling the transverse ligaments, the patellar ligaments and the hamstrings.
- Creating a 3D knee model of a female subject and repeating similar applications in order to evaluate the effect of gender difference on the knee joint performance under various loading.
- Conducting an experimental study to further investigate the proposed landing technique and the predicted results.
- Simulating menisci allograft scenarios to evaluate the procedure and its effect on restoring knee function.

REFERENCES

[1] Murphy, L. et al, (2012), "The Impact of Osteoarthritis in the United States: A Population-Health Perspective". *American Journal of Nursing*. Vol.112, No 3.

[2] Englund, M. et al, (2000), "Patient relevant outcomes fourteen years after meniscectomy: influence of type of meniscal tears and size of resection". *Journal of Rheumatology*. Vol 40, No 6.

[3] Fransen, M. et al, (2011) "The Epidemiology of Osteoarthritis in Asia," *International Journal of Rheumatic Diseases*, vol. 14, no. 2, pp. 113-121.

[4] Hefzy, M.S., Cooke, T.D.T, (1996), "Review of Knee Models: 1996 update", Journal of Applied Mech. Rev., Vol.49, No 10, part 2, S187-S193

[5] Kazemi, M. et al, (2012), "Recent advances in computational mechanics of the human knee joint". *Computational and Mathematical Methods in Medicine*, Vol. 2013, Article ID 718423.

[6] Moeinzadeh, M.H. et al, (1983). "Two-dimensional dynamic modeling of human knee joint". *Journal of Biomechanics* 16 (4), 253–264

[7] Engin A.E. et al, (1993), "Improved dynamic model of the human knee joint and its response to impact loading on the lower leg", *Journal of Biomechanical Engineering*., 115(2), 137-143.

[8] Abdel-Rahman E et al, (1993), "Three-dimensional Dynamic Modeling of the Tibio-Femoral Joint", *Advances in Bioengineering, ASME* BED Vol. 26, 315-318.

[9] Abdel-Rahman F. et al, (1994), "Improved Solution Algorithm for the Determination of the 3-D Dynamic response of the Tibio-Femoral Joint" in, Biomedical Engineering Recent Developments. Proc of l3th Southern Biomed Eng. Conference Washington DC, 368-371.

[10] Abdel-Rahman R. et al, (1994), "Determination of the three-dimensional Dynamic Response of the tibio-femoral Joint Using a DAE Solver," *Advances in Bioengineering, ASME* BED Vol. 28, 421-422.

[11] Tümer S.T. et al, (1993), "Three-body segment dynamic model of human knee*", Journal of Biomechanical Engineering 115(4), 350-356.*

[12] Blankevoort, L.et al, 1995. Validation of a three-dimensional model of the knee. *Journal of Biomechanics* 29 (7), 955–961.

[13] Wang, Y. et al, (2014). "Comparison of stress on knee cartilage during kneeling and standing using finite element models". *Journal of Medical Engineering and Physics*, 36:439-447.

[14] Ho, K. et al, (2013). "Comparison of patella bone strain between females wih and without patellofemoral pain: A finite element analysis study". *Journal of Biomehcanics*, 47:230-236

[15] Adouni, M. et al, (2012). " Computational biodynamics of human knee joint in gait: From muscle forces to cartilage stresses". *Journal of Biomechanics*, 45: 2149-2156

[16] Pena, E. et al, (2006). "A three-dimensional finite element analysis of the combined behaviour of ligaments and menisci in the healthy human knee joint". *Journal of Biomechanics* 39 1686–1701

[17] Ramaniraka, N.A. et al, (2005). "Effects of the posterior cruciate ligament reconstruction on the biomechanics of the knee joint: A finite element analysis". *Journal of Clinical Biomechanics.* 20:434-442

[18] Heegaard J. et al, (1995), "Biomechanics of human patella during passive knee flexion", *Journal of Biomechics* 28(11), 1265-1279.

[19] Hefzy M.S. et al, (1992), "Effects of tibial rotations on patellar tracking and patello-femoral contact area", *Journal of Biomedical. Engineering.*, 14, 329-343.

[20] Hefzy M.S. et al, (1993), "Three-dimensional anatomical model of the human patello-femoral joint to determine patello-femoral motions and contact characteristics", *Journal of Biomedical Engineering*., 15, 289-302.

[21] Matthews L.S. et al, (1977), "Load bearing characteristics of the patello-femoral joint" *Acta Orthopaedica Scandinavica*, 48, 511-516.

[22] Hirokawa S, (1991), "Three-dimensional mathematical model analysis of the patello-femoral joint", *Journal of Biomechanics*, 24, 659-671.

[23] Reithmeier E. et al, (1990), "Theoretical and numerical approach to Optimal positioning of the patellar surface replacement in a total knee endoprosthesis", *Journal of Biomechanics*, 23, 883-892.

[24] Van Eijden T.M. et al, (1986), "Mathematical model of the patello-femoral joint", *Journal of Biomechanics*, 19, 219-229.

[25] Yamaguchi G.T. et al, (1989), "Planar model of the knee joint to characterize the knee extensor mechanism", *Journal of Biomechanics*, 22, 1-10.

[26] Hefzy M.S. et al, (1993), Three-dimensional anatomical model of the human patello-femoral joint to determine patello-femoral motions and contact characteristics, *Journal of Biomedical Engineering.*, 15, 289-302.

[27] Blankevoort L. et al (1988), "The envelope of passive knee joint motion", *Journal of Biomechanics*, 21, (9), 705-720.

[28] Mommersteeg T.J.A. et al, (1996), “A global verification study of a quasi-static knee model with multi-bundle ligaments”, *Journal of Biomechanics*, 29, (12), 1659-1664.

[29] Heegaard J, Leyvraz PF, Curnier A, Rakotomanana L, and Huiskes R, (1995), “Biomechanics of human patella during passive knee flexion”, *Journal of Biomechanics,* 28(11), 1265-1279.

[30] Oshkour, A.A. et al. (2011). "Knee joint stress analysis in standing", 5th Kuala Lumpur International Conference on Biomedical Engineering. IFMBE Proceedings, 35:175-178.

[31] Sylvia, M. (2015). "Development of a human tibiofemoral joint finite element model to investigate the effects of obesity and malalignment on joint contact pressure". A Thesis presented to the faculty of California Polytechnic State University.

[32] Moglo, K.E. and Shirazi-Adl, A. (2003), "On the coupling between anterior and posterior cruciate ligaments, and knee joint response under anterior femoral drawer in flexion: A finite element study". *Journal of Clinical Biomechanics*, 18:751-759

[33] Fithian D.C. et al, (1990), “Material properties and structure-function relationships in the menisci”, *Journal of Clinical Orthopaedic and Related Research.*, 252, 19-31

[34] Shoemaker S.C. et al, (1986), “Role of the meniscus in the anterior-posterior stability of the loaded anterior cruciate-deficient knee: effects of partial versus total menisectomy”, *Journal of Bone Joint Surgery*, 63A, 71-79

[35] Newton, P.M. et al, (1992), “Effects of strain rate on the tensile properties of bovine meniscus”, *Journal of Orthopaedic Research. Society*, 17, 626.

[36] Thissakht, M. et al, (1995), “Tensile stress-strain characteristics of the human meniscal material”, *Journal of Biomechanics*, 28(4), 411-422.

[37] Thissakht, M. et al, (1991), “Nonlinear finite element analysis of the knee menisci: A composite- reinforced model”, *Journal of Orthopedic Research Society*, 16, 294.

[38] Deri, Y. et al, (2012), "Dynamic contact mechanics in the ovine knee joint following partial meniscectomy", *Journal of Biomechanics* 45(S169).

[39] Mononen, M. et al, (2013), "Effects of radial tears and partial meniscectomy of lateral meniscus on the knee joint mechanics during the stance phase of the gait cycle- A 3D finite element study". *Journal of Orthopedic Research* Vol 31(8):1208-1217.

[40] Pena, B.C. et al, (2005). "Finite Element Analysis of the effect of meniscal tears and meniscectomies on human knee biomechanics". *Journal of clinical biomechanics*, 20:498-507.

[41] Bendjaballah MZ. et al, (1995). "Biomechanics of the human knee joint in compression: reconstruction, mesh generation and finite element analysis". The Knee, 2:69-79

[42] Beutler, A. et al, (2009) "Muscle strength and qualitative jump-landing differences in male and female military cadets: The jump-ACL study". *Journal of Sports Science and Medicine* (8**):**663-671.

[43] Louw et al, (2006). "Knee movement patterns of injured and uninjured adolescent basketball players when landing from a jump: A case-control study". *BMC Musculoskeletal Disorders* (**7)**:22.

[44] Bellias, P. et al, (2004). A new method to investigate in vivo knee behavior using a finite element model of the lower limb. *Journal of Biomechanics*. 37 (7):1019-1030.

[45] Stephen, M. et al, (2007). The anterior cruciate Ligament: Reconstruction and Basic Science. *Elsevier Health Sciences.*

[46] Amis, A. et al. (2006) "Anatomy of the posterior cruciate ligament and the meniscofemoral ligaments" . Journal of *Knee Surgery, Sports Traumatology and Arthroscopy* 14 (3): 257–63.

[47] Chandrasekaran, S.et al (2012) "A review of the anatomical, biomechanical and kinematic findings of posterior cruciate ligament injury with respect to non-operative management.". *The Knee 19 (6): 738–45.*

[48] Janousek, A.T.et al (1999). "Posterior Cruciate Ligament Injuries of the Knee Joint". *The American Journal of Sports Medicine* 28 (6): 429–41.

[49] "Bone Patellar Bone ACL Reconstruction". *Wheeless' Textbook of Orthopaedics* Retrieved 2008-10-23.

[50] Moglo, K. et al, (2001) "Non-linear analysis using Finite Element analysis for the human knee joint during flexion", Thesis Presentation.

[51] Materialise, "Mimics Student Edition Course Book v13.1"

[52] Shirazi, R. et al, (2009) "Computation Biomechanics of Articular Cartilage of Human Knee Joint: Effects of Osteochondral Defect.," *Journal of Biomechanics*, vol. 42, no. 15, pp. 2458-465.

[53] Shirazi, R.et al, (2008) "Role of Cartilage Collagen Fibrils Networks in Knee Joint Biomechanics Under Compression," *Journal of Biomechanics*, vol. 41, no. 16, pp. 3340-3348.

[54] Pena, E. et al, (2006). "A three-dimensional finite element analysis of the combined behaviour of ligaments and menisci in the healthy human knee joint". *Journal of Biomechanics* 39 1686–1701

[55] Pena, E. et al. (2005). "Finite Element Analysis of the effect of meniscal tears and meniscectomies on human knee biomechanics". *Journal of clinical biomechanics* 20:498-507

[56] LeRoux, M.A. et al, (2002) "Experimental and biphasic FEM determinations of the material properties and hydraulic permeability of the meniscus in tension". *Journal of Biomechanical Engineering* 124(3):315-321

[57] Sakai, N. et al. (1996) " Quadriceps forces and patellar motion in the anatomical model of the patellofemoral joint". *The Knee* 3:1-7.

[58] Mesfar W, et al , (2005) "Biomechanics of the knee joint in flexion under various quadriceps forces". *The knee 12:424-434*

[59] Walker P.S. et al, (1975) "The role of the menisci in force transmission across the knee". *Journal of Clinical Orthopaedics and related research*, v.109, p.184.

[60] Im, H. S., et al (2015). "The effective quadriceps and patellar tendon moment arms relative to the tibiofemoral finite helical axis". *Journal of Biomechanics.* 48:3737-3742

[61] Ward, S.R., et al (2005). "Influence of patella alta on knee extensor mechanics". *Journal of Biomechanics.* 38, 2415–2422.

[62] Markolf, K.L. et al, (2014). "ACL forces and knee kinematics by axial tibial compression during a passive flexion-extension cycle". *Journal of Biomechanics*.

[63] Papaioannou, G. et al, (2008) "Specific knee joint finite element model validation with high-accuracy kinematics from biplane dynamic Roentgen stereogrammetric analysis." *Journal of Biomechanics 41: 2633–2638*

[64] Markolf, K. L.et al, (2008) "Contributions of the posterolateral bundle of the anterior cruciate ligament to anterior posterior knee laxity and ligament forces. *Journal of Arthroscopic and Related Surgery* 24:805-809

[65] Clements, K.M. et al, (2004) "The Spread of cell death from impact damaged cartilage lack of evidence for the role of nitric oxide and caspases". *Journal of Osteoarthritis and Cartilage* 12:577-585

[66] Chaoe et al , (2010)" Managing Osteoarthritis: A multidisplinary approach". *The Journal of Musculoskeletal Medicine* Volume 27-Number 10.

[67] Shirazi, A. et al, (2009) "Analysis of partial meniscectomy and ACL resonstruction in knee joint biomechanics under a combined knee loading". *Clinical Biomechanics* 24:755-761.

[68] Macnicol, M.F. et al, (2000) "The Knee after meniscectomy". *Journal of Bone and Joint surgery 82:157-159.*

[69] Dandy, D.J. et al, (1990) "The arthroscopic anatomy of symptomatica meniscal lesions". *Journal of Bone and Joint Surgery B72:628-633*

[70] Bobbert, M. F. et al, (1990) "Drop jumping as a training method for jumping ability . Journal of *Sports Medicine* 9:7–22.

[71] Devita, P. et al, (1992) "Effect of Landing Stiffness on joint kinetics and energetics in the lower extremity". *Journal of Medicine and Science in Sports and Exercise.* 24:108-115 .

[72] McNitt-Gray, J. L. et al. (2001) "Mechanical demand and multi-joint control during landing depend on orientation of the body segments relative to the reaction force". *Journal of Biomechanics* 34:1471-1482.

[73] Decker, M. J. et al. (2003) "Gender differences in lower extremity kinematics, kinetics and energy absorption during landing". *Journal of Clinical Biomechanics*. 18:662-669.

[74] AbdelRahman, E. M. et al, (1998) "Three dimensional dynamic behaviour of the human knee joint under impact loading". *Journal of Medical Engineering and Physics.20:276-290.*

[75] Shelburne, K. B. et al, (1997) "A musculoskeletal model of the knee for evaluating ligament forces during isometric contractions". *Journal of Biomechanics. 30:163-176.*

[76] Toutoungi, D. E. et al, (2000) "Cruciate Ligament forces in the human knee during rehabilitation exercises". *Journal of Clinical Biomechanics* 15:176-187.

[77] Zheng, N. G. et al, (1998) "An analytical model of the knee for estimation of internal forces during exercise". *Journal of Biomechanics* 31:963-967.

[78] Pflum, M. A. et al, (2004) "Model Prediction of ACL force during drop landings". *Journal of Medicine and Science in Sports and Exercise. 36:1949-1958.*

[79] Masouros, S.D. et al, (2008) "Biomechanics of the meniscus-meniscal ligament construction of the knee". *Journal of Knee surgery Sports Traumatology Arthoscopy* 16:1121-1132

[80] Rath,E. et al, (2001) "Meniscal Allograft transplantation". *American Journal of Sports Medicine* 29:410-414

[81] Schimmer, R.C. et al, (1998) "Arthroscopic partial meniscectomy: A twelve years follow up and two step evaluation of the long term course". *The Journal of Arthroscopic and related surgery* 14:136-142.

[82] Akizuki, S. et al., (1986) "Tensile properties of human knee cartilage and Influence of ionic conditions, weight bearing and fibrillation on the tensile modulus". *Journal of Orthopedics* 4:379-392.

[83] Kerin, A. J. et al, (1998) "The compressive strength of articular cartilage". *Proceeding of the Institution of Mechanical Engineers Part H. Journal of Engineering in Medicine* 212 (4):273-80.

[84] Quinn, T. M. et al., (2001) "Matrix and cell injury due to sub-impact loading of adult bovine articular cartilage explants: Effects of strain rate and peak stress". *Journal of Orthopedics* 19:242-249.

[85] Repo, R. U. et al, (1977)" Survival of articular cartilage after controlled impact". *Journal of Bone and Joint surgery* 59:1068-1076.

[86] Yang, N. et al, (2009) "The combined effect of frontal plane tibiofemoral knee angle and Meniscectomy on the cartilage contact stresses and strains", *Anuals of Biomedical Engineering* Volume 37, No. 11

[87] Mesfar, W. et al, (2006) "Knee joint mechanics under quadriceps–hamstrings muscle forces are influenced by tibial restraint". *Clinical Biomechanics* 21 841–848.

[88] Moglo, K. et al, (2003) "Biomechanics of passive knee joint in drawer: load transmission in intact and ACL-deficient joints. *The Knee* 10: 265–276.

[89] Brian, J. et al. Allograft Meniscal Transplantation. *Journal of bone and joint surgery*, 84:1236-1249.

[90] Distel, L.M.et al, (2011). "Prolotherapy: A clinical review of its role in treating chronic musculoskeletal pain. *The Journal of injury, function and rehabilitation*" 3(6):S78-81

[91] Spencer, S.J.et al, (2012) "Meniscal Scaffolds: early experience and review of the literature". *The Knee* 19(6):760-5.

[92] Crook, T.B. et al, (2009) "Meniscal Allograft Trasplantation: A review of the current literature". *The Annals of the Royal College of Surgeons of England* 91:361-365.

[93] Seynnes, O.R. et al (2013) "Effect of androgenic anabolic steroids and heavy strength training on patellar tendon morphological and mechanical properties". *Journal of Applied Physiology*. 115:84-89

[94] Amis, A. et al (2003). "Biomechanics of the PCL and related structures: posterolateral, posteromedial and meniscofemoral ligament" *Journal of knee Surgery, Sports Traumatology and Arthroscopy*. 11:271-281.

[95] Myers, C. et al (2010) "Alterations to movement mechanics can greatly reduce anterior cruciate ligament loading without reducing performance". *Journal of Biomechanics* 43(14):2657-2664.

[96] Bendjaballah M.Z. et al, (1998), "Biomechanics response of the passive human knee joint under anterior-posterior forces", *Journal of Clinical Biomechanics*. 13, 625-633.

[97] Brain J. et al, (2002) "Allograft Meniscal Transplantation". *Journal of bone and joint surgery* Volume 84-A, 1236-1249 .

APPENDIX A

Convergence Study

Table A.1: Convergence study of element type

Element Type	Number of Nodes	Von Mises stress
C3D4	4104	0.4 MPa
C3D8R	6326	0.75 MPa
C3D20R	14102	0.80 MPa
C3D10	41043	0.81 MPa

Four different element types were used to mesh the model part (as shown in Table A.1), A simple flexion of 60 degrees was conducted and the resulted Von Mises stress was recorded for each element type as well as the number of nodes resulted from the element type mesh. Von Mises stress value saturated at the value of 0.81. Selection of Element type C3D20R was based on choosing the element that gives the most accurate value (near saturation) and with less nodes to save computational time.

APPENDIX B

Contact Interactions, Constraints and Boundary Conditions

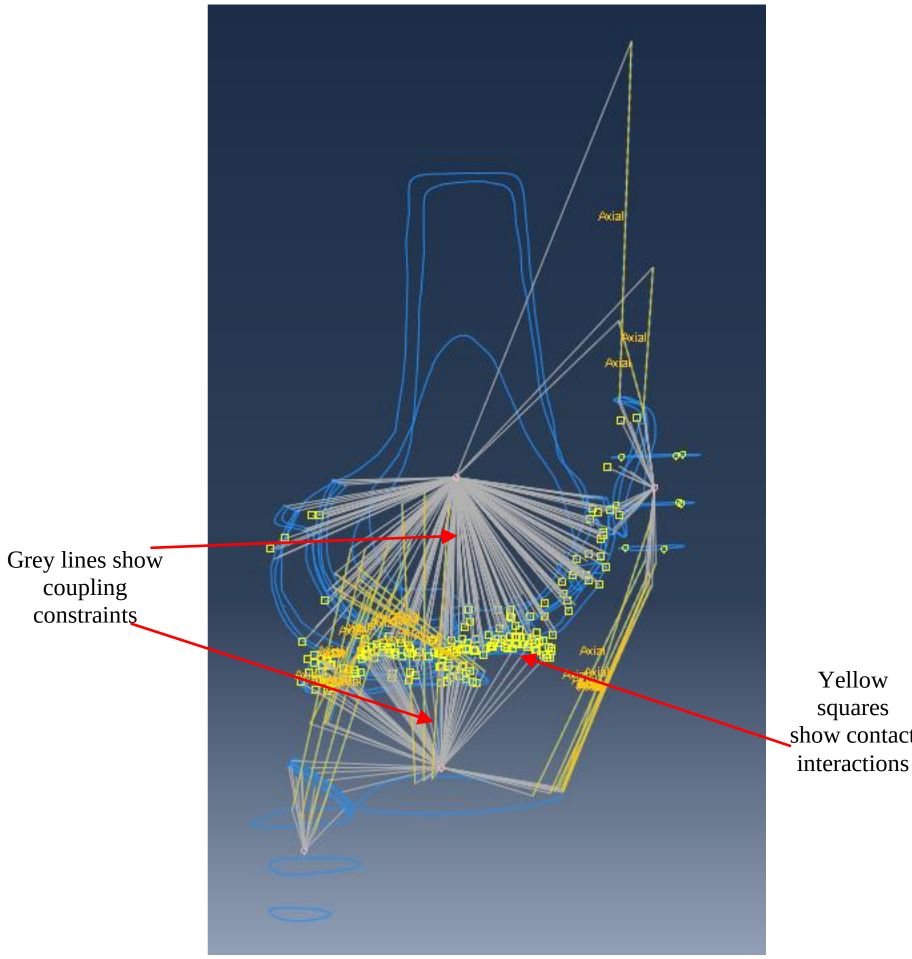

Figure B.1 Contact interactions and coupling constraints

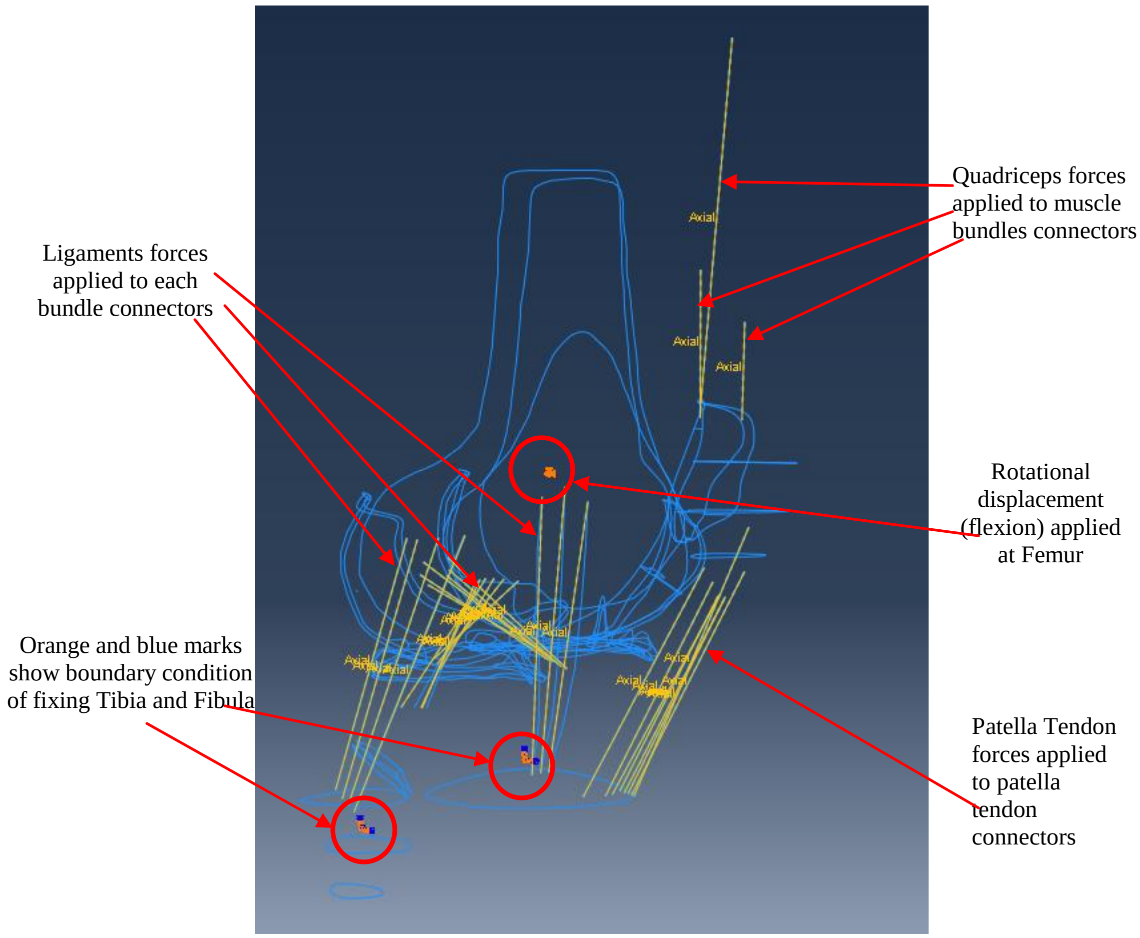

Figure B.2 Boundary Conditions and Loading